



POLITECNICO DI TORINO  
Repository ISTITUZIONALE

1,3-Dihydroxypropan-2-one (DHA) synthesis from Glycerol for pharmaceutical applications

*Original*

1,3-Dihydroxypropan-2-one (DHA) synthesis from Glycerol for pharmaceutical applications / Ripandelli, Simone. - (2015).

*Availability:*

This version is available at: 11583/2605356 since:

*Publisher:*

Politecnico di Torino

*Published*

DOI:10.6092/polito/porto/2605356

*Terms of use:*

openAccess

This article is made available under terms and conditions as specified in the corresponding bibliographic description in the repository

*Publisher copyright*

(Article begins on next page)



POLITECNICO DI TORINO  
FACOLTÀ DI INGEGNERIA INDUSTRIALE

SSD ING-IND/27 CHIMICA INDUSTRIALE E TECNOLOGICA

**Ph.D. thesis in Chemical Engineering**  
**XXVII cycle (2012-2014)**

**1,3-DIHYDROXYPROPAN-2-ONE (DHA) SYNTHESIS  
FROM GLYCEROL FOR PHARMACEUTICAL APPLICATIONS**

DEPARTMENT OF APPLIED SCIENCE AND TECHNOLOGY  
POLITECNICO DI TORINO

PH.D. CANDIDATE:  
SIMONE RIPANDELLI  
MAT.189215

ACADEMIC TUTOR PROF. GUIDO SARACCO

JANUARY 2015  
RESEARCH MONOGRAPH



---

# ABSTRACT

In the last century the amino alcohol serinol (2-amino-1,3-propanediol) has become a common intermediate for several chemical processes. Since the 40's serinol was used as precursor for synthesis of antibiotics (e.g. chloramphenicol). In the last years, new scopes of application were discovered. Serinol is used as building block in the synthesis of X-ray contrast agents, pharmaceuticals (anti-inflammatory or analgesic drugs) or in the cosmetics industry. It can either be obtained by chemical processes based on 2-nitro-1,3-propanediol, dihydroxyacetone (1,3-Dihydroxypropan-2-one or simply DHA) and ammonia [59]. One way to synthesize Serinol, in fact, is reacting DHA in a catalyzed reaction using Pt supported on carbon as catalyst.

The DHA can be synthesized from Glycerol (1,2,3-propanetriol or glycerine) with a selective oxydation of the secondary carbon. The reaction from Glycerol to DHA must be catalyzed and nowadays only one method is well known. The method to obtain DHA uses *gluconobacter oxydans* as catalyst for the selective glycerol oxydation. Anyway the method presents many drawbacks cost not yet solved such as low productivity and high production. It is fundamental to underline how nowadays glycerol plants are closing and others are opening that use glycerol as a raw material as a result of the large surplus of glycerol that is formed as a byproduct in manufacturing biodiesel fuel by transesterification of seed oils with methanol. Over the last twenty years, indeed, biodiesel emerged as a viable fuel and as a fossil diesel additive to replace sulfur, whose content is being progressively lowered according to tighter environmental legislation. However, the increasing production of biodiesel is not artificially sustained and is predicted to spread and increase, as biodiesel provides sufficient advantages to merit subsidy. Besides the closure of production plants, industry reacted to this situation stimulating research to find new applications of glycerol as a low-cost feedstock for functional derivatives either for mass consumption, such as additives for

concrete, or as a precursor of valued fine chemicals [60]. One investigated application of glycerol is exact its possible use as starting material for DHA synthesis (figure 1.4, chapter 1).

The aim of this work was to investigate for new possibilities to transform glycerol into DHA, avoiding *gluconobacter oxydans* utilisation. In particular the attention was posed on new catalytic solutions investigating inorganic catalysts for the selective oxydation of glycerol. Two catalytic system were investigated. An heterogenous solution using noble metal nanoparticles supported on carbonious supports (mono- and bi-metallic systems) and an homogeneous one using an organometallic catalyst based on Pd.

The study was approach from experimental and theoretical point of view because the reaction mechanism is not still clear.

The research bring us to investigate deeply many weakness of the reaction and not still clear in literature, such as an efficient analytical method, problems linked to the catalysts aging, their deactivation and synthesis.

---

# CONTENTS

<b>1</b>	<b>General introduction</b>	<b>1</b>
	General introduction	1
<b>2</b>	<b>The state of the art and the possible solutions analyzed</b>	<b>7</b>
2.1	Glycerol Oxidation . . . . .	7
2.2	A catalytic conversion using an Organometallic complex . . .	9
2.2.1	The best results in literature . . . . .	9
2.2.2	The problem of the decomposition . . . . .	11
2.3	The noble metals catalysts . . . . .	13
2.3.1	The important parameters for the performances of the catalysts . . . . .	20
2.4	The electrocatalysis . . . . .	23
2.5	Analytical methods . . . . .	25
<b>3</b>	<b>A preliminary study</b>	<b>26</b>
3.1	The electrocatalytic reaction . . . . .	28
3.2	The organometallic catalyst solution . . . . .	31
3.3	The heterogeneous solution with noble metal nanoparticles .	33
3.3.1	Deactivation of the heterogeneous catalysts . . . . .	34
3.4	An economical evaluation . . . . .	37
3.4.1	Homogeneous catalysts based on Pd complexes . . . . .	37
3.4.2	Heterogeneous catalysts based on Au nanoparticles . .	40
3.4.3	A comparison between the solutions proposed . . . . .	41
3.5	Conclusions and steps of reasearch . . . . .	43
<b>4</b>	<b>The catalysts synthesis and their characterization</b>	<b>45</b>
4.1	The organometallic catalyst . . . . .	46

4.2	The monomer form of the Pd catalyst . . . . .	48
4.2.1	The synthesis of the monomer complex . . . . .	49
4.2.2	The synthesis of the activated complex of Pd with CH <sub>3</sub> CN anhydrous . . . . .	52
4.2.3	The synthesis of the activated complex of Pd without CH <sub>3</sub> CN anhydrous . . . . .	54
4.2.4	The synthesis of the dimer form of the Pd complex . .	55
4.2.5	Considerations about the organometallic Pd complex .	58
4.3	The catalyst based on Au nanoparticles . . . . .	58
4.3.1	The different methods for Au NPs synthesis . . . . .	59
4.3.2	The improvement for the synthesis of the gold based catalyst . . . . .	62
4.4	The bi-metallic catalysts . . . . .	66
4.4.1	The catalysts synthesis . . . . .	67
4.4.2	The carbonious supports and the metals deposition . .	68
4.4.3	Bimetallic Pt-Bi on graphite oxide . . . . .	72
4.4.4	The EDX and XPS analysis . . . . .	75
4.4.5	Further results on the GOIV, GOV and GOVI . . . . .	80
4.4.6	Conclusions about the bi-metallic catalysts . . . . .	81
4.5	The tri-metallic AuPtBi catalyst . . . . .	84
<b>5</b>	<b>The analytical methods</b>	<b>86</b>
5.1	The GC-FID . . . . .	87
5.2	The GC-MS . . . . .	89
5.3	The HPLC methods . . . . .	90
5.3.1	The analytical method to follow the synthesis of PdNc(OAc) <sub>2</sub> complex . . . . .	91
5.3.2	The HPLC-RID for the DHA detection . . . . .	91
5.3.3	The RP-HPLC for the DHA detection with UV detector	92
<b>6</b>	<b>Experimental results</b>	<b>95</b>
6.1	The Pd complexes as catalyst . . . . .	100
6.2	The best results with Organometallic complexes and a study about the decomposition . . . . .	104
6.2.1	Conclusions . . . . .	109
6.3	The results from mono-metallic catalyst . . . . .	111
6.4	The experiments with the bi-metallic catalysts . . . . .	111
6.5	The experiments with the tri-metallic catalyst . . . . .	116
<b>7</b>	<b>Conclusions</b>	<b>118</b>
<b>8</b>	<b>Appendix A</b>	<b>121</b>
8.1	The Graphite Oxide (GO): classical method . . . . .	121
8.2	The Graphite Oxide (GO): the modified methods . . . . .	122

<b>9</b>	<b>Appendix B</b>	<b>125</b>
9.1	The gold mono-metallic catalyst . . . . .	125
9.2	The Pt-Bi bi-metallic catalysts . . . . .	126
<b>10</b>	<b>Appendix C</b>	<b>129</b>
10.1	A brief introduction to DFT calculation . . . . .	129
10.2	Quantum Espresso and the approach to the model . . . . .	130
10.3	Conclusions about the DFT calculation . . . . .	134



---

# LIST OF FIGURES

1.1	The reaction scheme for the Iopamidol synthesis . . . . .	2
1.2	The reaction scheme for the Serinol synthesis . . . . .	2
1.3	The glycerol business from 2004 until 2011 . . . . .	5
1.4	Overview of conversion pathways for glycerol . . . . .	6
2.1	Chemicals from glycerol by oxidation (commercial price of glycerol and oxidation products - when available): glycerol refined = 0.74 Euro/kg , lactic acid = 1.2 Euro/kg, dihydroxyacetone = 15 Euro/kg) . . . . .	8
2.2	general mechanism of Palladium-Catalyzed alcohols oxidation .	11
2.3	Catalytic oxidation of glycerol and 1,2-propanediol with Palladium neocuproine organometallic complex . . . . .	11
2.4	The proposed mechanism for aerobic alcohol oxidation from Waymouth and co-workers . . . . .	14
2.5	Catalytic results from literature about the bi metallic catalysts based on Pt-Bi . . . . .	16
2.6	Effect of (A) the platinum loading (Bi/Pt ration between 0.52-0.67) and (B) the Bi/Pt ratio on the activity of Bi-Pt/C catalysts (5 wt%) [4] . . . . .	17
2.7	Effect of Au loading on the activity of Bi-Pt/C catalysts (3 wt%Pt, Bi/Pt ratio 0.5) [4] . . . . .	18
2.8	The two routes to DHA by the catalytic oxidation of glycerol [4] . . . . .	18
2.9	Some typical results of catalytic oxidation of glycerol investigated by several groups . . . . .	19
2.10	General reaction scheme for electrochemical alcohol oxidation mediated by TEMPO . . . . .	24
2.11	Electrochemical oxidation of glycerol mediated by TEMPO in water effords DHA and, after longer reaction times, HYPAC	25

3.1	Curve gain on cost; in accord with the results obtained from literature, with the yellow mark the cost compared with the yield following the heterogeneous catalysts, while with the red mark the cost related to the homogeneous solution; the green triangle is related to the electrocatalytic results . . . . .	28
3.2	The catalyst TEMPO . . . . .	28
3.3	The electrocatalytic reaction scheme . . . . .	29
3.4	The electrocatalytic reactor scheme . . . . .	29
3.5	The reaction scheme for the solution with the organometallic catalyst based on Pd . . . . .	32
3.6	The scheme of the reactor with the amount of reagents for each cycle . . . . .	32
3.7	The scheme of the reactor for the heterogeneous catalyst . . .	34
3.8	The conversion of glycerol following the models proposed in the equations 3.1, 3.2 and 3.3 . . . . .	35
3.9	A zoom on the chart presented in figure 3.8 in order to evaluate the necessary time to reach the glycerol conversion level required . . . . .	36
3.10	the scheme proposed for the heterogeneous catalyst solution; MWCNTs: multiwalled carbon nanotubes . . . . .	37
3.11	the scheme of the volumes needed for the reaction in function of the cycles per day . . . . .	38
3.12	The conversion estimation referred to the experimental data from literature . . . . .	39
3.13	The flowchart about the reaction costs . . . . .	39
3.14	The cost hypothesis without evaporation with nanoparticles solution . . . . .	40
3.15	The cost hypothesis with evaporation with nanoparticles solution . . . . .	40
3.16	the scheme concerning the all potential sources of cost . . . .	41
3.17	the scheme of the volumes necessary for the reaction function of the cycles per day . . . . .	42
3.18	The economical estimation for the three different solutions; metal based catalyst with a longer life . . . . .	42
3.19	The economical estimation for the three different solutions; metal based catalyst with a shorter life . . . . .	43
3.20	The economical estimation for the three different solutions; organo-metallic catalyst with a longer life . . . . .	43
3.21	The economical estimation for the three different solutions; organo-metallic catalyst with a longer life . . . . .	44
4.1	neocuproine-Pd(OAc) <sub>2</sub> . . . . .	46
4.2	[neocuproine-Pd( $\mu$ -Ac)] <sub>2</sub> (OTf) <sub>2</sub> . . . . .	46

4.3	The reaction scheme for the alcohols oxidation using the Pd complex [44]; the carboxylate form of the complex (5) is an inactive form of the catalyst . . . . .	47
4.4	The chemical reactions to obtain the dimer Pd-complex: (I) the activation of CH <sub>3</sub> CN with the acid;(II) the reaction to obtain the Pd-complex (PdNc-C) in its activated form (PdNc-A);(III) the final reaction to obtain the dimer (PdNc-D) [44]	48
4.5	The reaction scheme for the synthesis of the complex in its monomeric form, Neocuproine-Pd(OAc) <sub>2</sub> . . . . .	49
4.6	An example of the reactor for the complex synthesis in its monomeric form . . . . .	50
4.7	The HPLC chromatogram for the only Neocuproine . . . . .	51
4.8	The HPLC chromatogram of the complex after the filtration: the chromatogram is related to the final product after the filtration . . . . .	52
4.9	The H-NMR analysis of the complex; as solvent was used the CH <sub>3</sub> CN . . . . .	52
4.10	The ICP analysis to define the amount of Pd of the Pd-complex monomer . . . . .	53
4.11	The Karl-Fischer results to evaluate the water amount in the Pd-complex monomer . . . . .	53
4.12	The H-NMR spectrum for the activated form of the complex	54
4.13	The H-NMR spectrum for the activated form of the complex using the no anhydrous CH <sub>3</sub> CN; the two signals related to the two methyl groups have a area ratio equal to 2:1 . . . . .	55
4.14	The ICP analysis to define the amount of Pd of the activated Pd-complex . . . . .	55
4.15	The KF analysis to define the amount of water of the activated Pd-complex . . . . .	55
4.16	The theoretical structure of the dimer form of the PdNc complex	56
4.17	The simple scheme shows the possible behavior of the Pd complex in solution when is used as catalyst . . . . .	56
4.18	The MALDI spectrum for the dimer . . . . .	57
4.19	The KF analysis to define the amount of water of the dimer Pd-complex . . . . .	58
4.20	The ICP analysis to define the amount of Pd of the activated Pd-complex . . . . .	58
4.21	The FESEM image takes from the sample with Au NPs synthesized with impregnation method; support: carbon black . . . . .	60
4.22	The FESEM image takes from the sample with Au NPs synthesized with double impregnation method; support: carbon black . . . . .	61
4.23	The FESEM image takes from the sample with Au NPs synthesized with LPRD method; support: carbon black . . . . .	62

4.24	The FESEM image takes from the sample with Au NPs synthesized with LPRD method; support: mesoporous carbon . . .	63
4.25	The FESEM image takes from the sample with Au NPs synthesized with LPRD method; support: graphite without pH control . . . . .	65
4.26	The FESEM image takes from the sample with Au NPs synthesized with LPRD method; support: graphite with pH control	66
4.27	The FESEM image takes from the sample with Au NPs synthesized with LPRD method using NaOH 1 M; support: graphite with pH control . . . . .	67
4.28	The FESEM image takes from the sample with Au NPs synthesized with LPRD method; support: carbon with pH control	68
4.29	The FESEM image takes from the sample with Au NPs synthesized with LPRD method; support: carbon with pH control	69
4.30	The FESEM image takes from the sample with Au NPs synthesized with LPRD method using CTAB . . . . .	70
4.31	The graphite sheet (a) and a graphite oxide sheet (b) . . . . .	70
4.32	The XRD on the graphite and on the GO; the XRD shows the shift on the graphite peak . . . . .	71
4.33	The XRD on the graphite and on the GO; the XRD shows the shift on the graphite peak . . . . .	71
4.34	The XRD comparison between the two GO weakly functionalized . . . . .	72
4.35	The XPS on the graphite by Sigma-Aldrich . . . . .	72
4.36	The XPS on the GO IV obtained in laboratory; see the Appendix B for the synthesis description . . . . .	73
4.37	Pt Bi nanoparticles on graphite oxide; deposition using subsequent impregnation . . . . .	73
4.38	Pt Bi nanoparticles on graphite oxide (GO II) using the STEM	74
4.39	Pt Bi nanoparticles on graphite oxide (GO II) using the STEM	75
4.40	Pt Bi nanoparticles on graphite oxide (GOIII) using the STEM	75
4.41	the XPS of graphite on the C binding energy range . . . . .	76
4.42	the XPS of graphite oxide GOII on the C binding energy range; were put in evidence the functional groups . . . . .	76
4.43	the XPS of graphite oxide GOIII on the C binding energy range, were put in evidence the functional groups . . . . .	76
4.44	the XPS of graphite after the impregnation; together with the C binding energy are presented the Pt and the Bi binding energy ones . . . . .	77
4.45	the XPS of GOII after the impregnation only with Pt metal precursor; together with the C binding energy are presented the peaks of Pt . . . . .	78

4.46	the XPS of GOIII after the impregnation; together with the C binding energy are presented the Pt and the Bi binding energy ones . . . . .	78
4.47	the EDX analysis on the PtBi based catalyst on graphite . . .	79
4.48	the EDX analysis on the PtBi based catalyst on GOII; this EDX analysis was a further information about the absence of the Bi on the surface . . . . .	79
4.49	the EDX analysis on the PtBi based catalyst on GOIII; the EDX analysis was done on the entire area presented in the small window on the right side of the spectra . . . . .	80
4.50	the EDX analysis on the PtBi based catalyst on GOIII; the EDX was done on the same sample of the figure 4.49 but in a punctual zone . . . . .	80
4.51	An image from the STEM analysis on the sample GO IV after the Pt and Bi deposition; it is possible to observe the Nps displacement on the surface . . . . .	81
4.52	This image from STEM, Pt on GO V, shows the presence of the metal NPs on the surface of the functionalized support; moreover it shows how the NPs are localized on the functionalized part of the support, the finest one; the STEM permits to have an idea of the thickness of the support that it is very thin in correspondance of the functionalisation. It is possible to see, indeed, the carbon lattice of the copper grids for the FESEM microscopy through the sample . . . . .	82
4.53	This image from STEM, Pt on GO V, permits to have an idea of the NPs; moreover the distribution seem to be homogeneous	82
4.54	This image from STEM to observe the NPs of Pt on the GO VI . . . . .	83
4.55	This image from STEM, Pt on GO VI, permits to have an idea of the NPs dimension . . . . .	83
4.56	The STEM analysis on the tri-metallic catalyst . . . . .	85
4.57	The STEM analysis on the tri-metallic catalyst . . . . .	85
5.1	The scheme of the possible structures from the oxidation of the glycerol [60] . . . . .	87
5.2	The GC-FID chromatogram with the external standard . . .	88
5.3	The GC-FID chromatogram with the external standard . . .	89
5.4	The GC-MS spectrum for a solution with pure glycerol; with the blu square is underlined the signal m/z relative to the the CF <sub>3</sub> from TFAA after the derivatization; with the red ellipsis the signal m/z related to the glycerol . . . . .	90

5.5	The GC-MS spectrum for a solution with pure glycerol; with the blu square is underlined the signal m/z relative to the the CF <sub>3</sub> from TFAA after the derivatization; with the yellow ellipsis the signal m/z related to the DHA . . . . .	90
5.6	The chromatogram from the HPLC analysis at the start and at the end of PdNc(OAc) <sub>2</sub> synthesis . . . . .	91
5.7	The chromatogram from the HPLC analysis from a reaction solution . . . . .	92
5.8	The RP-HPLC elution gradient . . . . .	93
5.9	The RP-HPLC analysis, on the abscissa the retention time [min]; UV detector at 263 nm . . . . .	94
5.10	The RP-HPLC analysis, on the abscissa the retention time [min]; UV detector at 215 nm . . . . .	94
6.1	The selective oxidation of glycerol to obtain the DHA . . . .	95
6.2	The scheme represents how the impeller works coupled with the oxygen tube; this is not the best solution for a real reactor, but is one of the best solution for a kinetic study . . . . .	96
6.3	The interior of the reactor; it is possible to observe the holed impeller, the cooling loop on the right side and the pipe for the gas injection . . . . .	97
6.4	This table shows the results obtained at different volume ratios of water and CH <sub>3</sub> CN prepared to test the solubility of the glycerol and DHA (1.0 M) before to start the experiments	98
6.5	The solubility of O <sub>2</sub> in water solution and different temperatures	98
6.6	The solubility of O <sub>2</sub> in CH <sub>3</sub> CN solution and different temperatures . . . . .	98
6.7	The form to collect data from the laboratory experiments . .	99
6.8	The reaction mechanism proposed by Waymouth and co-workers	101
6.9	The table summarized some operational conditions using the dimer form of the Pd catalyst . . . . .	101
6.10	The reaction scheme from the literature [7] . . . . .	102
6.11	The graph about the yield evaluation for the DHA at different temperatures . . . . .	103
6.12	Results about conversion of glycerol and yield to DHA for three reaction at 10 bar of O <sub>2</sub> , 40°C, MR = 1600 and in different solutions of CH <sub>3</sub> CN; the analysis were done with the GC-FID and subsequently confirmed by HPLC-RID . . .	104
6.13	Results from reactions at 60 Celsius degree and 30 bar, for different solution of acetonitrile to water and different molar ratio glycerol to catalyst; for every test is reported the value of the glycerol conversion ( $\zeta$ ) computed at the end of the reaction . . . . .	105

6.14	Glycerol conversion and DHA Yield at 60°C, 30 bar of oxygen at MR=16,160,1600, CH <sub>3</sub> CN:water (10:1) used as solvent . . .	106
6.15	Glycerol conversion and DHA yield at 60°C, 30 bar of oxygen at MR=16,1600; pure water used as solvent . . . . .	106
6.16	Glycerol conversion and DHA yield at 60°C, 30 bar of oxygen at MR=16; pure water and CH <sub>3</sub> CN:water (10:1) were used as solvent . . . . .	107
6.17	Glycerol conversion and DHA yield compared; two reactions at 40°C, 10 bar and 60°C, 30 bar of oxygen; MR=16; pure water used as solvent . . . . .	108
6.18	Glycerol conversion and DHA yield at 40°C, 10 bar of oxygen at MR=16,160,1600; pure water and CH <sub>3</sub> CN:water (1:1) were used as solvent . . . . .	108
6.19	The regeneration factor . . . . .	109
6.20	A comparison about the glycerol conversion with monomer and dimer for three different solutions . . . . .	110
6.21	The DHA yield compared using three different solvents and the organometallic catalyst in its monomeric and dimeric form; the error bars are tuned with the instrumental error . . . . .	110
6.22	In this H-NMR the spectrum at the bottom represents the analysis of the powder recovered from the reactor; the spectrum is compared with the signal of the catalyst and with the DAH and glycerol ones . . . . .	112
6.23	The EDX on the powder recovered from the reactor at the end of the reaction . . . . .	113
6.24	The GC-FID chromatograph obtained analyzing the samples from the reactions with gold on carbon catalysts . . . . .	113
6.25	The table shows some significant example did with the Au catalyst; in the last column the results about the selectivity to DHA at the end of the reaction are equal to 0% . . . . .	114
6.26	The tests conducted with bi-metallic PtBi catalysts on GOIII and GOV . . . . .	114
6.27	The tests conducted with bi-metallic PtBi catalysts on graphite and GOVI . . . . .	115
6.28	The conversion of the glycerol . . . . .	116
6.29	Results from the tests into the batch reactor at different pH .	117
8.1	This picture was taken during the reaction and 2 hours mixing (after water addition at 98°C) . . . . .	123
9.1	This picture was taken during the reaction and 2 hours mixing (after water addition at 98°C) . . . . .	127

10.1	One of the proposed mechanism of reaction presented in literature . . . . .	129
10.2	This scheme summarized how the simulation took place to solve the Schroedinger equations . . . . .	131
10.3	The glycerol and DHA molecules; the two structures correspond to the two configurations calculated with software Quantum Espresso . . . . .	131
10.4	The computed crystal for gold atoms . . . . .	132
10.5	The computed crystal for gold atoms from the top; it is possible to recognize the hexagonal lattice typical for the bcc crystals, Au(111) . . . . .	132
10.6	The system for which the Hamiltonian is solved; in this system it is possible to recognize glycerol, the Au nanoparticles and the -OH functional group, in accord with one of the model proposed as main mechanism of glycerol de-protonation . . . . .	133



---

---

# CHAPTER 1

---

## GENERAL INTRODUCTION

The amino alcohol serinol (2-amino-1,3-propanediol) has become a common intermediate for several chemical processes. Since the 40's serinol was used as precursor for synthesis of antibiotics (chloramphenicol). In the last years, new scopes of application were discovered. Serinol is used as building block in the synthesis of X-ray contrast agents, pharmaceuticals (anti-inflammatory or analgesic drugs) or in the cosmetics industry. It can either be obtained by chemical processes based on 2-nitro-1,3 propanediol, dihydroxiacetone (DHA) and ammonia [59].

In Bracco Imaging S.p.A., an italian pharmaceutical company operating in the field of the diagnostic imaging, the serinol finds an application in the Iopamidol synthesis (figure 1.1). Iopamidol is a non-ionic iodinated X-ray contrast agent. The Bracco company is looking for a solution to reduce the cost for the Iopamidol synthesis.

The serinol employed as starting material in the preparation of contrast media must have a high degree of purity in order to obtain products with very low levels of impurities. This requirement is due to the total amount of administered product, which is much higher than that of other medications. Currently Bracco buys all its requirement from Angus Chemical Company. Anyway the serinol production was running from the beginning of 90's and ended in 2011 when the process became not-cost effective. Serinol was produced by Bracco from the reaction of dihydroxiacetone (DHA) with ammonia to give as intermediate an oxazole derivative. Followed a reduction with  $H_2$  in presence of catalyst into amino compound (figure 1.2). The serinol process became not cost-effective cause the high cost of the DHA as starting material.

Nowadays the DHA is produced on an industrial scale by microbial fermentation of glycerol. Although microbial fermentation processes can provide

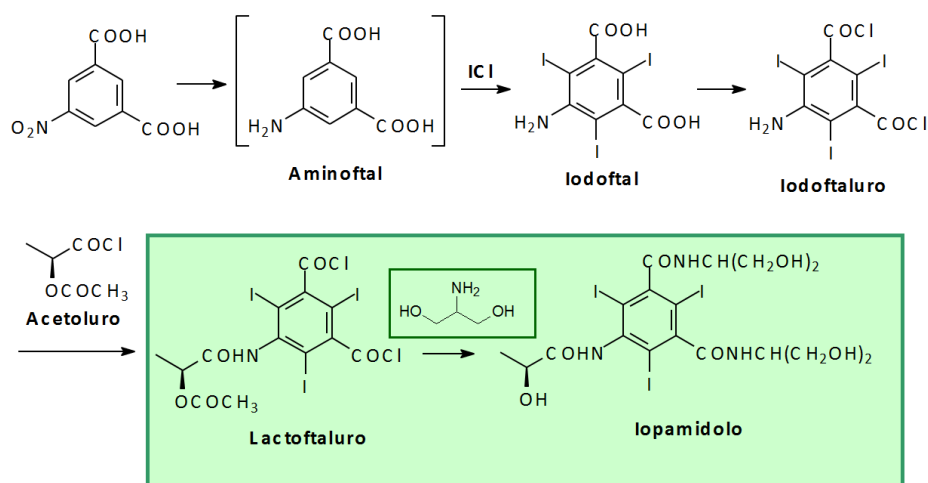


Figure 1.1: The reaction scheme for the Iopamidol synthesis

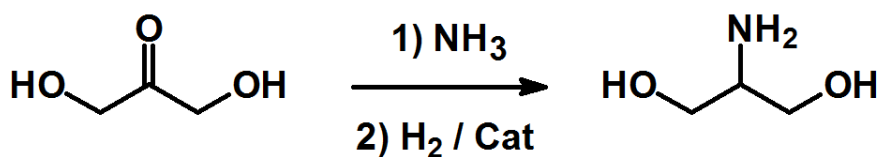


Figure 1.2: The reaction scheme for the Serinol synthesis

high selectivity to DHA, they have some drawbacks such as low productivity and high production cost.

## The structure of the thesis

In this section is presented the structure of the thesis.

The thesis is divided in 10 chapters three of them dedicated to complementary information and three Appendices: A, B and C. The first chapters are dedicated to a general introduction presenting the problem studied. The chapter 2 is dedicated to the state of the art for the problem studied. In chapter 3 there is a brief introduction to the problem with the preliminary study that involved the first six months of the Ph.D. In this period a bibliography research was conducted and it was helpful to focus the problem. Then, in order to focus size of the problem, three possible scenarios were proposed. The chapter 4 presents all the catalytic systems studied. From the organometallic, passing through the heterogeneous mono-metallic catalyst based on Au

nanoparticles (NPs) and the bi-metallic catalyst system.

The first part of this chapter is considered central because it was dedicated to the organometallic catalysts. The catalyst based on Pd and Neocuproine. It is reported a complete description about the synthesis and the characterisation about this catalysts. Some considerations on the catalyst are underlined in this section. A 90% of the work did about the organometallic catalyst was done at Research Center of Bracco Imaging (CRB) in Colleretto Giacosa, Ivrea, Italy.

The research about the mono-metallic catalyst occupied eight months with interesting results about the catalytic activity in contrast with the literature results. The reason about these conflicting results has been associated to the impossibility to use this kind of catalyst for the reaction studied and in accord with the *errata corrige* published by Rodrigues *et alii* [1] in 2011.

Concerning the bi-metallic catalyst: Pt and Bi on carboniuos supports. This catalyst was studied looking for a new solution to the Au on carbon as heterogeneous catalyst. The research on this catalyst starts at the end of 2013. Aim of this part of the Ph.D. study was to improve the results obtained and already presented in literature [47] using a new kind of support, graphite oxide (GO).

Finally it is important to underline how this "new" catalyst has found an interesting application in other research area and opened new scientific collaborations. The catalyst found application in the selective oxydation of glucose to D-saccharid acid, used as starting material for the adipic acid synthesis. The research work is still ongoing.

In the same chapter is also reported a brief study performed in collaboration with the research group of prof. Laura Prati, Department of Inorganic Chemistry, University of Milan. The collaboration involved experiments on a tri-metallic Pt-Au-Bi catalyst.

The chapter 5 presents the analytical method developed. The development of the analytical methods occupy an important part of the work in order to be sure about the real activity of the catalysts. Moreover the errors committed by Rodrigues and co-workers [54] have taught the necessity to pay attention at a correct development of a reproducible and a reliable analytical method.

In the chapter 6 the experimental results from laboratory tests are presented and compared.

The chapter 7 is dedicated to a brief conclusion about the entire work. The entire work became important in order to underline all the problems related to the selective oxydation of the glycerol into DHA. These problems, in fact, were not still extensively studied and presented in literature to date.

The Appendices are divided as follow:

- A the description of the graphite oxide used as support for the bi-metallic catalysts: this appendix describes the original method by Hummers

(1958) [52] and its modification

B the description of the heterogeneous catalysts synthesis, mono- and bi-metallic

C the *shape ab initio* study: the density functional theory (DFT) approach to the problem in exam

## The Glycerol as chemical platform

Glycerol (1,2,3-propanetriol or glycerine), an organic molecule isolated by heating fats in the presence of ash (to produce soap) as early as 2800 B.C., is an industrial chemical with tens of applications. Following the discovery of synthetic surfactants, glycerol has been produced from epichlorohydrin obtained from propylene (and thus from fossil oil) and later large chemical companies initiated its synthetic production. Today, however, glycerol plants are closing and others are opening that use glycerol as a raw material (including for the production of epichlorohydrin itself) as a result of the large surplus of glycerol that is formed as a byproduct in manufacturing biodiesel fuel by transesterification of seed oils with methanol. To illustrate this trend, the global glycerol market started to increase from 2005, with a peak in 2008, together with a progressive reduction of its cost (figure 1.3).

Over the last decade, biodiesel has emerged as a viable fuel and as a fossil diesel additive to replace sulfur, whose content is being progressively lowered according to tighter environmental legislation. Until the recent increases in petroleum prices, high production costs made biofuels unprofitable without government subsidies. However, the increasing production of biodiesel is not artificially sustained and is predicted to spread and increase, as biodiesel provides sufficient advantages to merit subsidy. Besides the closure of production plants, industry reacted to this situation by starting research to find new applications of glycerol as a low-cost feedstock for functional derivatives either for mass consumption, such as additives for concrete, or as a precursor of valued fine chemicals [60].

During its production via transesterification of oils from plants, about 100 kg of glycerol is produced for every ton of biodiesel. The glycerol is a waste chemical produced in large quantity. Currently, biodiesel companies face serious issues to identify high added value outlets for the crude glycerol. Crude glycerol typically has a purity of 40-70% and refining is required to produce pharmaceutical grade glycerol (99% purity), to be used in cosmetics, paints, automotive parts, food, tobacco, pharmaceuticals, paper, leather and the textile industry. This market is continuously increasing, and this trend is expected to keep constant. Moreover the rapid expansion of the global production of biodiesel has created a major surplus of glycerol, leading to a decline in glycerine pricing. Consumption of this extra glycerol is a neces-

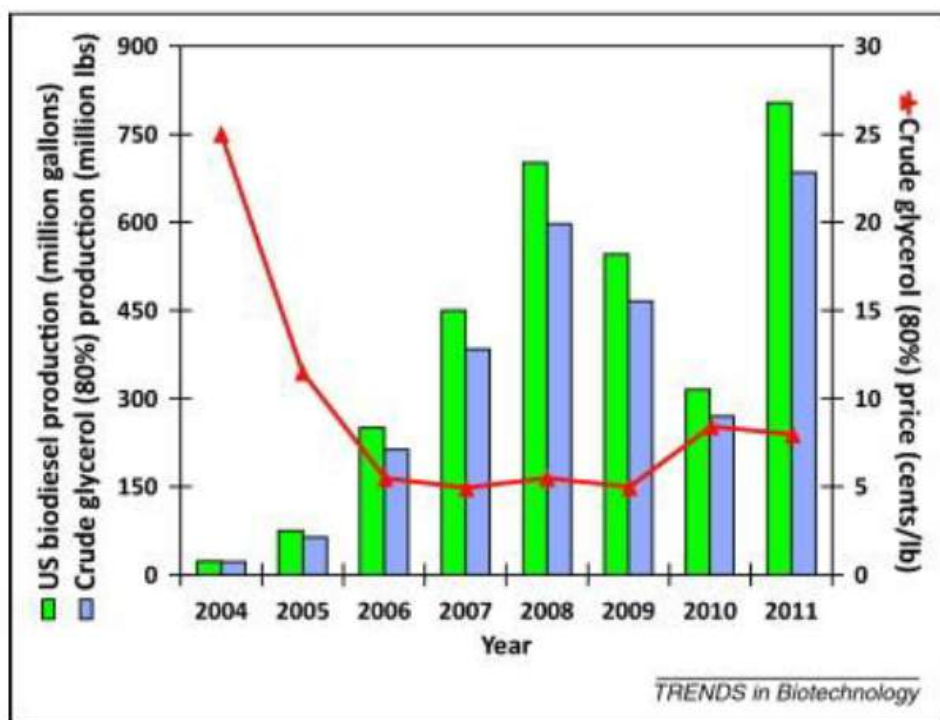


Figure 1.3: The glycerol business from 2004 until 2011

sary requisite for the commercial viability of biodiesel production [1,3]. For this reason a large number of publications and reviews have appeared in the recent years on glycerol conversions using either chemo-catalytic or biochemical methods. Glycerol may be converted to a multitude of products using oxidation, hydrogenolysis, etherification, esterification, polymerization, dehydration, halogenation and reforming (figure 1.4).

## The DHA as byproduct

Among byproducts from the glycerol oxydation, the 1,3-dihydroxy-2-propanone (DHA) is main topic of this work. The research was focused on the selective oxidation of glycerol to DHA and the work was developed directly in collaboration with Bracco Imaging S.p.A.

Compared to the price of the DHA, about 15 Euro per kilo, and thanks to its molecular structure, the glycerol became an interesting starting material. In the last years many groups of research have started to study how to use the glycerol as starting material by selective catalyzed reactions [1,2,3,4,5,6,7,50]. The selective oxidation of the glycerol to DHA (selective oxydation on the secondary carbon) is is a possible reactions, one of the most

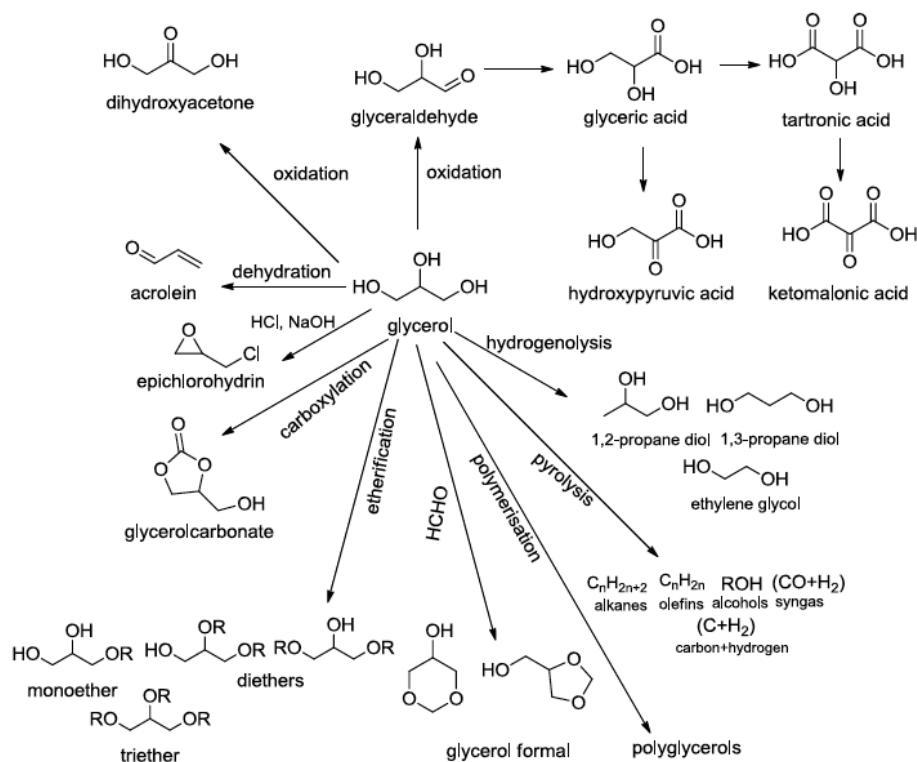


Figure 1.4: Overview of conversion pathways for glycerol

difficult but, in practice, all oxidized chemicals obtained by the process are commercially relevant.

Unfortunately the extensive functionalisation of the triol glycerol molecule with hydroxy groups of similar reactivity makes difficult the selective oxydation. Glycerol is easily converted to formaldehyde, formic acid, and CO<sub>2</sub> and in some cases mass balances as low as 20% are observed [61,62]. Good selective conversion is difficult to achieve due to rapid overoxidation, and high selectivities become more difficult as the compound become more oxidised. The research moved on this scenario. Ph.D. course can be summarized in three parts:

1. a study of the state of the art in order to understand what was done in the recent past
2. a preliminary evaluation of the possibility to scale-up the reaction
3. laboratory experimentation

---

---

## CHAPTER 2

---

# THE STATE OF THE ART AND THE POSSIBLE SOLUTIONS ANALYZED

### 2.1 Glycerol Oxidation

The glycerol oxidation are currently receiving a lot of attention. Many oxidation products exist apart DHA. Glyceraldehyde, glyceric acid, tartronic acid, mesoxalic acid, and oxidative degradation products glycolic acid, oxalic acid and formic acid are the main byproducts. Primary oxidation products are not yet commercially available in large quantities. To get some insights in the potential market, the price levels of selected derivatives in a typical chemical catalogue are given in figure 2.1. Clearly, there is an economic incentive to identify technology to produce these products starting from glycerol [1,3,8]. So in particular the liquid phase catalytic oxidation seems to be a promising route to the valorisation of glycerol by its conversion into useful compounds, provided that catalysts used are sufficiently active and selective for the formation of compounds such as glyceric acid (GLYCEA) and di-hydroxyacetone (DHA), potential useful as chemical intermediates in the fine chemicals industry, particularly in pharmaceuticals. However, the extensive functionalisation of the glycerol molecule, with similar reactive hydroxyl groups, renders its selective oxidation particularly difficult [5,6,12]. Nowadays a traditional way of synthesis exists to produce DHA: an incomplete microbial fermentation of glycerol by *Gluconobacter Oxydans* [1,4,47]. Although microbial fermentation process can provide high selectivity to DHA, there are some drawbacks, low productivity and high production cost. Moreover the market about this product is divided between no more than five

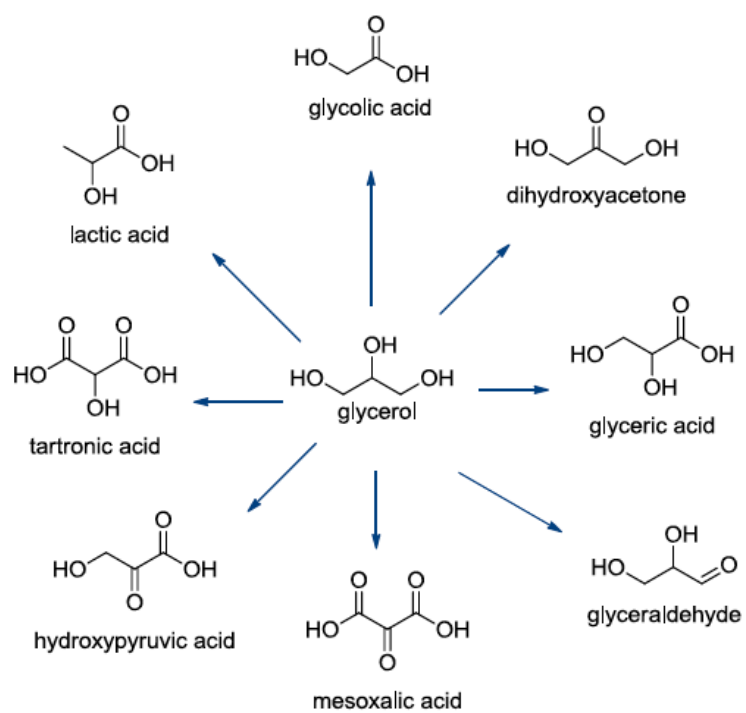


Figure 2.1: Chemicals from glycerol by oxidation (commercial price of glycerol and oxidation products - when available): glycerol refined = 0.74 Euro/kg , lactic acid = 1.2 Euro/kg, dihydroxyacetone = 15 Euro/kg)



companies and none of them use a catalytic oxidation reactions. For this reason, recently, a series of novel catalytic conversion processes are carried on. Given its high boiling point, the selective oxidation of glycerol with air or oxygen is normally carried out in the liquid phase using water as the solvent . There are many studies dealing with this topic and using different catalytic solution. It is possible to summarize them in:

- organometallic complexes as homogeneous catalysts in a bi-phase reactors [7]; it offers an high selectivity to DHA with the higher conversion than the other two catalytic systems
- supported noble metals nanoparticles as heterogeneous catalysts in a three-phase reactors [1,2,3,47]; the heterogeneous nature of the catalyst permits an its easier recovering at the end of the reaction
- some ideas concerning the electrocatalytic reactions [8], interesting because no wasterwaters or byproducts are produced

Every solution shows its peculiar advantages.

Concerning the heterogeneous catalysts an important Review was published in 2011 [4]. This Review summarized the most important results obtained on the selective oxidation of glycerol. The work highlight that the selectivity not only depends on the type of the active phase, but is also influenced by numerous parameters such as the metal particles size, the nature of the support and the pH of the reaction medium.

Among the various target compounds presented in this review there is a chapter dedicated to DHA. Finally about the electrocatalysis very few information were available in literature.

## **2.2 A catalytic conversion using an Organometallic complex**

### **2.2.1 The best results in literature**

One possible catalyst system for the selective oxidation of glycerol into DHA was an organometallic complex of Pd (Palladium Neocuproine) [44].

In an effort to develop highly active oxidation catalysts for potential use in low temperature fuel cells, the research group of prof. Robert M. Waymouth (Stanford University, USA) observed active catalysts system that suggested that appropriately ligated Pd(II) complexes can mediate selective oxidative transformation with air (or oxygen) as terminal oxydant. In particular, the Pd-catalyzed aerobic oxidation of alcohols to aldehydes and ketones.

Sigman and co-workers reported that the Pd N-heterocyclic carbene complex catalyzes the oxidation of alcohols at room temperature in air [44,63]. Since the first report of ligand-accelerated catalysis using Pd(OAc)<sub>2</sub> and

pyridine by Uemura and co-workers[64], a variety of ligands have been employed, including triethylamine [63,65], substituted phenantrolines [66,67,68], N-heterocyclic carbenes [64], and sterically encumbered pyridines[69,70]. While high attention has been given to the effect of ligand modulation on catalyst activity, there are only a few examples of effective catalyst systems that use Pd salts other than Pd(OAc)<sub>2</sub> [66,65]. Sigman and Jensen [71] attribute the success of acetate to its dual role as an anionic ligand and as a base for intramolecular deprotonation of the Pd-bound alcohol species. However, the use of *non-coordinating* ions to make cationic Pd(II) complexes with an open coordination site has also been shown the dramatic increase of the rate of aerobic oxidations. Moreover Waymouth and co-workers reported that cationic neocuproine palladium acetate complexes exhibit very fast initial rates of alcohol oxidation at room temperature in air but undergo competitive ligand oxidation from hydroperoxide intermediates generated from the partial reduction of O<sub>2</sub>.

On the basis of Sheldon's work that substituted (Neocuproine)Pd(OAc)<sub>2</sub> complexes to the Pd(OAc)<sub>2</sub>, that were active alcohol oxidation catalysts under 30 bar of air at 80°C, Waymouth and co-workers developed a synthetic route to obtain a cationic (Neocuproine)Pd(OAc)(OTf) complexes. They reasoned that a palladium(II) complex with both a basic, coordinating acetate ion and a non coordinating triflate counterion should yield a more active alcohol oxidation catalysts. These complexes were investigated for the catalytic oxidation of glycerol to DHA. The results obtained was very good (figure 2.3) even if problems on the catalyst decomposition (the general scheme is presented in figure 2.2 ) came out as confirmed by the works of Kevin Chung and Bradley A. Steinhoff [43]. These two works proposed two mechanistic studies on the catalyst decomposition mainly due to the formation of mirror Pd (Pd<sup>0</sup>), an inactivated form of Pd during the reaction. This reductive form of Pd results no more active, becoming a "black hole" for the catalyst: when decomposition (figure 2.2) starts, process results irreversible. The best results, in fact, were obtained using a large amount of catalyst (low values of molar ratio (MR)), equivalent to the ratio between the moles of substrate with the moles of catalyst), using DMSO or CH<sub>3</sub>CN as solvents and benzoquinone as terminal oxydant (figure 2.3).

The reaction time was another crucial parameter when the mild conditions were adopted. With the idea of a scale-up to an industrial application the research posed the accent on these critical aspects: solvents, time and oxydant agents. In this work the study of the Pd-Neocuproine organometallic catalyst was performed in order to get both a deepen understanding about the catalyst and meanwhile reaction improvement in a batch reactor.

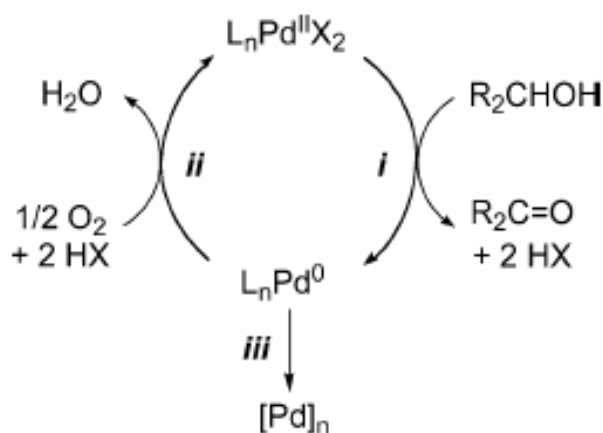


Figure 2.2: general mechanism of Palladium-Catalyzed alcohols oxidation

N°	Solvent	MR	Ox.	Time	z	s	y
[·]	[·]	[Gly/cat.]	[·]	[h]	[%]	[%]	[%]
1	CH <sub>3</sub> CN:H <sub>2</sub> O (10:1)	10	O <sub>2</sub>	4	95	/	69
5	CH <sub>3</sub> CN:H <sub>2</sub> O (10:1)	10	air	18	/	/	73
2	DMSO	20	air	24	47	80	/
3	CH <sub>3</sub> CN	20	benzoquinone	24	97	99	/
4	CH <sub>3</sub> CN:H <sub>2</sub> O (7:1)	20	benzoquinone	3	97	99	/

Figure 2.3: Catalytic oxidation of glycerol and 1,2-propanediol with Palladium neocuproine organometallic complex

### 2.2.2 The problem of the decomposition

For every work present in literature the organometallic catalyst presented decomposition problems during the oxidation.

This behavior is applied to Pd(OAc)<sub>2</sub> both for 2,9-methyl-1,10-phenantroline-Pd(OAc)<sub>2</sub> complexes. The precise mechanism of catalyst decomposition is not known; however, the formation of catalytically inactive palladium black during the reactions suggests that decomposition is associated with catalyst aggregation. Metal aggregation has been studied extensively in the context of colloid formation and nanoparticle synthesis, and both unimolecular (figure 1.2) and bimolecular pathways have been implicated in these processes [43]. By analogy, catalyst decomposition in the present reactions could oc-

cur via both unimolecular and bimolecular pathways. Decomposition pathways that might exhibit a unimolecular dependence on  $[\text{Pd}(\text{OAc})_2]$  include nucleation events associated with interactions between soluble Pd(0) and impurities in the solvent, the solvent itself, and/or the wall of the reaction vessel, for example. The most straightforward bimolecular decomposition mechanism is direct interaction of two Pd centers in a nucleation or particle-growth process. The kinetics of palladium decomposition (i.e., aggregation) have direct implications for catalyst performance. Oxidation of the catalyst should exhibit a first-order dependence on  $[\text{Pd}]$  (e.g., rate  $k_{ii}[\text{Pd}][\text{O}_2]$ ). If the catalyst decomposes via a unimolecular pathway, the first-order dependence of both catalytic turnover and catalyst decomposition (steps ii and iii, Scheme 1) results in a linear dependence of the turnover rate on  $[\text{Pd}]$ . Such trend was observed in the oxidation of the secondary alcohol. If decomposition proceeds via a bimolecular pathway, the decomposition rate will increase more rapidly than the catalytic rate at elevated  $[\text{Pd}]$ . Therefore, the rate exhibited a nonlinear dependence on the  $[\text{Pd}]$ . Such trend was observed in the oxidation of the primary alcohol. The origin of the differences between the catalyst decomposition pathways in reactions involving primary and secondary alcohols cannot be clearly discerned from the present study. Nevertheless, it is noteworthy that the catalyst decomposition pathway is substrate dependent. This observation may be related to the observation by Hiemstra and co-workers that colloidal palladium formed in Pd(OAc)<sub>2</sub>/DMSO-catalyzed oxidative heterocyclization of alkenes retains catalytic activity. In contrast, the aggregated palladium formed during alcohol oxidation is inactive. Bradley A. Steinhoff and Shannon S. Stahl proposed a study insights the catalyst decomposition pathways by evaluating the full timecourse of the reactions at different Pd(OAc)<sub>2</sub> concentrations.

$$\frac{d[\text{Gly}]_t}{dt} = k_i[\text{Gly}]_0[\text{Pd}] \quad (2.1)$$

$$[\text{Gly}]_t = [\text{Gly}]_0 e^{-k_i[\text{Pd}]t} \quad (2.2)$$

Where  $[\text{Gly}]_0$  is the initial glycerol concentration. Considering the catalyst decomposition during the course of the reaction, the concentration of active Pd catalyst decrease and the rate will decrease proportionately. The effect of catalyst decomposition on the rate was modeled by incorporating a time-dependent catalyst concentration term,  $[\text{Pd}]_t$ , into the original rate equation. The identity of this term depends on whether proceeds via unimolecular or bimolecular process(es). This treatment is elaborated for the unimolecular decomposition pathway(s) and in equations for the bimolecular pathway(s). This analysis yields three separate integrated rate laws that can be used to evaluate the experimental timecourse data. The rate law for unimolecular catalysts decomposition is expressed as follows:

$$\frac{d[\text{Pd}]_t}{dt} = k_{uni}[\text{Pd}]_0 \quad (2.3)$$

where  $[Pd]_0$  is the initial catalyst concentration. That incorporated to equation 1.1 gives:

$$[Gly]_t = [Gly]_0 e^{\frac{k_i [Pd]_0}{k_{uni}} (e^{-k_{uni} t} - 1)} \quad (2.4)$$

Bradley A. Steinhoff and Shannon S. Stahl proposed another one decomposition model. The rate law for bimolecular catalysts decomposition is expressed as follow:

$$\frac{d[Pd_t]}{dt} = k_{bi} [Pd]_0^2 \quad (2.5)$$

That incorporated to equation 1.1 gives:

$$[Gly]_t = [Gly]_0 (1 + k_{bi} [Pd]_0 t)^{\frac{k_i}{k_{bi}}} \quad (2.6)$$

A similar decomposition behavior appears in the work of Waymouth *et alii*. Despite the fast initial rates of alcohol oxidation with the complexes, the rates decrease rapidly with conversion, implicating that these catalysts are deactivated, even under mild conditions. Analysis conducted after 24 h from the start of the reaction revealed the presence of the cationic palladium carboxylate (structure 5 in figure 1.4), indicating that during the reaction one of the methyl groups of the neocuproine ligands is oxidized to the carboxylate. This complex was inactive as a catalyst. The formation of the inactive carboxylate complex during the course of the reaction implies that either oxygen degrades the ligand in competition with alcohol oxidation.

Even in this work the problem of the decomposition was observed. Moreover this phenomena resulted not dependent to the nature of the solvent (water and  $CH_3CN$  were investigated).

## 2.3 The noble metals catalysts

Efforts to improve productivity and selectivity have included use of heterogeneous catalysts in which a careful design is required to control the chemoselective orientation of the process. In the early 1990's, Kimura *et alii* [72] discovered that carbon supported platinum (Pt/C) had a weak activity in the catalytic oxidation of glycerol into DHA in acid media, which was confirmed later on by Garcia *et alii* in 1995 [73,74]. Nevertheless, the catalytic performance for unmodified Pt/C catalysts was limited, as the yield in DHA did not exceed 4%. Then, Kimura *et alii* focused on the optimization of Pt/C catalysts using promoters [74]. The best catalytic performance was observed when using bismuth as a promoter (Pt-Bi/C). For this type of catalyst, the highest yield in DHA (20%) was observed at a 5% (figure 1.3) platinum loading with a Bi/Pt ratio of 0.2. Further studies by Kimura *et alii* in the effect of promoters revealed that the addition of cerium leads to an increased catalytic activity. Pt-Bi-Ce/C catalysts, indeed, exhibit the

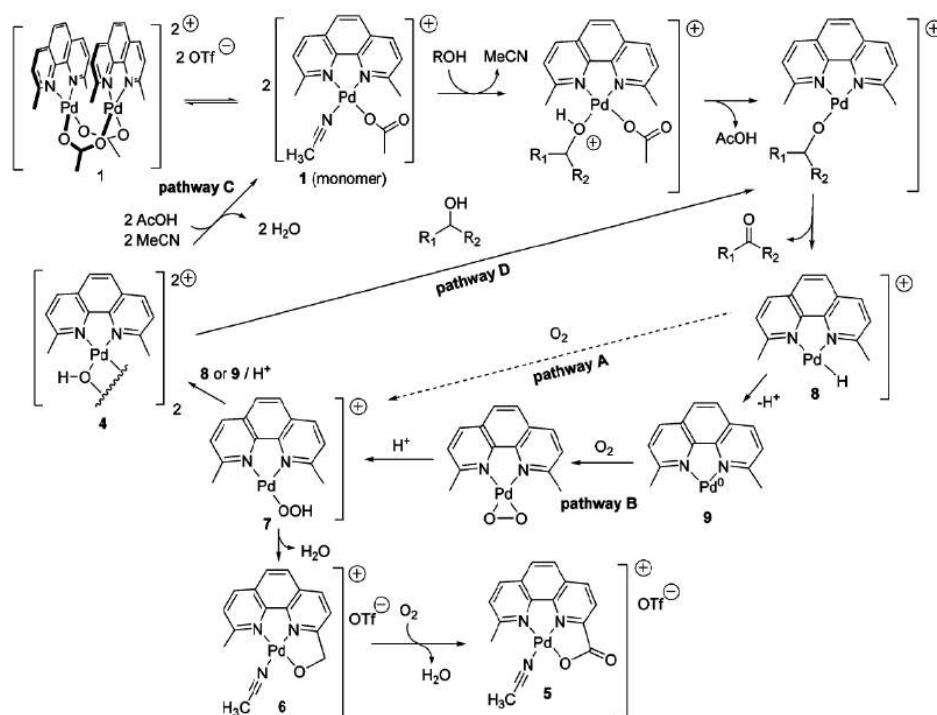


Figure 2.4: The proposed mechanism for aerobic alcohol oxidation from Waymouth and co-workers

same conversion as that of the Pt-Bi/C catalysts, but at the much lower reaction temperature of 0 °C *versus* 50 °C. With these optimized catalysts, a continuous synthesis of DHA was demonstrated using a trickle bed reactor. A maximum yield of 52.5 % was obtained. The authors also demonstrated the long-term performances of their catalysts over 1000 h, which is an important feature when targeting commercial applications.

Whereas Kimura *et alii* focused on the study of potential promoters, Garcia *et alii* achieved an increase in performances of non-ceria-doped Pt-Bi/C catalysts by optimizing both the reaction conditions and the activation method, whereby the yield in DHA could reach 28%. In 2010, Hu *et alii* gave a presentation on the catalytic synthesis of DHA using Pt-Bi/C catalysts. The bi-metallic catalysts were optimized in terms of Pt/Bi ratio, amount of metal and type of support. The optimum composition was 3%Pt-0.6%Bi on activated carbon. The optimum Pt and Bi loadings and Pt/Bi ratio were similar to those reported by Kimura *et alii* [75].

From the aforementioned results of Kimura, Garcia and Hu, it was obvious that the Pt/Bi ratio played an important role on the catalytic performances. Therefore, Brander *et alii* performed a thorough study by varying the Bi/Pt ration between 0 and 0.3 at a fixed Pt amount of 5% [76]. They found that the optimum ratio was around 1.0, which was remarkable as this value is five

times larger than the initially reported by Kimura. Kimura, in fact, found an optimum Bi/Pt ratio of no more than 0.2 [75]. Nowadays it is not totally clear why both groups found different optimal ratios, but when comparing the catalytic results and conditions, one can see the reaction temperature and oxygen pressure applied by Brandner *et alii* are significantly higher (120 °C versus 50 °C and 10 bar versus 1 bar) to obtain the same conversion as Kimura and co-workers.

Facing this discrepancy, Xie *et alii* also decided to study the effect of the Pt loading and of the Bi/Pt ratio on the DHA yield, as well as the effect of various preparation and activation methods for the Pt-Bi/C catalysts [77]. In contrast to the findings of Brandner and Kimura, they reported an even-higher optimum value for the Bi/Pt ratio of 1.8 for a yield in DHA of 33% at 1 wt% of platinum content [75,76]. In conclusion the Bi/Pt ratio has indeed an important impact on the catalytic results. The analyzed results are quite different between the different studies. Summarizing these data from literature it is possible to say:

- the glycerol conversion - and therefore the DHA yield - is proportional to the platinum content of the catalyst. In consequence, the highest conversion (82%) is observed for 9 wt% of platinum
- the selectivity to DHA was apparently independent of the Pt amount
- the doping with Bi increases the catalytic activity. Although the trend is less clear than for the impact of the amount of Pt, which might be the explanation for different optimum ratios reported by several researches
- like in the case of the amount of Pt, the selectivity to DHA seem unaffected when varying the Bi/Pt ratio

In figure 1.5 are summarized the results obtained with Bi-Pt/C catalysts used in a continuous batch reactor and a continuous fixed-bed one. Anyway it is important to underline how the stirred tank reactor was the Bracco's favourite technological solution for the glycerol conversion into DHA.

In 2007, a new generation of catalysts entered the scene. Claus *et alii* reported for the first time the synthesis of DHA by the catalytic oxidation of glycerol over carbon-supported gold nanoparticles with platinum as a promoter ( $Au_{0.8}Pt_{0.2}$ ) [78,79]. Among the numerous researchers who studied the catalytic oxidation of glycerol over Au-based catalysts, they were the first ones to succeed at synthesizing DHA. The oxidation was performed at atmospheric pressure in a basic media (pH=12), which is in direct contrast with the Bi-Pt catalysts that use acidic reaction conditions (pH 2-5)[72,77]. In the first attempt of using a Au/C catalyst, Claus *et alii* reported a yield of DHA only up to 6.6% [79]. However in 2009 Dimitratos *et alii* reported a

Support	$S_{\text{mer}}$ ( $\text{m}^2 \text{g}^{-1}$ )	Loading (wt%)			Reaction conditions				DHA (%)			Ref.	
		Pt	Bi	Bi/Pt mole ratio	$T/^\circ\text{C}$	$P$ (bar)	pH	$t$ (h)	GLY conv. (%)	Sel.	Yield		
Batch experiments													
Carborafin	1430	5	1	0.2	50	1	2-4	4	30	66	20	20	
CECAS05*	nc.	7.4	2.9	0.4	60	1	2	nc.	75	49	37	21	
		8.4	1.2	0.1	60	1	2	nc.	70	49	34	21	
nc.	1701	5	5	1.0	60	1	2	nc.	40	77	30	21	
		9	5	0.5	55	1	—	6-8	82	40	32	28	
		—	—	—	—	—	—	—	50	100	50	50	28
		7	4.5	0.6	55	1	—	6-8	58	46	27	28	
		5	5	0.9	55	1	—	6-8	57	38	22	28	
		5	1	0.2	55	1	—	6-8	46	38	18	28	
		3	5	1.6	55	1	—	6-8	51	37	19	28	
		3	0	0.0	55	1	—	6-8	15	37	6	28	
		1	5	0.2	55	1	—	6-8	33	32	10	28	
		5	5.4	1.0	100	1	4	nc.	59	51 <sup>b</sup>	—	26	
AC7	1224	4	2	0.5	70	7.9	—	—	—	—	24		
Aldrich	600	5	2	0.4	70	—	2	83	50	42	25		
		3	0.6	0.2	80	3.1	2	80	60	48	25		
Continuous experiments													
KL	1500	3	0.6	0.2	50	1	—	16.6 <sup>e</sup>	75	70	53	20	
WH2C	1200	3	0.6	0.2	50	1	—	7.1 <sup>e</sup>	—	—	14 <sup>d</sup>	20	
AC1	867	5	5.4	0.9	100	10 <sup>e</sup>	4	6.7 <sup>e</sup>	97-87	88-50	85-44	26	

nc.: not communicated. <sup>a</sup> Commercial catalyst. <sup>b</sup> At 20% conversion. <sup>c</sup> Calculated as 1/LHSV. <sup>d</sup> LHSV = 0.15 h<sup>-1</sup>. <sup>e</sup>  $P_{\text{O}_2}$  = 1 bar.

Figure 2.5: Catalytic results from literature about the bi metallic catalysts based on Pt-Bi

more efficient DHA synthesis over Au/C catalysts, using a continuous down-flow slurry bubble column reactor yielding 15% in DHA (53% of selectivity and 30% of conversion). In the later developments, the concept of Bi-Pt and gold-based catalysts were combined. Xie *et alii* reported that gold-doped Bi-Pt catalysts supported on active carbon (Au-Bi-Pt/C) exhibited interesting catalytic activity in the oxidation of glycerol to DHA [77]. The doping with gold resulted in a significantly higher selectivity to DHA (up to 64%), whereas the conversion did not surpass 40%. This low catalytic activity conversion might be due to the acidic reaction conditions, which are unfavourable for gold catalysts.

From the results observed over Bi/Pt (figure 2.6) and Au-doped Bi/Pt catalysts (figure 2.7), it was possible to figure out that the reaction mechanism that end up into DHA formation in basic and acidic media were completely different. Thus, doping of Bi/Pt catalysts with gold seemed to be not very promising in the oxidation of glycerol when targeting DHA. Indeed, in acidic media, which was generally used for Bi-Pt/C catalysts, DHA is formed by direct catalytic oxidation of the secondary hydroxyl group of glycerol (figure).

On the other hand, the reaction mechanism in basic conditions is based on the oxidation of a primary hydroxyl groups. The corresponding glycerldehyde (GLYA) is then trasformed into DHA by base-catalyzed interconversion. This reaction pathway was also reported in literature for the enzyme-catalysed bio-reaction [80]. Figure 2.5 summarizes results of catalytic oxidation of glycerol reported by several groups with different catalyst. Anyway recently, between 2011 and 2013, together with the results just presented another one solution with Au proposed interesting results. The



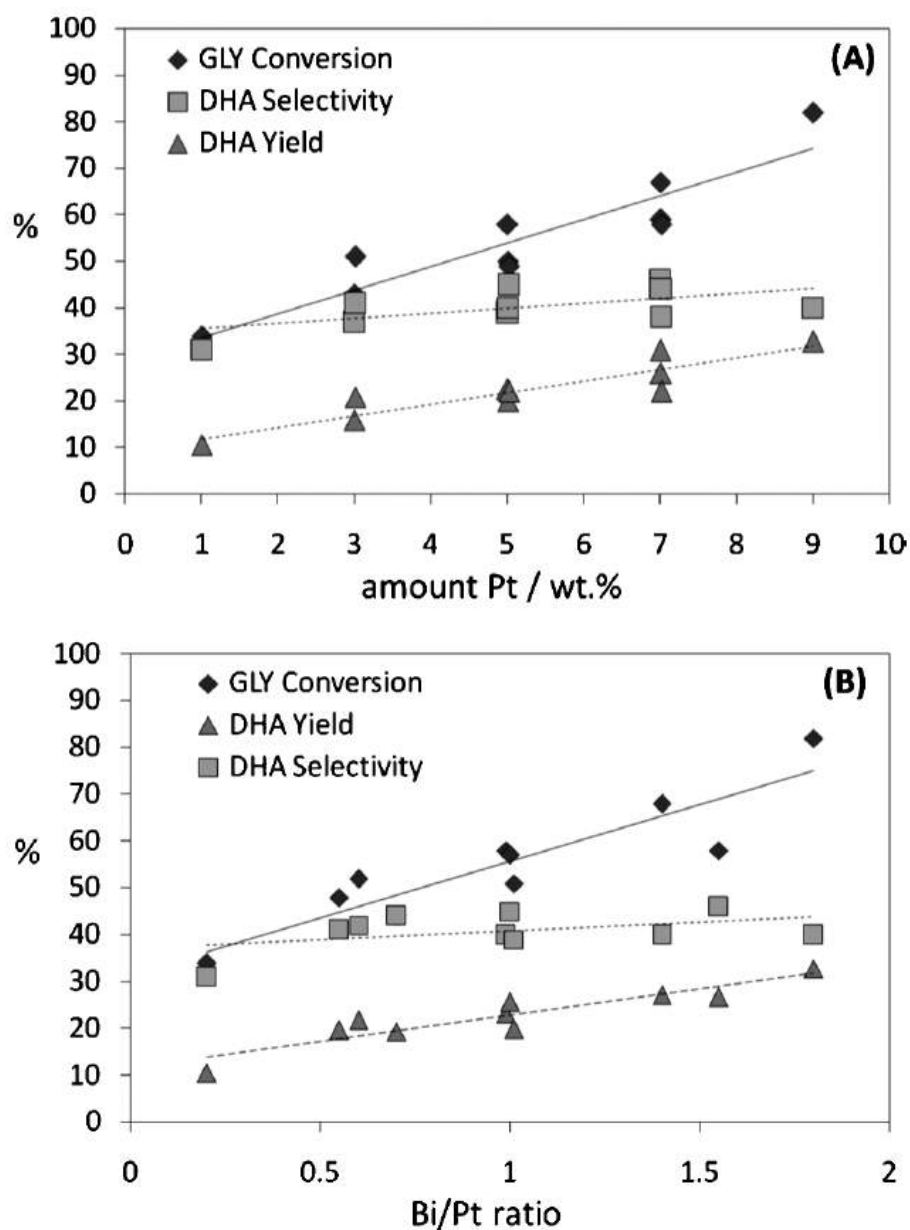


Figure 2.6: Effect of (A) the platinum loading (Bi/Pt ratio between 0.52-0.67) and (B) the Bi/Pt ratio on the activity of Bi-Pt/C catalysts (5 wt%) [4]

reaction found application as catalytic reaction in a stirrer tank reactor. Rodrigues *et alii* [1,2,5] between 2011 and 2012 published new results with gold structured on multi walled carbon nanotubes and on activated carbon to the selective oxidation of glycerol into DHA and GLYA respectively. Initially Rodrigues proposed gold nanoparticles on activated carbon for the glycerol de-protonation obtaining interesting results about the selective ox-

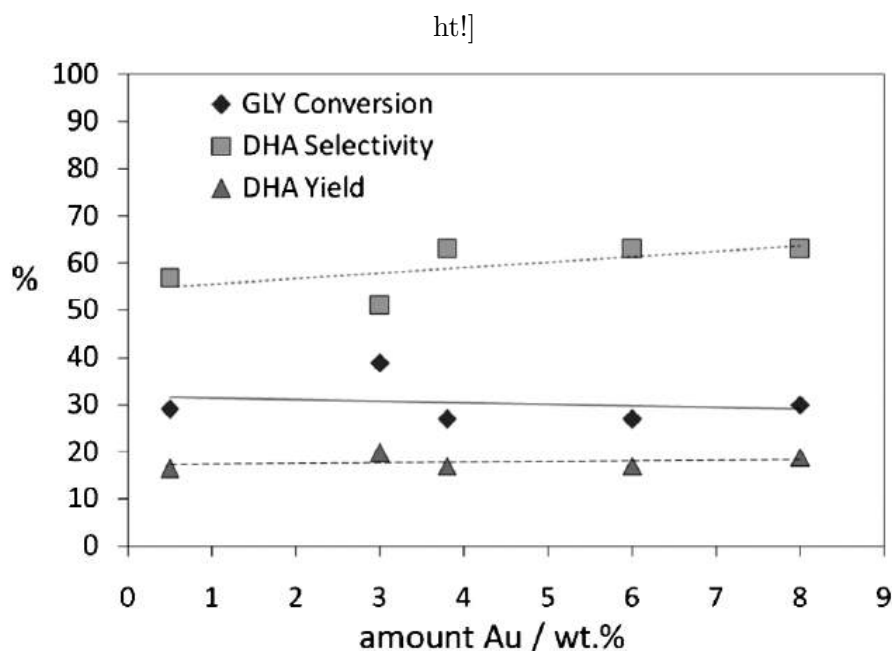


Figure 2.7: Effect of Au loading on the activity of Bi-Pt/C catalysts (3 wt%Pt, Bi/Pt ratio 0.5) [4]

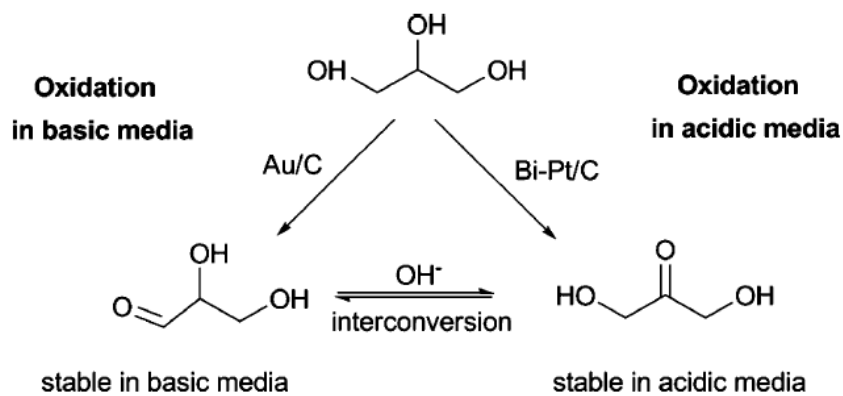


Figure 2.8: The two routes to DHA by the catalytic oxidation of glycerol [4]

oxidation to GLYCEA [5]. So using activated carbon as support for Au, Rodrigues and co-workers observed the formation of large amount of glyceric acid and a small amount of DHA. Later, in 2012, the same group presented a job about the selective oxidation to DHA. The multi-walled carbon nanotubes (MWCNTs) were used as support and the results obtained were different from that ones with activated carbon. The use of multi-walled carbon nanotubes as support for Au nanoparticles results in the preferential

Catalysts	Oxidants	pH	Other reaction conditions	Glycerol conversion	Selectivity or yield	Researchers and year	Ref.
Pt/charcoal	air (0.1 MPa)	2-4	10% GLY, 323 K, 4 h	37%	4% (Y <sub>DHA</sub> ) <sup>b</sup>	Kimura, 1993	35,36
Bi-Pt charcoal	air (0.1 MPa)	2-4	10% GLY, 323 K, 4 h	30%	20% (Y <sub>DHA</sub> )	Kimura, 1993	35,36
Pt-Bi/charcoal <sup>a</sup>	air (0.1 MPa)	—	50% GLY, 323 K, O <sub>2</sub> /GLY = 2 (mol/mol)	80%	80% (S <sub>DHA</sub> )	Kimura, 1993	35,36
5% Pd/C	air (0.1 MPa)	11	10% GLY 333 K, 30% NaOH, 5 h	100%	8% (S <sub>DHA</sub> ), 70% (S <sub>GLYAC</sub> )	Garcia <i>et al.</i> , 1995	37
Bi-Pt/C	air (0.1 MPa)	2	10% GLY, 333 K, 5 h	75%	50% (S <sub>DHA</sub> )	Garcia <i>et al.</i> , 1995	37
5%Bi-5%Pt/C	O <sub>2</sub> (0.02 MPa)	5.5	8 mmol GLY/60 ml H <sub>2</sub> O, 338 K, 3 h	—	25% (Y <sub>DHA</sub> ), 20% (Y <sub>HYPAC</sub> )	Abbadì <i>et al.</i> , 1996	40
Ti-Si co-gel	H <sub>2</sub> O <sub>2</sub> (10% w/v)	7	10 g GLY, 353 K, 24 h	22%	37% (S <sub>GLYALD</sub> )	McMorn <i>et al.</i> , 1999	68
1%Au/charcoal	O <sub>2</sub> (0.3 MPa)	basic	12 mmol GLY/20 ml H <sub>2</sub> O 333 K, 3 h, 12 mmol NaOH	56%	100% (S <sub>GLYAC</sub> )	Carretin <i>et al.</i> , 2002	54
5%Pt/C	Air (0.1 MPa)	11	1 M GLY, 333 K, 21 h, 30% NaOH	60%	47.5% (S <sub>GLYAC</sub> )	Carretin <i>et al.</i> , 2003	55
1% Au/C	O <sub>2</sub> (0.3 MPa)	basic	0.3 M GLY, NaOH/GLY = 4 (mol/mol), 303 K, 20 h	100%	92% (S <sub>GLYAC</sub> )	Porta <i>et al.</i> , 2004	57
1% Pd/graphite	O <sub>2</sub> (0.3 MPa)	basic	0.3 M GLY, NaOH/GLY = 4 (mol/mol), 50 °C, 1 h	90%	62.4% (S <sub>GLYAC</sub> )	Dimitratos <i>et al.</i> , 2005	58,60
1% (Pd + Au)/graphite	O <sub>2</sub> (0.3 MPa)	basic	0.3 M GLY, NaOH/GLY = 4 (mol/mol), 323 K, 2 h	100%	39.1% (S <sub>GLYAC</sub> )	Dimitratos <i>et al.</i> , 2005	58,60
1% (Au@Pd)/graphite	O <sub>2</sub> (0.3 MPa)	basic	0.3 M GLY, NaOH/GLY = 4 (mol/mol), 323 K, 2 h	100%	45.5% (S <sub>GLYAC</sub> )	Dimitratos <i>et al.</i> , 2005	58,60
1% Pt/C	O <sub>2</sub> (0.3 MPa)	basic	0.3 M GLY, NaOH/GLY = 4 (mol/mol), 50 °C, 4 h	81.6%	50% (S <sub>GLYAC</sub> )	Dimitratos <i>et al.</i> , 2006	61
1%(Au + Pt)/C	O <sub>2</sub> (0.3 MPa)	basic	0.3 M GLY, NaOH/GLY = 4 (mol/mol), 323 K, 4 h	69.3%	58.3% (S <sub>GLYAC</sub> )	Dimitratos <i>et al.</i> , 2006	61
Au/C	O <sub>2</sub> (0.1 MPa)	12	1.5 M GLY, NaOH/GLY = 2 (mol/mol), 333 K, 3 h	30%	75% (S <sub>GLYAC</sub> )	Dimirel, 2005	63
Au/C	O <sub>2</sub> (0.1 MPa)	12	1.5 M GLY, NaOH/GLY = 2 (mol/mol), 333 K, 1.5 h	50%	26% (Y <sub>DHA</sub> ), 44% (Y <sub>HYPAC</sub> )	Dimirel <i>et al.</i> , 2007	63
Au-Pt/C	O <sub>2</sub> (0.1 MPa)	12	1.5 M GLY, NaOH/GLY = 2 (mol/mol), 333 K, 1.5 h	50%	36% (Y <sub>DHA</sub> ), 30% (Y <sub>HYPAC</sub> )	Dimirel <i>et al.</i> , 2007	63

<sup>a</sup> Fixed bed reactor. <sup>b</sup> Selectivity to the product given in parentheses.

hetecat.png

Figure 2.9: Some typical results of catalytic oxidation of glycerol investigated by several groups

chemoselective orientation of glycerol oxidation towards the reaction of the secondary alcohol hermorefunction. Treating with the glycerol, indeed, the main oxidation product was DHA. The role played by the support resulted fundamental. The results obtained by Rodrigues using Au were the best ones obtained in the last twenty years for the selective oxidation of glycerol to DHA [1,2]. Thanks to these results the work of Rodrigues was presented in a review published in 2013 about the selective oxidation of glycerol [53]. In this review the solution of Au on MWCNTs was presented as the best promising route to the valorisation of glycerol by its selective oxidation to DHA. For this reason our attention was posed on these results.

Later in the 2013 the same research group published an *errata corrige* [54] about the published results. In this publication Rodrigues declared that the HPLC method used for the anlysis was not good for the detection of the DHA. The DHA observed was actually formi-acid, a product of third oxidation of glycerol. No presence of DHA was actually detected.

The wrong results presented by Rodrigues suggested to abandon the mono-metallic solution. The results from the experiments conducted with similar catalysts and synthetized in our laboratories confirmed the no selectivity of these catalysts to DHA.

Furthermore for the samples analysis a GC-FID method was developed at the CRB laboratories.

In this work the choices of the Au/C and Au/MWCNTs as heterogeneous catalysts were the first catalyst systems studied. After the publication of the *errata corrige* the attention moved on the bi-metallic catalysts: thanks

to the results on the selective oxyation into DHA. Even if the conversion and selectivity levels were lower respect to the ones proposed by Rodrigues, they seemed to be reliable.

The research moved on the direction to improve the glycerol conversion level and the DHA yield starting from the good results just discussed.

### **2.3.1 The important parameters for the performances of the catalysts**

The oxidation of the glycerol depends on the choice of the catalyst and on the reaction conditions. Anyway there were other parameters that have been indentified as having an important impact on the catalytic performances, such as the size of the metal particles, the nature of the support and finally the pH of the reaction medium.

#### **The particle size**

Platinum has been just described as highly active for the oxidation of polyols in the liquid phase. To study the influence of the particle size on the catalytic performances, Liang *et alii* prepared a series of carbon-supported platinum catalysts with particle sizes ranging from 1.2 to 26.5 nm [81]. From their results it is possible to see that the activity was increased for particle sizes of less 6 nm. On the other hand when the particle size was larger than 6 nm, the catalytic activity dropped, which was ascribed to the lower metallic surface area.

Using a colloidal deposition method, Prati and co-workers tuned the particles size from 2 nm to 16 nm [82].

Also the gold-based catalysts were found highly active in the oxidation of diols. Moreover, compared to platinum-based catalysts, gold appears to be more resistant to oxygen poisoning [83]. Due to this higher resistance, the reaction can be performed with higher oxygen partial pressures, which results in higher activity and selectivity.

In some of their studies, Carrettin *et alii* focused on the influence of the gold particles' size. When they changed the particle size from 25 to 50 nm, at iso-quantity of gold, the conversion decreased to 0.

At the same time, Prati and Porta also performed studies on the influence of the particle size on the catalytic performances over carbon-supported gold nano-particles in the range of 6 nm to 20 nm [87]. At a constant gold loading, they found that the small size particles, 6 nm, showed an about 10 times higher activity. Obviously this behavior can be associated to the higher surface exposition of the metal when using small size particle, which results in higher activity. Moreover, they also found that the selectivity was influenced by the particle size. Indeed when lowering the particle size, the amount of gold particle edges increases, and the latter are claimed to be

active centres for oxygen activation.

These results were also confirmed by Demirel *et alii* [88]. They showed that catalysts with smaller gold particles were more active than bigger ones (ranging from 2.7 nm to 42 nm). Moreover they showed how the catalysts with larger gold nano-particles showed increased selectivity to less oxidized products such as DHA.

Finally even though various studies have demonstrated the influence of the gold particle size on the catalytic performances in the reaction of oxidation of glycerol, it seems that there was no general consensus about the mechanism. Nevertheless, it is possible to conclude as follows:

- the catalytic activity of the gold catalysts is proportional to the amount of active phase
- small gold particles exhibit higher catalytic activity which is ascribed to the increased number of edges that are claimed to be the active centres
- the selectivity is not always correlated to the nature and the size of the nanoparticles: discussion are still on-going concerning this point

### **The effect of the support**

From the literature it is possible to enhance the importance of the support. Nowadays, most of the catalysts for glycerol oxidation use carbon-type compounds as supports which are well recognized in industrial chemistry for being stable in acidic and basic conditions. Furthermore, this kind of support offer the possibility of an easy recovery of metals by burning off the support. It was also reported that carbon enables conservation of the size and the morphology of deposited gold particles during liquid phase oxidation in water solutions.

The group of Claus and co-workers studied the influence of the carbon support on the catalytic performances in liquid phase glycerol oxidation [79,87,89]. By analysing the preparation of gold catalysts on various active carbon supports, they found a correlation between the pore size distribution of the support and the catalytic activity. A high ratio of micropores resulted in an increased activity.

Gao *et alii* [90] studied the use of multi-wall carbon nanotubes (MWCNTs) as catalyst supports. They found the MWCNTs-supported platinum (for example) catalyst gave a significantly higher conversion than that the active carbon-supported on (70.1% versus 46.7%) with a similar selectivity. The increased activity over MWCNTs-supported platinum was ascribed to the facilitated accessibility of the reactants (glycerol and oxygen) to the metals. Electron microscopy evidenced that the platinum particles were located outside the nanotubes, whereas the impregnation on the active carbon led

to the incorporation of the metal particles inside the network.

Liang *et alii* focused on the influence of the pre-treatment of active carbon on the catalytic performances of platinum. In this study the nitric acid and the hydrogen peroxide were used as pre-treating agent, and they found that the latter resulted in increased surface area, pore volume and metal nanoparticles distribution compared to the non-treated support. This functionalisation were found to be favourable for the catalytic performances in the oxidation of glycerol [85]. This result suggested to use the functionalisation as a favourable pre-treatment for every supports.

### The effect of the pH

Together with the support the pH of the reaction and the type of the catalyst influence the glycerol oxidation. It is generally admitted that the glycerol oxidation occurs in acidic or basic pH conditions when using Pt or Pd, while the activity of gold is exclusively limited to basic media.

In 1997, Galezot and co-workers studied the catalytic activity of carbon-supported platinum catalysts at pH 6 and 12. They found that the catalyst was significantly less active when used in acidic conditions. The initial glycerol specific conversion rate was calculated at  $40 \text{ h}^{-1}$  at pH 6, whereas it reached  $110 \text{ h}^{-1}$  at pH 12. Unfortunately, the authors did not give selectivity of the different products, but the overall yield of the identified products (GLYA, DHA and tartronic acid) was 35% in the acidic conditions and 70% in the basic ones. The oxidation of glycerol using carbon-supported platinum in acidic media was also studied by Kimura [75], Liang [85] and Villa [91]. While Kimura reported low activity for this catalyst, Liang and Villa claimed a 50% and a 78% conversion respectively. Indeed, it is difficult to clearly cross-evaluate the catalytic results, as the reaction conditions are too different. Nevertheless, all the authors report an important selectivity to C1 compounds, namely carbon dioxide and formic acid. To highlight the impact of the pH, Garcia *et alii* [73] chose carbon supported platinum (5%Pt/C) as a catalyst. As expected, the initial rates of glycerol oxidation are pH dependent, whereby the highest reaction rate ( $375 \text{ mmol h}^{-1} \text{ mmol}^{-1}$ ) was reported for neutral media. In terms of selectivity, GLYA was identified as the main product as in the case of palladium catalysts. Nevertheless, the yield in GLYA decreased (70% versus 55%) whereas that of DHA increased (8% versus 12%). No explanation was formulated for explaining the observed products selectivities. Fordham *et alii* studied the oxidation of glycerol but using a catalyst with a high loading of platinum (7 wt% Pt/C). They reported an increase in the tartronic acid yield at higher pH, whereas formation of DHA was limited to neutral or acid conditions, which is in good agreement with the work of Garcia *et alii*. Very similar results were reported by Carretin *et alii* [84-86]. After 3 h of reaction with 5 wt% Pt/C

at 60 °C, the glycerol conversion increased from 27% to 56% with the increase of the NaOH/glycerol molar ratio from 0 to 2. At the same time, the selectivity to GLYA increased from 28% to 69%. Moreover, the use of different metal hydroxides dramatically changed the catalyst activity. For the same reaction conditions, the glycerol conversion decreased in the sequence: NaOH (63.1%) , CsOH (52%), LiOH (48.9%), RbOH (37%), KOH(35.4%). On the other hand, a correlation with the change in selectivity was not so obvious, as the highest (87%) and the lowest (13.7%) selectivities to GLYA were recorded for KOH and RbOH, respectively. Nevertheless, a systematic study of the impact of the pH on the catalytic activity and selectivity of platinum based catalyst is still missing.

The research on gold-based catalysts for the oxidation of glycerol has dramatically increased in the recent years. As previously mentioned, the use of gold as a catalyst limits the reaction conditions to basic media, where sodium hydroxide is generally the first choice. The basic conditions are supposed to favour the initial hydrogen abstraction from the hydroxyl groups, which is the first reaction step of the oxidation mechanism. This “activation” of the -OH group is claimed to be impossible for gold catalysts alone. In that case, the main product, with a yield of up to 90%, is always the sodium salt of GLYA. Nevertheless, Carretin *et alii* reported the influence of the NaOH/glycerol ratio and claimed that an increased ratio leads to a decreased formation of the tartronic acid but an increased formation of GLYA. Recently, Prati *et alii* and Villa *et alii* [92,93] published about glycerol oxidation using gold-based catalysts in a base-free medium. By increasing the reaction temperature to 80°C, they obtained up to 10% of conversion of glycerol after 6 h of reaction using a 1 wt% Au/C catalyst. The main products were formic acid and carbon dioxide, which is a result completely different than the tests using basic media, where the main product is generally GLYA. Furthermore, traces of hydroxypyruvic acid were detected, which is a product that was never claimed when the reaction was performed in basic media. Therefore, one can assume a drastic change in term of reaction mechanism when a base-free medium is used. In this case, the first step for the oxidation process might be a hydride abstraction with the formation of a hydrogen-gold species as proposed by Villa *et alii* and Prati *et alii*. This species may be then oxidized by molecular oxygen (O<sub>2</sub>) leading to the formation of hydrogen peroxide (H<sub>2</sub>O<sub>2</sub>), which is, as already mentioned, well known to promote the C–C cleavage leading to C1 compounds.

## 2.4 The electrocatalysis

The electrocatalyst system [8] it is a clean and direct conversion of glycerol into DHA by anodic oxidation in the presence of catalytic TEMPO. The general reaction scheme for electrochemical alcohol oxidation mediated by

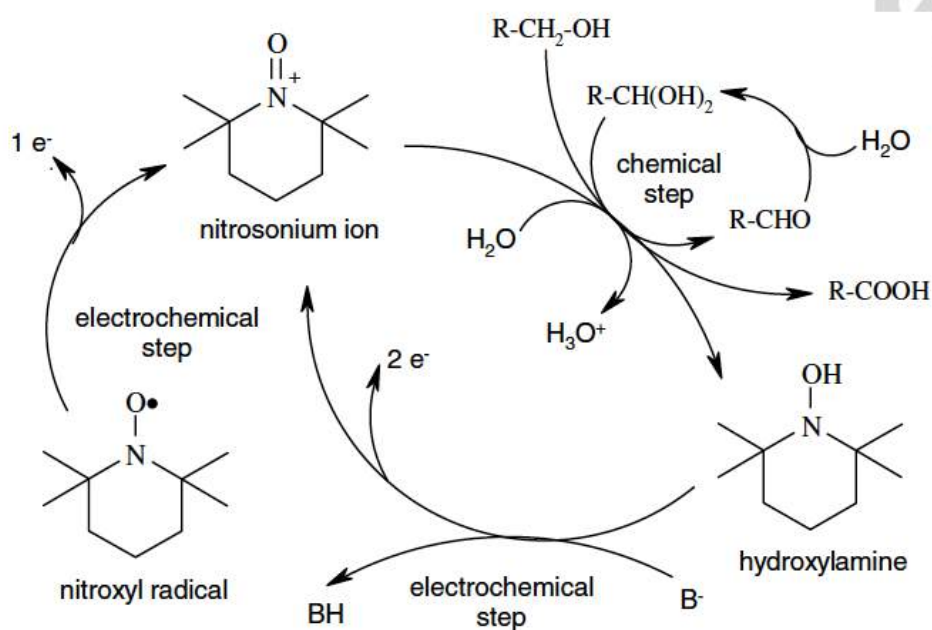


Figure 2.10: General reaction scheme for electrochemical alcohol oxidation mediated by TEMPO

TEMPO is proposed in figure 1.10 [8]. The entire process gives yields (25%) that are comparable to that of the cumbersome biotechnological process actually used in industry. Moreover the radical TEMPO can be entirely recovered at the end of the reaction [8]. So with a simple one-pot, waste-free oxidation of glycerol to DHA at the anode can be achieved by simply applying a small electric potential (1.1 V with Ag/AgCl) to a glycerol solution (0.05 m) in water buffered with bicarbonate (0.2 M) at pH 9.1 in the presence of 15 mol% TEMPO: after 24 h, a yield of 25% was obtained. It is important to put in evidence how Ciriminna and co-workers underlined that extending the reaction time causes over-oxidation of DHA and an increase in amount of hydroxypyruvic acid (HYPAC).

No reaction was observed in the absence of added TEMPO. Similar pronounced alteration in the selectivity of electrocatalytic oxidation of alcohols mediated by TEMPO was recently reported [8].

Anyway this solution was only recently introduced and not many information were present in literature to plan a scale-up. Moreover even if with a selectivity of 99.9%, a low value of conversion is reliable (25%) after 24 hours, that it is no good for an industrial application. For both reasons we did not see an industrial application for this approach.



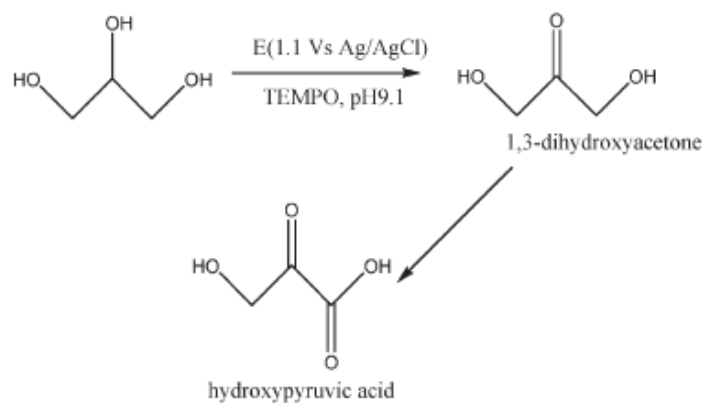


*Figure 2.11:* Electrochemical oxidation of glycerol mediated by TEMPO in water affords DHA and, after longer reaction times, HYPAC

## 2.5 Analytical methods

Studying the literature related to the selective catalytic oxidation of glycerol it was not trivial to find a detailed analytical method to identify the oxidation by-products.

For this reason an important part of my work was dedicated to an analytical method development. In chapter 4 are described the analytical methods developed.

The importance to have a performed analytical method

---

---

## CHAPTER 3

---

### A PRELIMINARY STUDY

A preliminary proof of concept study was performed in order to understand economical benefits of such a research.

Research protocol was prepared after a literature review.

The economical evaluation taking into account the following parameters:

- total amount of DHA required per year, 500 tons
- total hours of work per year: 7500 (or 313 days)
- DHA price (purity  $\geq$  94%): 15 Euro/kg
- glycerol price: 0.8 Euro/kg
- cost per year for the direct supply of the DHA: 7.500.000,00 Euro
- utilisation of stirrer tank reactor

was analyzed three catalytical reactions analyzed were:

- an heterogeneous catalyst using gold nano-particles based on carboni-  
uos supports [1,2]
- an homogeneous catalyst; with an organometallic one based on Pd [4]
- an electrocatalytic reaction [8]

The bi-metallic catalyst proposed was intially ignored because the yield in DHA was not higher such as the yield obtained using Au/C catalysts.

Even if each of these three approaches presented some adavantages only two of them were developed and studied. Heterogeneous catalyst using metal nano-particles based on carboniuous supports and homogeneous solution with an organometallic one using the Pd as metal.

The Au nanoparticles based on carbon offered a catalyst with a long life. The Au nano-particles have a longer life in a strong oxydant environment [1].

The second solution seemed to have the highest level of conversion and selectivity. On the other hand the life of these catalysts is not well known and not many information were available.

The third approach was the most eco-friendly. Using only the catalyst and water (as main solvent) to obtain an extremely pure product. Anyway the conversion level (only 25% after a reaction 24 hours long) was too low to have an industrial application.

In the international literature, all of these three solution offered possibility to work in mild conditions: low temperature, no higher than 60 °C, and at low oxygen pressure (3 to 10 bar). Moreover for each solution the reaction time was lower than the traditional organical way of synthesis, about three-four hours versus more than 24 hours.

Starting from these considerations a preliminary study was conducted.

The choice was made considering the amount of DHA requested by Bracco S.p.A. per year. About 500 tons/year is the current consumption of DHA with a cost of 7.500.000,00 Euro. The main goal at this step was to propose a new solution, reducing the current cost and in order to obtain the DHA directly from the glycerol de-protonation.

Comparing the cost of the glycerol as starting material, the first analysis was computation curve gain on cost (figure 3.1). The yield, as a product of conversion time selectivity, was also estimated with an exponential behavior. It could be worth to remember that at this step the curve of yield was based on the data from others published studies used as starting point for the research. Anyway, even if the solution seems to be simple, many problems come out from this reaction. Better solution is the one that offer the highest level on yield but considering the costs of the catalysts and its medium life (and eventually the necessity to regenerate it). Moreover the costs related to the entire reactions were also important.

To have a general idea it was necessary to make a list of the main aspects were taken into account:

- The reaction volumes
- The separations of the products: DHA is only one of the possible numerous products of reaction (see the introductive chapter)
- The separation of the catalysts for a new reaction [10,11,12,13]
- The waste treatments
- The purification of the products (an high purity was necessary to employ the product in the subsequent reactions)

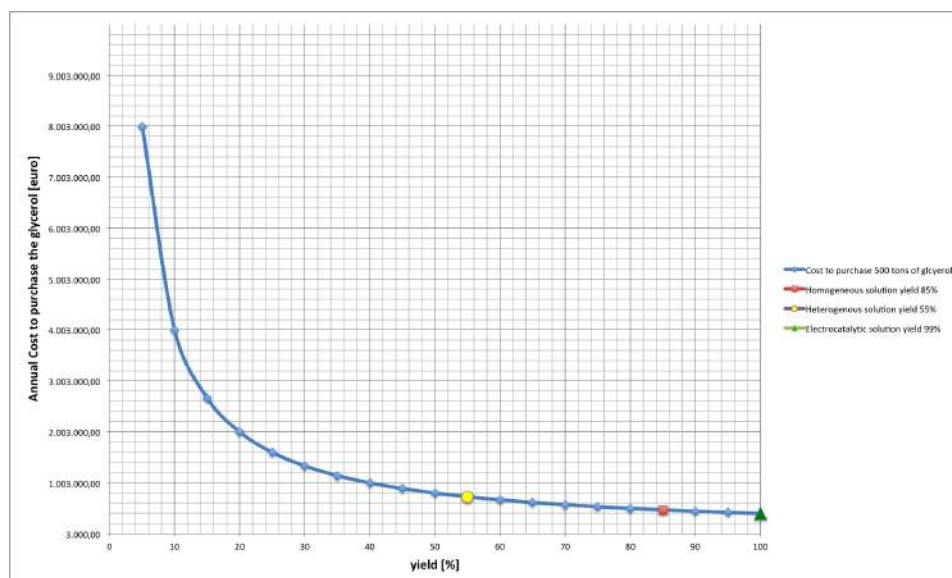


Figure 3.1: Curve gain on cost; in accord with the results obtained from literature, with the yellow mark the cost compared with the yield following the heterogeneous catalysts, while with the red mark the cost related to the homogeneous solution; the green triangle is related to the electrocatalytic results

In the next sections the three solutions will be deeply described taking into account every aspect presented.

### 3.1 The electrocatalytic reaction

At the beginning of the study the electrocatalysis way for the glycerol oxydation was considered the most interesting. Due to the high level of selectivity, the electrocatalysis gave the possibility to obtain a very pure product and working only with water as main solvent. It tooks in account the utilisation of a main reactor, equipped with two electrodes. The catalyst, presented in solution with  $\text{NaHCO}_3$ , is a commercial one, the (2,2,6,6-Tetramethylpiperidin-1-yl)oxyl, commonly named TEMPO (figure 3.2). This catalyst

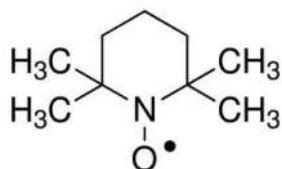


Figure 3.2: The catalyst TEMPO

is oxydized at the anod and, once in solution, and it is active for the deprotonation of the glycerol to form DHA. The reaction scheme is summarized

in figure (3.3). At the cathod the catalyst reduced itself to be ready for a

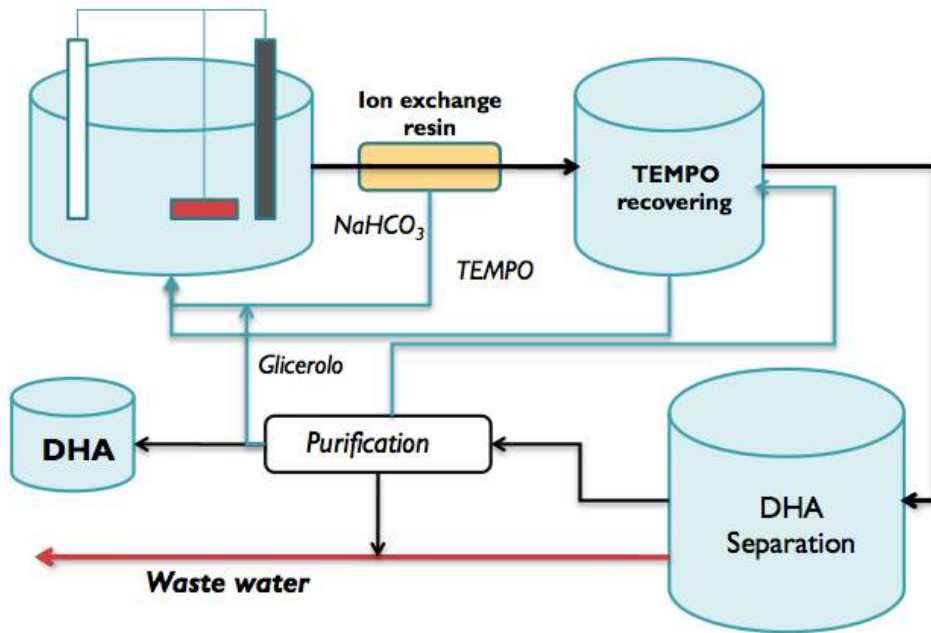


Figure 3.3: The electrocatalytic reaction scheme

new de-protonation. A simplified reactor scheme is presented in figure 3.4. The calculus was made in accord with the data obtained from literature

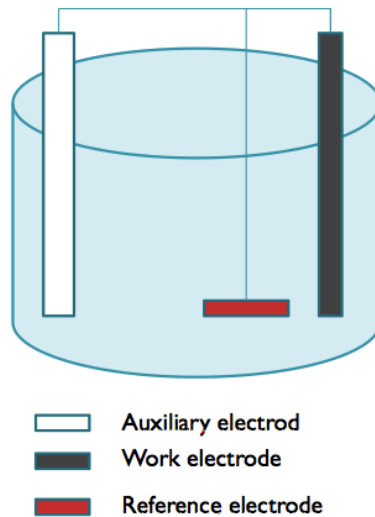


Figure 3.4: The electrocatalytic reactor scheme

[8]. In order to obtain the amount of DHA required, 500 tons per year, a

reactor of 1400  $m^3$  was retained necessary. Working in  $\text{NaHCO}_3$  solution 0.2 M, with TEMPO (7.5 mM) and glycerol 0.05 M, a retention time of 20 h is required to obtain the product. The yield evaluated is equal to 25% with a selectivity near to 99.9%. On the other hand, even considering this high selectivity, the conversion resulted to be too low and not good for an industrial application. Anyway this solution showed many advantages:

- purity of the final product (no problems related to separation)
- absence of byproducts could offer the possibility to think about a periodical taking of the solution with a following crystallization: the possibility to work without stop
- no byproducts and re-circulation of the solvent allow a low production of waste-water

Anyway the possibility to take into account the electrocatalysis presented other problems. The first problem was the operative concentration of glycerol. Thinking to an industrial application, it was necessary to take into account possibility to work with a higher glycerol concentration in order to reduce cost of the plant. The concentration modification clearly influenced the reaction: modification on the ohmic resistance of the solution with a consecutive influence on the energetic cost to bring forward the reaction, the reaction yield and, eventually, modification on the reaction pathway and technological problems linked to the reactor design. Because impossibility to make prevision about this problem the only possible solution was to start with an experimental campaign to define the unknown (or unclear) specific aspects related to this electrochemical solution.

Another similar problem was the behavior of the catalyst TEMPO after every cycle: any poisoning or deactivation occurs? What was the medium life of the catalyst at different conditions? Even in this case non data from literature were available.

Working between the glycerol concentration used from Ciriminna and co-workers [8] and the solubility limit of glycerol in water, separating DHA from glycerol not reacted, an high volumes of water must be evaporate, with a consumption of energy variable from 4300 kW to 830 kW (the variability is function of the concentration level of glycerol in water) to evaporate the total initial solution at each batch. In order to avoid the evaporation step (cause the thermolability problems of the products), due to a big volumes, a fractional crystallization was considered as a good solution working with a mix of water and ethanol.

The test was not brought forward cause the electrocatalyst system was not considered suitable from Bracco S.p.A. Too many open problems caused the rejection of the electrocatalysis as possible approach. The company did not consider interesting to explore the research anymore. Finally the economical evaluation for this solution was not computed even if, maybe in the

future, this solution could be an interesting research field.

## 3.2 The organometallic catalyst solution

Other ways tested for the selective glycerol oxydation into DHA were analyzed in details. Studying the solution with the organometallic catalyst some aspects became evident:

- referring to literature's experiments the possibility to work with a higher concentration of glycerol
- an high level of conversion for the catalyst based on Pd with levels of selectivity higher than 96%
- difficulties to separate the catalyst from the solution when the reaction is overcome: this problem is mainly due to the fact that the catalyst works in a homogeneous phase
- no information about the life cycle of the catalyst
- always referring on the literature information the volumes used for the reaction resulted very big: in order to study the scale-up of the reaction become necessary to think to work with different volumes
- the fractional crystallization was not taken into account due to the fact that, differently from the electrocatalyst system, some byproducts could be present
- the time for the reaction was estimated equal to 3h30', 1 to 6 respect the other solution: the reaction is fast and then became possible to consider more than one cycle per day

Anyway major problems were volume of reaction and formation of mirror Pd, a no active form of Pd, during the reaction.

Concerning the volume one of the main goal was to test the possibility to work with more concentrated solutions. Always referring to the literature data, the amount of energy required to evaporate the total solution was estimated equal to  $2.45 \cdot 10^4$  kW per cycle.

Even in this case it was possible to make a scheme of the reaction (figure 3.5).

Focusing on the batch reactor (figure 3.6) it is possible to have an idea about how the reactor works. From the scheme in figure 3.6 it is possible to estimate the volume of the reactor. There is the possibility to reduce the dimension varying the concentration of glycerol: a parameter not evaluated in the reference papers [1]. Finally the theoretical possibility to work with

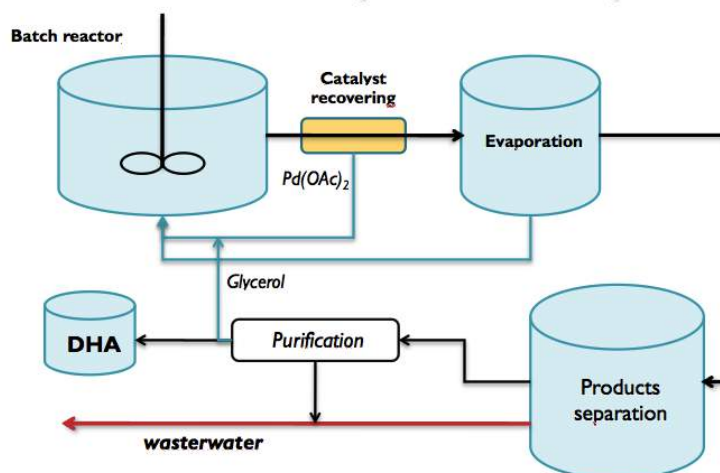


Figure 3.5: The reaction scheme for the solution with the organometallic catalyst based on Pd

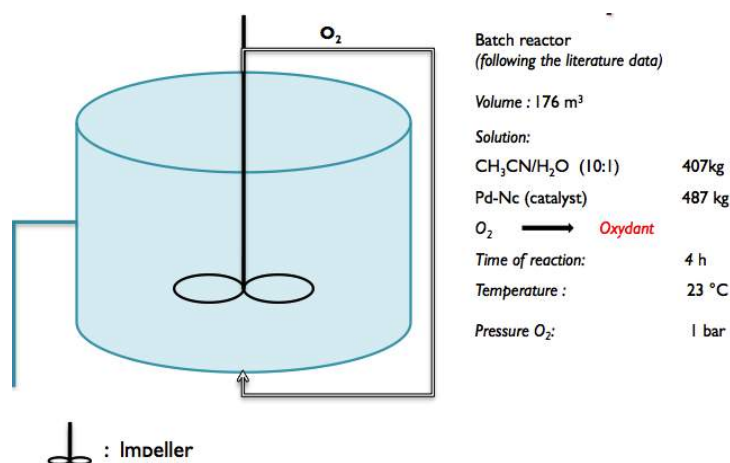


Figure 3.6: The scheme of the reactor with the amount of reagents for each cycle

smaller volumes made this solution more interesting.

Another important aspect that must be taken into account is the composition of the solution. Not only water but a solution with a 10:1 v/v of CH<sub>3</sub>CN:H<sub>2</sub>O is required. This composition is worst than a simple water solution cause is less "environmental friendly" and could become another important cost parameter treating with the waterwastes.

Even in this case become necessary separation of the catalyst from the solution. The catalyst in homogeneous phase could be separated with diethyl ether and separated by filtration. Then the final product and the other co-products must be separated. The separation of these products from the solution passed trough the impossibility to reach high temperature cause the



risk of a subsequent degradation of the same products at temperatures higher than 60°C - 80°C. The impossibility to reach high temperature to separate the species suggested to work at pressure lower than the atmospheric one. This solution is the main responsible of two important aspects: increasing cost for the products separation and reaction times. The problem of the products separation is a parameter function of the reaction volumes and, without a specific study, difficult to foresee.

### **3.3 The heterogeneous solution with noble metal nanoparticles**

This solution took inspiration from a work of Rodrigues [1]. Differently from other catalysts present in literature this one was chosen because of his mono-metallic nature. Moreover, compared to the results obtained with Pt-Bi nanoparticles, the best bi-metallic solution for this kind of reaction, the levels of yield were higher than other results in literature. This kind of catalysts represented the best solution in literature for the oxidation of glycerol to DHA [47].

This solution guaranteed possibility to work at mild conditions like the other solutions, 60 °C and 3 bar of oxygen. Reaction time was similar to test with Pd organometallic complex, even if the yield remained lower than this reaction and equal to 56%. Anyway this catalyst offered the possibility to reach an high conversion level near to 93%. This conversion level was a good solution in accord with the requests of Bracco. The catalyst used for this reaction was directly synthesized on multi walled carbon nanotubes (MWCNTs). Even if the industrial preliminary study was conducted on the results published on the reviews, possibility to find other more economical supports was hypothesized during experimental laboratory research. The choice to use the gold as catalyst was due to the higher resistance of this metal to the poisoning, respect other ones as Pt or Pd, in a strong oxydant environment. The reaction scheme for this solution it very similar to the one presented in figure 3.5 for the Pd. In figure 3.7 is reported the scheme of the batch reactor using Au/MWCNTs as catalyst. It is important to underline two aspects about this solution. The first is low amount of the volumes treated. Second reason is that this reaction, basing on the results published in literature, is faster than other solutions proposed.

As for the other two solution the evaluation of this solution passed from the possibility to make some assumption. Differently from the organometallic catalyst, where hypothesis of catalyst regeneration was done during the reaction in presence of the O<sub>2</sub>, here the authors observed a progressive de-activation of the catalyst from the first until the fifth cycle with a progressively reduction of the yield. This consideration had permitted a construction of a de-activation model for this catalyst useful during the economical eval-

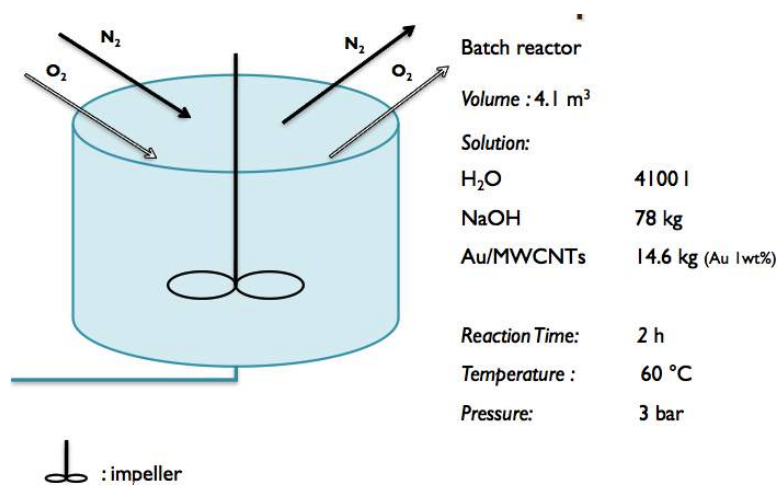


Figure 3.7: The scheme of the reactor for the heterogeneous catalyst

uation.

### 3.3.1 Deactivation of the heterogeneous catalysts

This brief section is useful to understand hypothesis behind the economical evaluation with this catalyst. These considerations became important in particular at the preliminary step of the research when not many experimental data were suitable.

Even if in this case the behavior of the catalyst was well known became necessary to test its behavior after two hours and for longer period. There were two reasons:

- to take into account the possible de-activation of the catalyst
- to evaluate reaction time to reach the required level of conversion considered acceptable at the industrial scale (99.95%)

Models proposed were compared to the experimental data from literature. The first one was a simply exponential model of conversion without any de-activation of the catalyst. The model considered a first order kinetic (3.1): the kinetic constant remained fixed during the reaction.

$$\zeta = 1 - e^{-k_0 t} \quad (3.1)$$

where  $k_0$  is the kinetic constant.

In the second model was considered a de-activation. In the simplest way the kinetic constant varied with time, considering the poisoning of the activated sites on the catalyst. The poisoning was taken into account with a parameter  $\delta$ .

$$\zeta = 1 - e^{-\delta k_0 t} \quad (3.2)$$

The last consideration was made on the variation of the de-activation with time (exponential variation): in this model a double exponential behavior appears.

$$\zeta = 1 - e^{-\frac{k_0}{\delta}(1-e^{-\delta t})} \quad (3.3)$$

The following proceedings:

- for the first model  $k_0$  was evaluated fitting the experimental data considering a new catalysts at the first cycle
- for the model with de-activation,  $k_0$  and  $\delta$ , the experimental data considered were the ones after the first cycle
- the final step was to consider an exponential decreasing of the kinetic constant

The second model with de-activation (equation 3.2) was used only as the first step before to compute the parameters for the equation 3.3. The two different curves are presented in figure 3.8. These two models became impor-

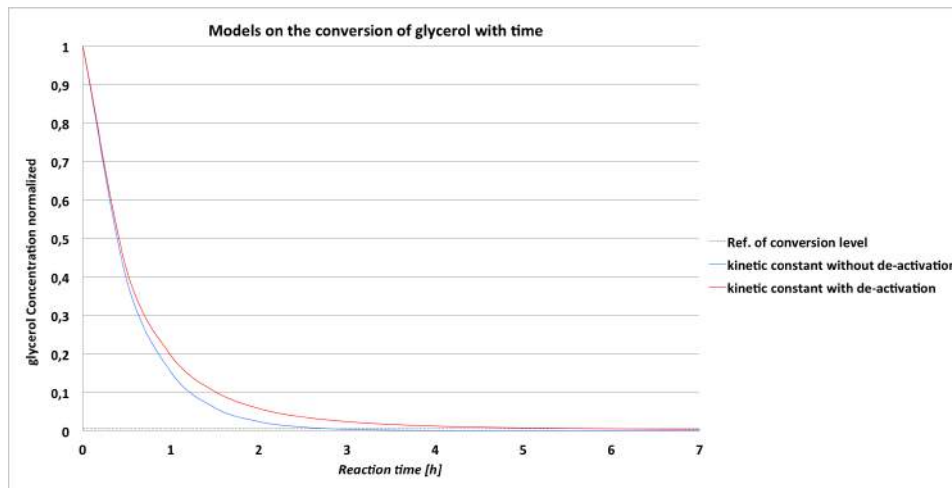


Figure 3.8: The conversion of glycerol following the models proposed in the equations 3.1, 3.2 and 3.3

tant in order to estimate the reaction time necessary to reach the conversion level requested. On figure 3.9 a zoom on the conversion behavior after 2 h is presented. The dashed line represents a conversion level equal to 99.95%. It is evident the time gap between the two models with and without de-activation. The importance of these evaluation was linked to the necessity to understand the maximum possible cycles number per day (24 h). The conversion level required and retained optimal at the production level was equal to 99.95%. With a de-activation behavior one cycle must be carried on until the sixth hour after the start of the reaction. This requirement

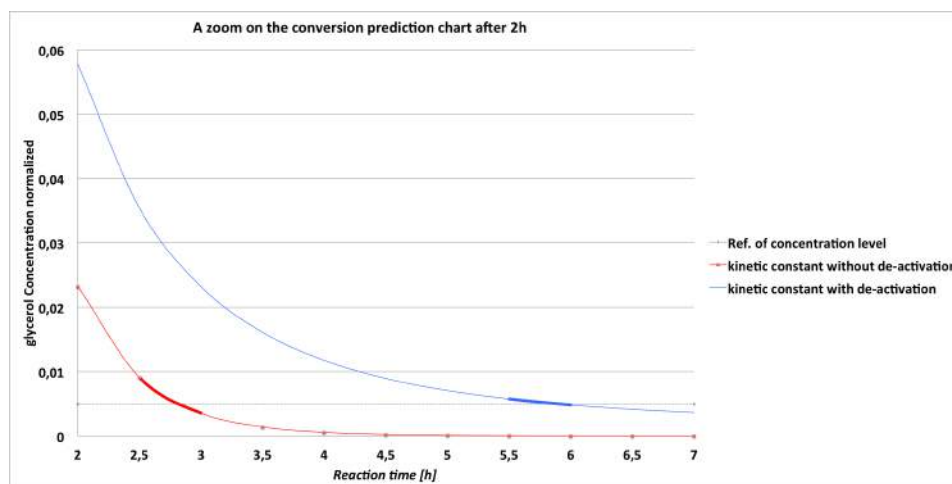


Figure 3.9: A zoom on the chart presented in figure 3.8 in order to evaluate the necessary time to reach the glycerol conversion level required

reduced drastically the cycle numbers per day with a following modification of the treated volumes for the DHA annual production. As done before a list of process needed were considered:

- reagents supply
- catalyst supply or, eventually, *in loco* catalyst production
- pure Oxygen line
- solvents (in this case the water were the only one)
- reactor heating and temperature control during the reaction
- products separation
- products crystalization
- waterwaste post-treatment

The scheme of the process (figure 3.10) is quite similar to the other one presented in figure 3.5. The main difference is the possibility of the catalyst recovering. One of the advantages to work with an heterogeneous catalyst is the easier separation of it from mother waters and an easier re-utilisation for the following reaction. Even if the nanotubes were proposed as supports for gold nanoparticles the idea to use more economical ones (e.g. carbon black or graphite) was carried on.

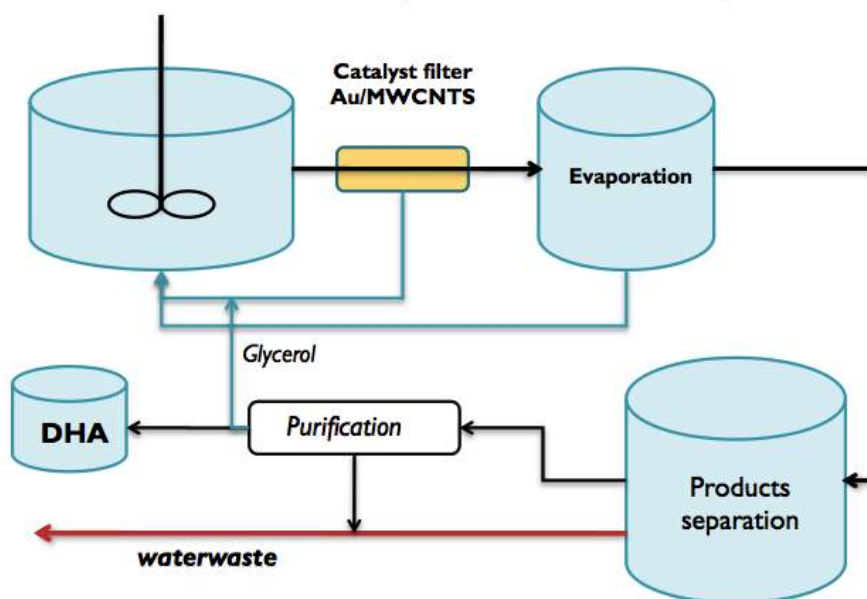


Figure 3.10: the scheme proposed for the heterogeneous catalyst solution; MWCNTs: multiwalled carbon nanotubes

### 3.4 An economical evaluation

After analyzing possible solutions, an economical and process evaluation was performed, in order to evaluate the most feasibility catalyst system. First of all after the preliminary evaluation the electrocatalytic solution was abandoned. The reasons are mainly two:

- Bracco Imaging S.p.A. does not have the possibility to work with an electrocatalytic reactor
- electrocatalysis proposed had a too low conversion (25%) level and a too long reaction time (24 h)

#### 3.4.1 Homogeneous catalysts based on Pd complexes

This catalytic system proposed was initially not considered cause the problem links with the big volumes treated. Working with an homogeneous catalyst, at the end of every batch the separation of the catalyst from the solution became necessary. Its separation and a sedimentation were evaluated as the only possible way: a ten times the reaction volume was the amount of diethyl ether (DE) estimated to precipitate the catalyst. Anyway:

- volume of diethyl ether (DE) was over estimated, only with laboratory experiments the volume could be reduced

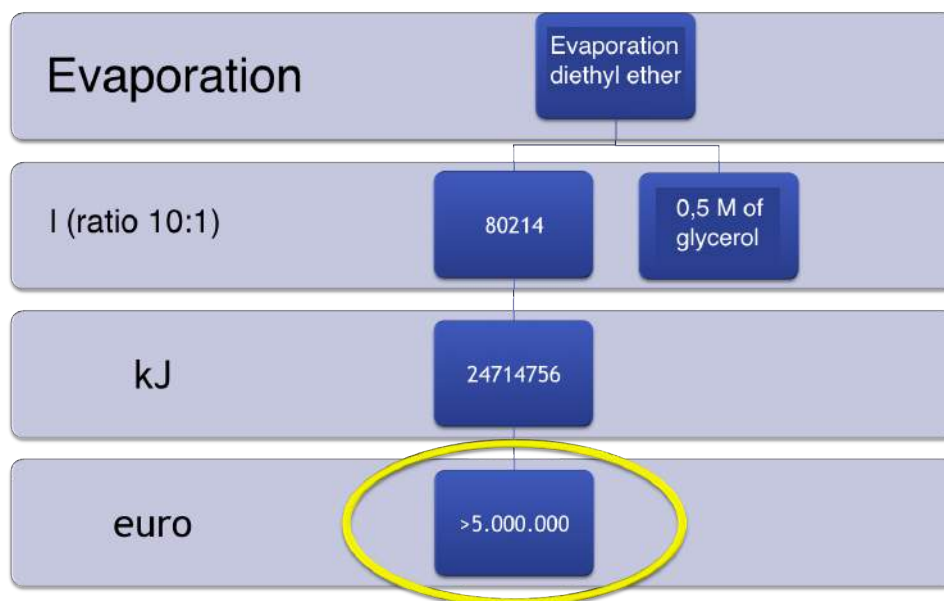


Figure 3.11: the scheme of the volumes needed for the reaction in function of the cycles per day

- diethyl ether must be re-cycled at each step
- diethyl ether must be separated

So, in this preliminary evaluation, the problem links to the separation of the catalyst became a big problem: with no more information and without experimental data only a simply evaluation, as presented in figure 3.11, was possible. Referring to the hypothesis just presented the cost about the step with diethyl ether was too high, more than 5.000.000,00 Euro. This way of synthesis was not considered the best one for the DHA production.

Anyway in 2009, Mifsud and co-workers [3] suggested an heterogeneous solution starting from the Pd-Neocuproine complex. This study proposed the utilisation of Palladium nanoparticles. This result suggested to have the possibility to recover the catalyst at the end of the reaction. In a batch reactor a solution of Pd-Neocuproine showed to have good results with an high selectivity (about 99%) and a good conversion level (72%) at 1,5 hours. Even in this case a simple exponential model was built in order to estimate the time necessary to reach the minimum conversion required. Batch time estimation comes from figure 3.12 and a modification was made on the process cost estimation. In figure 3.13 a flow chart with the estimation of the volumes is presented. In this last figure it is important to underline the presence of a new reagent, the sodium acetate. The role of this salt was to increase the catalyst's activity [7,43].

Moreover in figure 3.14 and 3.15 are presented the estimation of the costs

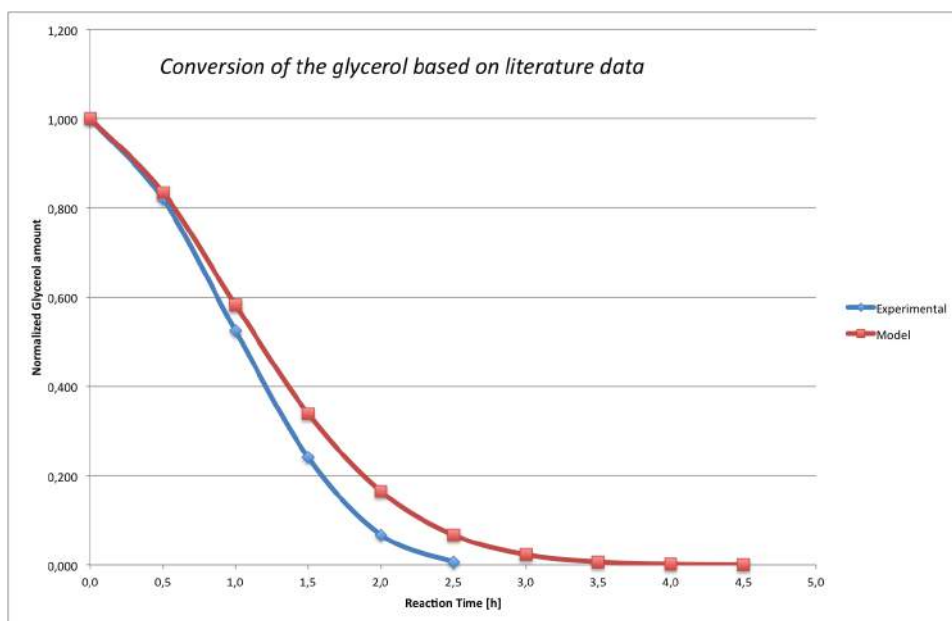


Figure 3.12: The conversion estimation referred to the experimental data from literature

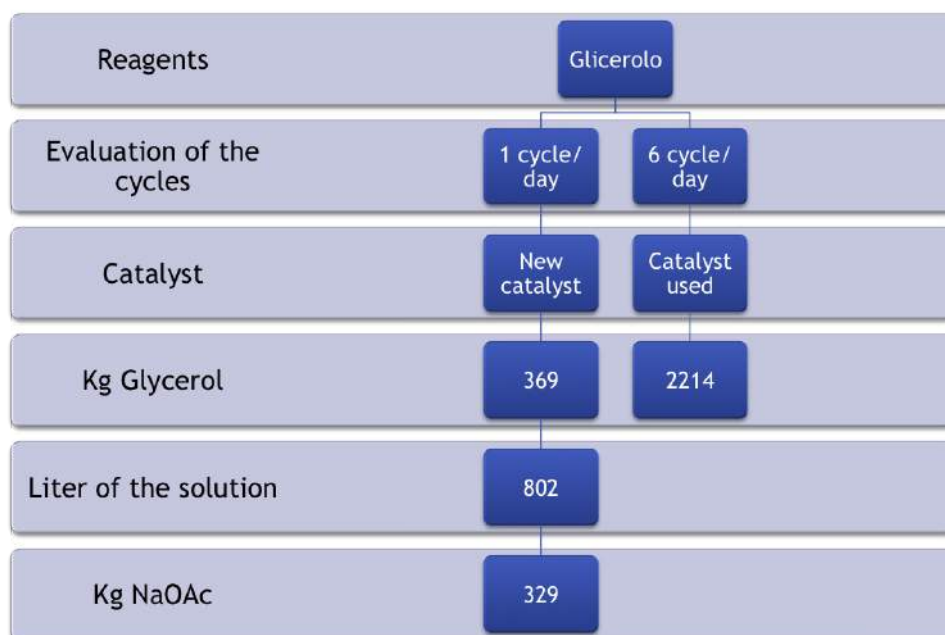


Figure 3.13: The flowchart about the reaction costs

for two solution: reaction with and without evaporation having modified the volumes in function of the catalyst in its homogenous and heterogenous phase. The possibility to recover the catalyst at the end of the reac-

Glycerol [euro/year] 553.000	Catalyst [euro/year] 191.000 - 2.300.000 + 10% (cost for the catalyst synthesis)	NaOAc [euro/year] 3.000 - 17.000
Evaporation [euro/year] /	Heating cost [euro/year] 14.300	Oxygen and (Nitrogen) [euro/year] 550.000

Figure 3.14: The cost hypothesis without evaporation with nanoparticles solution

Glycerol [euro/year] 552.000	Catalyst [euro/year] 191.000 - 2.300.000 +10%(synthesis of the catalyst)	NaOAc [euro/year] 3.000 - 17.000
Evaporation [euro/year] Etanolo: 180.000	Heating [euro/year] 14.300	Oxygen and (Nitrogen) [euro/year] 523.000

Figure 3.15: The cost hypothesis with evaporation with nanoparticles solution

tion as Pd nanoparticles was the main reason that making attractive the organometallic catalyst.

### 3.4.2 Heterogeneous catalysts based on Au nanoparticles

This solution was considered very interesting cause of the low volumes treated. For the annual production was made this estimation about the reagents amount:

- NaOH in molar ratio 2:1 with glycerol
- catalyst 25 g for every kg of glycerol (2.5 wt%)
- glycerol 5 M (45 wt% - the limit is 10 M even if in the paper the quantity used was 0,3 M)



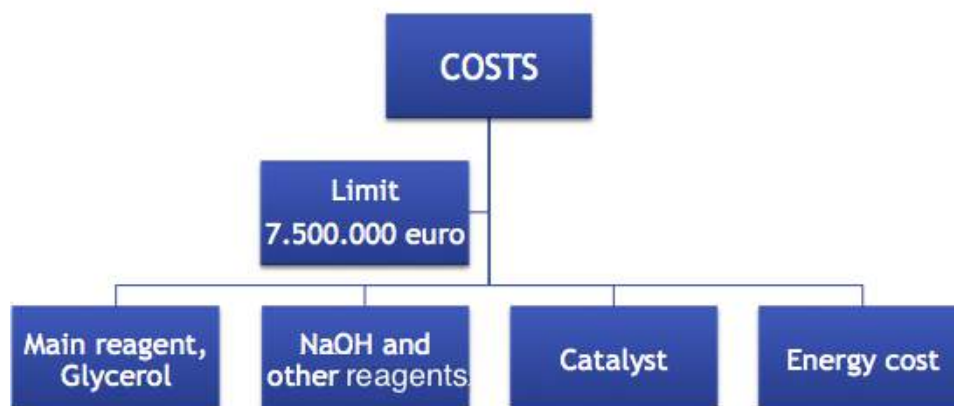


Figure 3.16: the scheme concerning the all potential sources of cost

- for the crystallization of the products a quantity of ethanol with a ratio 3-4:1 w/w ethanol to water

The crystallization step is an option. The DHA, indeed, is used for a synthesis of the serinol by amination, so the DHA produced can be used directly. In this situation the crystallization is not necessary with a big influence on the final costs.

Based on the consideration done in the previous chapter about the required time to reach the almost total conversion of the glycerol (99.95%), we estimated to perform no more than 2 cycle per day.

In accord with this last consideration and referring to the scheme in figure 3.16, total volumes needed for each batch reaction are reported in figure 3.17.

Two further scenarios must be evaluated, presence or absence of evaporation. In the case of evaporation, the differential cost per year compared with the solution without ethanol, is equal to a surplus of 170.000,00-190.000,00 Euro. The small volumes used with this solution would give the possibility to maintain low costs of the post-reaction procedures.

### 3.4.3 A comparison between the solutions proposed

In order to permit an easier comparison between the three solution, in figure 3.18 it is possible to compare cost estimations. The diagram shows how the solution with Pd as homogeneous catalyst is not economically available unless a reduction of the reaction volume.

Another estimation, more conservative, was proposed in order to consider a

Reagent	Glycerol			
Cycles number	1 cycle/day		2 cycle/day	
Catalyst	Cat.New	Cat.Used	Cat.New	Cat.Used
Kg Glycerol	2867	5797	1434	2899
l solution	6233	12607	3117	6301
Kg NaOH	5735	11594	2867	5797

Figure 3.17: the scheme of the volumes necessary for the reaction function of the cycles per day

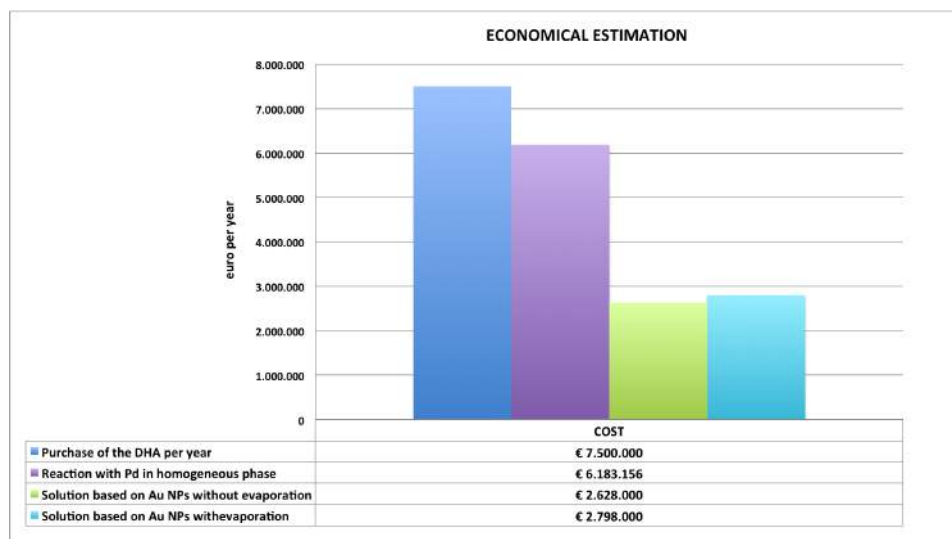


Figure 3.18: The economical estimation for the three different solutions; metal based catalyst with a longer life

shorter life of the catalyst, another more conservative estimation was made (figure 3.19) considering the catalyst aging.

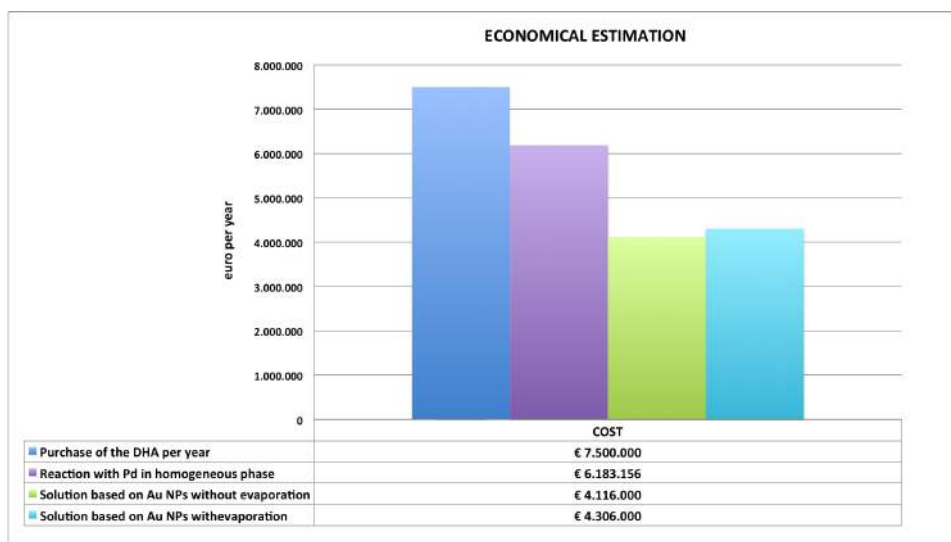


Figure 3.19: The economical estimation for the three different solutions; metal based catalyst with a shorter life

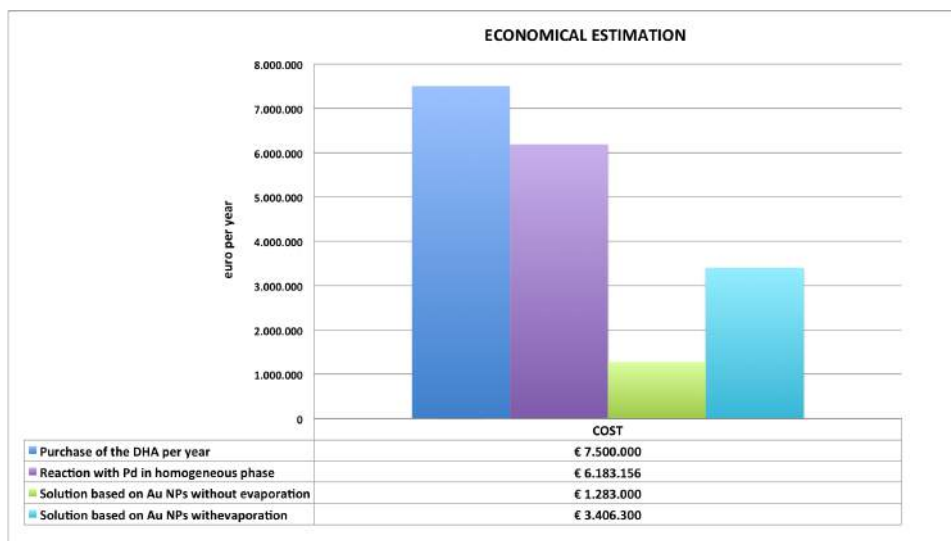


Figure 3.20: The economical estimation for the three different solutions; organo-metallic catalyst with a longer life

### 3.5 Conclusions and steps of reasearch

Some aspects came out after analyses of data from the preliminary economical evaluation:

- unknown if the medium life of the catalyst (no evaluation about their poisoning) offers only a big uncertainty related to the cost evaluation (compare the figure 3.18 with 3.19 and 3.20 with 3.21)

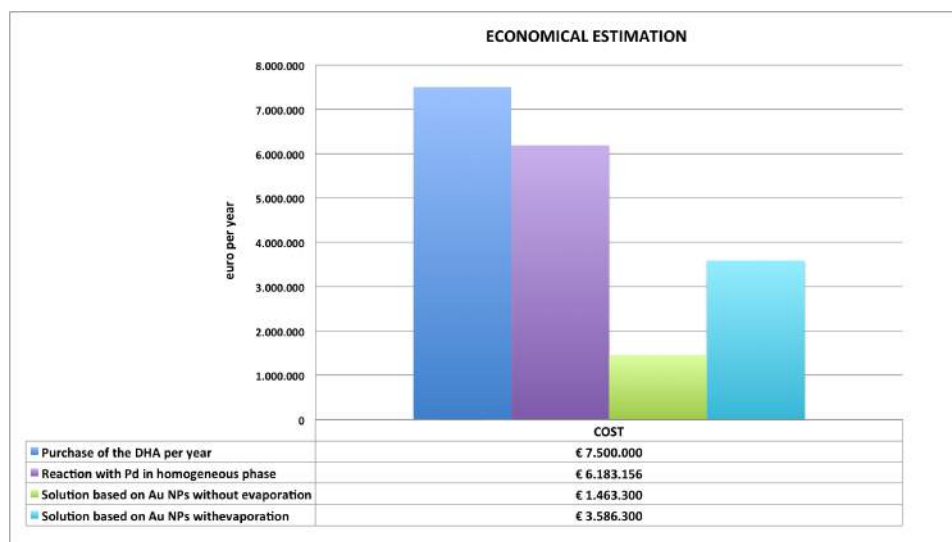


Figure 3.21: The economical estimation for the three different solutions; organo-metallic catalyst with a longer life

- the post-treatment of the reaction volume has an important influence on the final cost of the DHA synthesis. It could be useful to mind differences between evaporation and no-evaporation processes (see figures - 3.18, 3.19, 3.20, 3.21)
- to not have economical advantages due to costs related to a big plant

This economical analysis has permitted to focus the main problems. The study, from this point of view, started by hypothesizing to obtain a better knowledge of the reaction collecting the amount of data necessary to think to a scale-up.

Moreover it is important to underline how initially the reactor and the reaction design were two of the principal goals of this research.

---

---

## CHAPTER 4

---

# THE CATALYSTS SYNTHESIS AND THEIR CHARACTERIZATION

This chapter is dedicated to the description of the synthesis of the different catalytic systems studied.

The organometallic catalyst system was well known in literature cause the works of Waymouth and co-workers [4,7]. The organometallic catalysts was based on two different Pd complexes showed. The possibility to recover the catalyst at the end of the reaction as Pd nanoparticles was the main reason that transforms attractive the organometallic catalyst (figures 4.1 and 4.2): neocuproine-Pd(OAc)<sub>2</sub> and [neocuproine-Pd( $\mu$ -Ac)]<sub>2</sub>(OTf)<sub>2</sub>.

The three heterogeneous catalysts were related to the use of the noble metal nanoparticles: Au, Pt-Bi as coupled system and Au-Pt-Bi as tri-metallic one.

The research was based on these metals because of the good results already obtained in literature. Efforts to improve selectivity, indeed, have included the use of heterogeneous catalysts, where a liquid-phase batch reactor with Au/C, bi-metallic AuPd/C or PtBi/C catalysts yielded near full conversion of glycerol to a complex solution, with main products glyceric acid (45%) and DHA (from 10% to 46%) [1,20,47]. Catalysts based only with Pt were also investigated, but were more selective for oxidation of the primary hydroxyl groups. Only the Bi, in a coupled catalytic system, Pt-Bi gave a DHA selectivity [43].

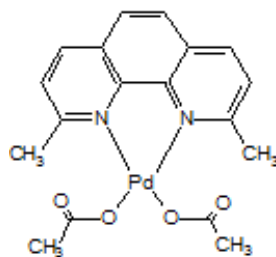


Figure 4.1: neocuproine-Pd(OAc)<sub>2</sub>

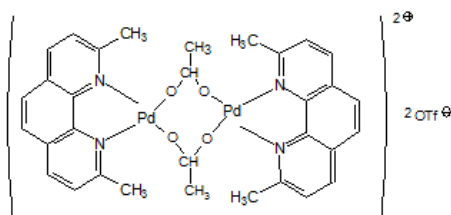


Figure 4.2: [neocuproine-Pd( $\mu$ -Ac)]<sub>2</sub>(OTf)<sub>2</sub>

## 4.1 The organometallic catalyst

The idea to approach the reaction with this catalyst was taken from literature [4,7]. With this organometallic complex an oxidation of glycerol could be conducted in mild condition to obtain an high yield of DHA near to 90%. The first step, in accord with the preliminary study, was to verify the data in order to reproduce the results and to scale-up the reaction. In fact, was necessary to evaluate the feasibility of the reaction before to move to an industrial scale. The approach expected:

- a study about the possibility to work at higher concentration
- to obtain information for the reactor design
- to study the possibility to modify the nature of the solution reducing the CH<sub>3</sub>CN amount: the preferred solvent was pure water
- to evaluate the effective activity of the catalyst at repetute cycles

The behavior of the catalyst during the reaction was still unknown from some points of view apart its decomposition [44,46]. One of the most common mechanism proposed in literature is the scheme reported in figure 4.3. In this scheme the catalyst works as a monomer complex (in two different structures, 1 and 4) but is synthesized in a dimeric form (PdNc-D).

In order to obtain this dimer form three steps are necessary:

- the first step is the synthesis of the monomer complex of Palladium

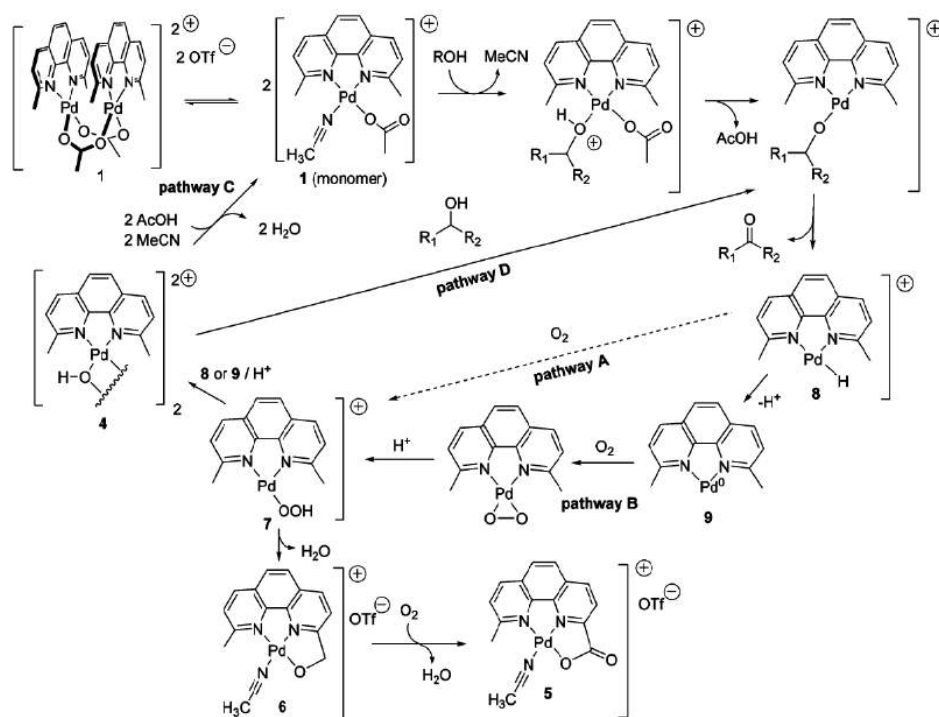


Figure 4.3: The reaction scheme for the alcohols oxidation using the Pd complex [44]; the carboxylate form of the complex (5) is an inactive form of the catalyst

- the second step is the activation of this monomer complex using the trifluoromethanesulfonic acid (a super-acid named TfOH)
- the third step is finally the synthesis of the dimer using the monomer and an its activated form as starting chemicals

In figure 4.4 it is possible to observe the three chemical reactions just described. In the following sub sections will be treated the synthesis of the three structures step by step.

For every step an accurate analysis was did on the product obtained at the end of the synthesis. An HPLC method was developed to follow the synthesis of the monomer Neocuproine- $\text{Pd}(\text{OAc})_2$ . The method, described below, permits to follow the entire reaction until the complete Neocuproine consumption.

The Nuclear Magnetic Resonance (NMR) was used to verify the three structures of the Pd complexes. This technique uses the nuclear spin of the H atoms and its interaction with an external induced magnetic field.

The Karl-Fischer (KF) analysis and the Inductively Coupled Plasma (ICP) completed the characterization. These two techniques were used to define the water amount of the sample and the Pd assay, respectively.

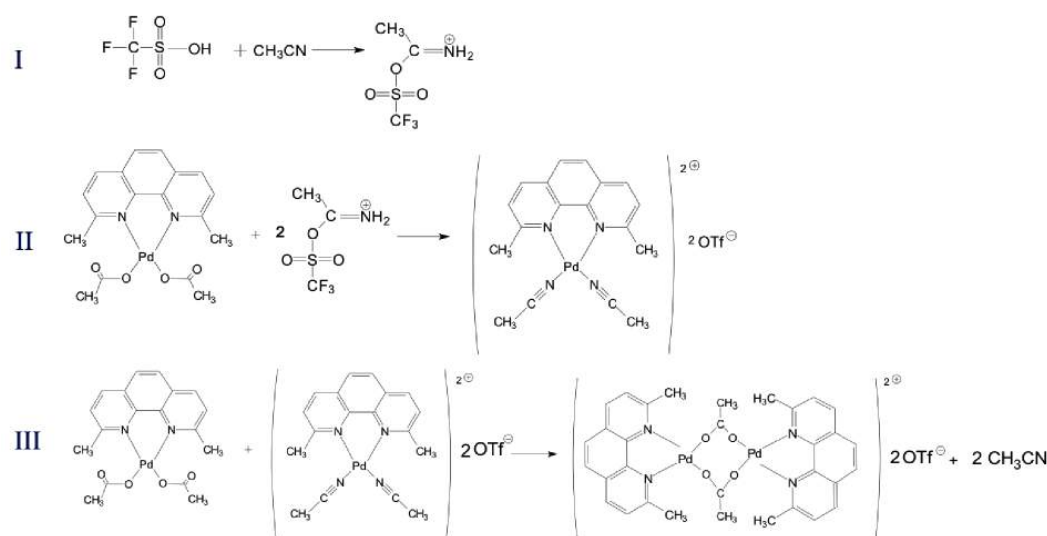


Figure 4.4: The chemical reactions to obtain the dimer Pd-complex: (I) the activation of  $\text{CH}_3\text{CN}$  with the acid; (II) the reaction to obtain the Pd-complex (PdNc-C) in its activated form (PdNc-A); (III) the final reaction to obtain the dimer (PdNc-D) [44]

## 4.2 The monomer form of the Pd catalyst

The first step was the synthesis of the monomer form of the organometallic Pd catalyst. The  $\text{Pd}(\text{OAc})_2$  (by Sigma-Aldrich, Pd assay higher than 98%) reacts with an organic molecule, the 2,9-methyl-1,10-phenanthroline (Neocuproine or Nc, Sigma Aldrich, purity higher than 99.9%). The synthesis of the monomeric Neocuproine- $\text{Pd}(\text{OAc})_2$  is necessary in order to obtain the dimeric complex. This dimeric structure of the catalyst is that one used by Waymouth and co-workers in the selective oxidation of the glycerol to DHA [4].

With the idea to have an accurate method of synthesis for the catalyst, necessary to reproduce the reaction at an industrial scale, the step of the monomer synthesis was developed in different ways. It is possible to divide the study of the catalysts synthesis in two different macro-area:

- an analytical method developed to follow the synthesis step by step until the completely reaction of the reagents
- an analysis about the purity of the catalyst to evaluate the Pd assay and water content

The thin layer chromatography (TLC), high pressure liquid chromatography (HPLC) and NMR analysis were used to analyze the catalyst. The TLC did not give any results and was impossible to follow the reaction with this technique. The unsuccessful with the TLC brought to develop an HPLC method to follow the reaction. The HPLC resulted useful only during the



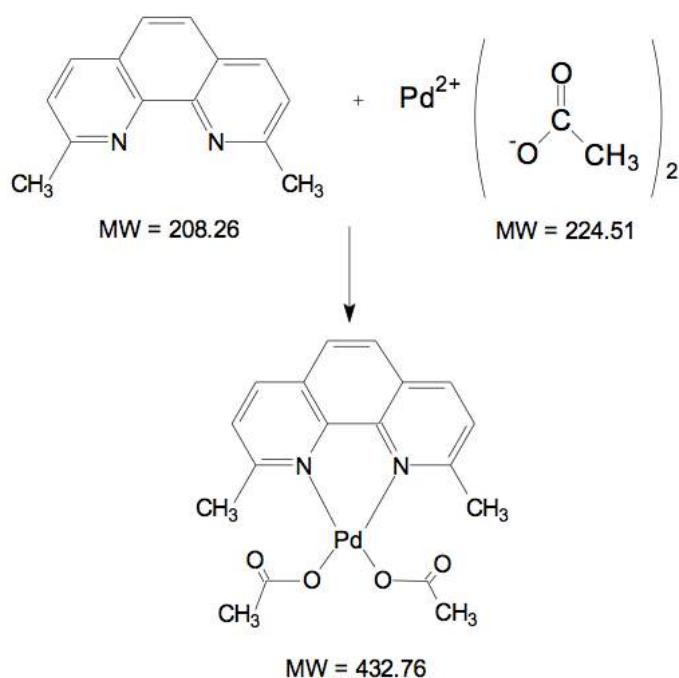


Figure 4.5: The reaction scheme for the synthesis of the complex in its monomeric form, Neocuproine-Pd(OAc)<sub>2</sub>

synthesis of the monomer Neocuproine-Pd(OAc)<sub>2</sub>.

After the synthesis an ICP analysis was done to determine the amount of Pd in the complex, an NMR analysis to define the structure and the Karl-Fischer technique to evaluate the water amount into the sample. The water was always present even if the synthesis reactions were always conducted in anhydrous conditions.

#### 4.2.1 The synthesis of the monomer complex

The reaction scheme proposed for the synthesis of the complex is reported in figure 4.5. The reaction was conducted in a flask (500 ml) with four necks. With the flask were used a Liebig refrigerator to permit the reflux and another tube at the top with CaCl<sub>2</sub> to maintain an anhydrous environment during the reaction (figure 4.6). The synthesis of the complex can be described as follows:

- 5.28 g (23.52 mmol) of Pd(OAc)<sub>2</sub> dissolved in 250 ml of Toluene (anhydrous): mixing time of 95 minutes
- preparation of a solution of 5.00 g (24.00 mmol) of Neocuproine in 50 ml of CH<sub>2</sub>Cl<sub>2</sub>; during this addition a dark-yellow suspension forms
- dropwise of the Neocuproine solution in 3h24'



*Figure 4.6:* An example of the reactor for the complex synthesis in its monomeric form

- the solution is left under stirring for 16 hours
- after 16 hours 500 ml of petroleum ether (PE) are added to permit the filtration of the suspension and for the precipitation of the solid

after the addition of the PE it was possible to observe a precipitation of a solid compound. The solid was filtered by silica filter and washed four time with acetone (4 per 10 ml). The solid appeared of a dark yellow and it is dry by vacuum for 5 hours with a yield that was evaluated equal to 87.54%. This yield was estimated without considering the presence of impurities.

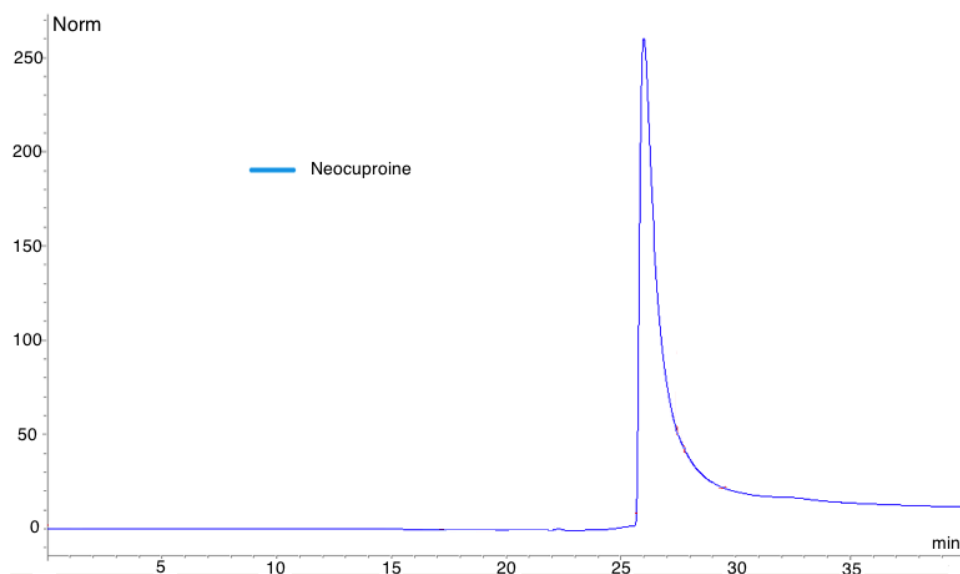


Figure 4.7: The HPLC chromatogram for the only Neocuproine

### The monomer characterization

During the reaction the solution was analyzed in order to follow the reaction: an HPLC method was prepared to do this (C18 column). In the figures 4.7 and 4.8 it is possible to observe HPLC chromatograms. In the first one it is possible to observe the peak related to the Neocuproine (blu line). In the second chromatogram is showed the peak related to the Pd complex (red line) after the filtration. On the other hand it is important to underline how the Pd precursor is not visible with this method. This HPLC method permits to follow completely the reaction in a fast way. However, in order to be sure about the nature of the product an NMR analysis was made. Anyway the HPLC is going to be a fast way to follow the complex synthesis for possible industrial application of the catalyst.

The NMR analysis was made only on the proton. No C-NMR was necessary to confirm the structure of the complex. For each peak a number was associated and correlated to the theoretical structure (figure 4.9). Even if the synthesis was conducted in anhydrous conditions, a water peak appears. This peak influences the purity of the complex, but a part of it derived from the solvent used to conduct the NMR analysis. To evaluate the amount of water in the catalyst a Karl-Fischer was done and, together with the ICP analysis, was possible to define the purity of the catalysts synthesized. In figure 4.10 the results about the ICP analysis on the sample. These results permitted to evaluate the yield, estimated to be equal to 87.5%, and a purity equal to 95.52%. With the Karl-Fischer analysis a water amount was estimated (figure 4.11). The value was equal to the 7.86 wt%.

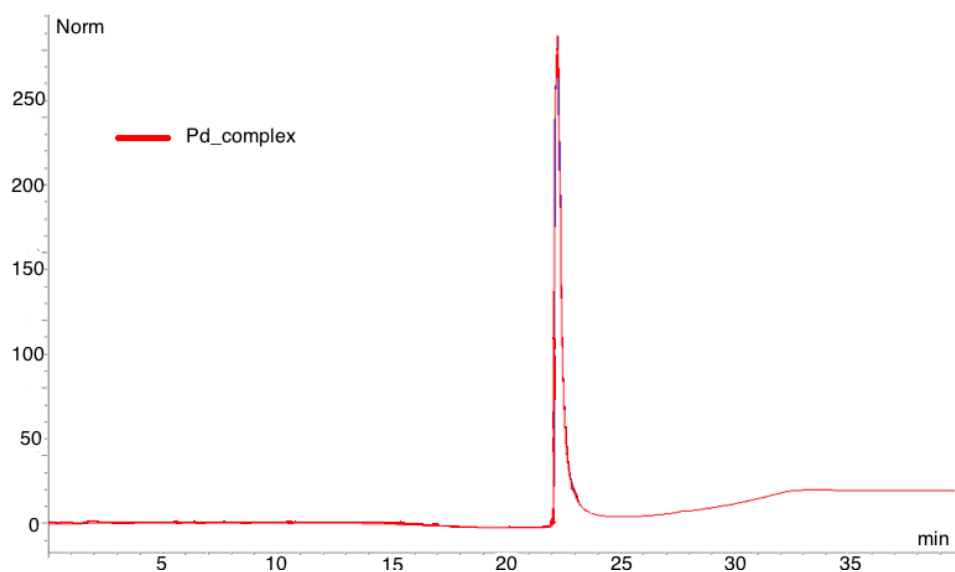


Figure 4.8: The HPLC chromatogram of the complex after the filtration: the chromatogram is related to the final product after the filtration

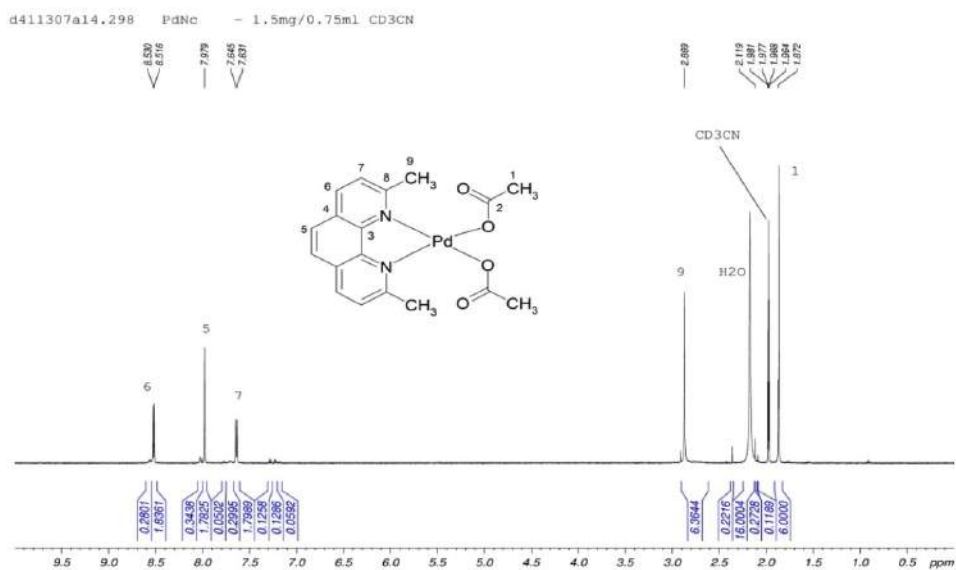


Figure 4.9: The H-NMR analysis of the complex; as solvent was used the CH<sub>3</sub>CN

#### 4.2.2 The synthesis of the activated complex of Pd with CH<sub>3</sub>CN anhydrous

The structure of the activate form of this molecule is presented in the figure 4.12 (PdNc-A).

Sample	Weight	Pd amount	Average	$\sigma$
[-]	[mg]	[%w/w]	[-]	[-]
A	8.95	20.932	21.7	$\pm 0.6$
B	8.62	22.082		
C	9.44	21.960		

Figure 4.10: The ICP analysis to define the amount of Pd of the Pd-complex monomer

Sample	Weight	Water Amount	Average
[-]	[mg]	[wt%]	[wt%]
A	109.2	8.70	7.86
B	103.1	7.69	
C	101.9	7.20	

Figure 4.11: The Karl-Fischer results to evaluate the water amount in the Pd-complex monomer

The synthesis required two steps: the activation of the  $\text{CH}_3\text{CN}$  [38, 39] and the synthesis of the PdNc-A.

The first step is conducted in an anhydrous environment, in a four necks flask and using  $\text{CH}_3\text{CN}$  anhydrous. In the flask a solution of trifluoromethanesulfonic acid (triflic acid) 0.33 M (3.3 mmol of acid) is dissolved with  $\text{CH}_3\text{CN}$  anhydrous [44]. Immediately an amount of this solution is used for the activation of the PdNc-C complex.

In a flask of 25 ml, 0.221 g (0.51 mmol) of PdNc-C are dissolved in 2 ml of anhydrous  $\text{CH}_3\text{CN}$ . 4 ml of the solution 0.33 M are added dropwise (molar ratio triflic acid: PdNc-C equal to 2.5:1) in ten minutes. After the addition the solution changes its color from yellow to orange. The solution becomes clear, no slurry.

After fifteen minutes 10 ml of diethyl ether (DE) are added to precipitate a yellow solid. Before the filtration the solid suspension is left under stirring for 30 minutes.

After the first filtration the solid is precipitated two more times. At the end of the third precipitation the solid is washed with DE (2 per 2ml).

Finally the solid is dried under vacuum overnight.

The H-NMR technique was used to characterize the activated (PdNc-A). For the characterization the attention is posed on the two methyl groups  $\text{CH}_3$  that appeared in the molecule (figure 4.12). The two methyl groups are different for the chemical shift, but the integration of the signal must have a ratio equal to one (1:1). In figure 4.12 the H-NMR for the activated form of the complex. Such as for the monomer even for the PdNc-activated were necessary the KF (figure 4.15) and the ICP (figure 4.14) analysis to complete the characterization. Finally the activated PdNc complex the yield was estimated equal to 84.15% (yield from literature 31%) and the ICP assay

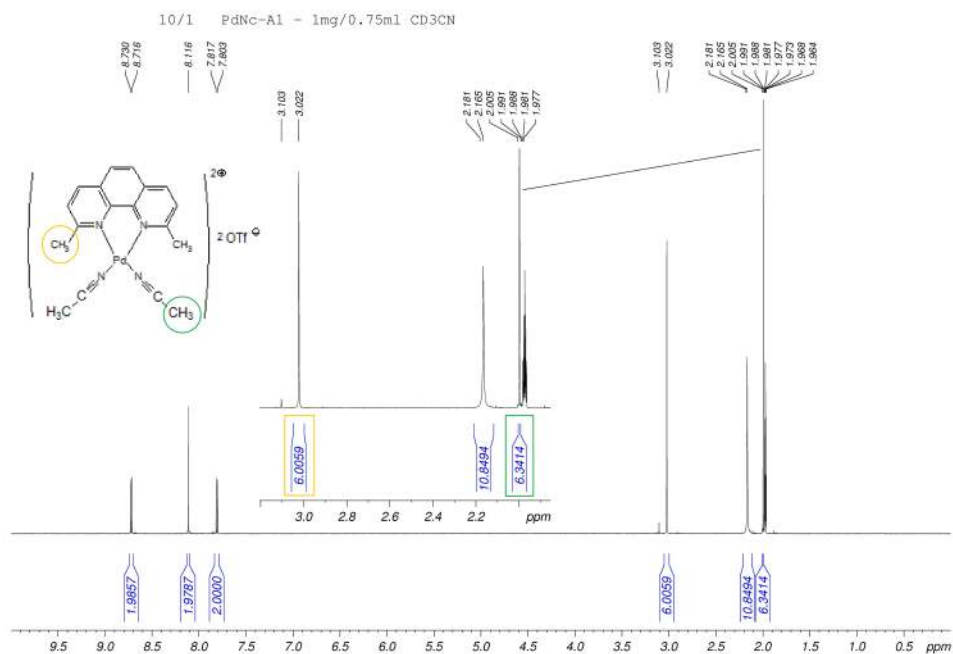


Figure 4.12: The H-NMR spectrum for the activated form of the complex

equal to 96.9%.

#### 4.2.3 The synthesis of the activated complex of Pd without CH<sub>3</sub>CN anhydrous

The synthesis of the PdNc-A cannot be done with no anhydrous CH<sub>3</sub>CN. Using not anhydrous acetonitrile the triflic acid is not able to activate it (figure 4.13, the first step described) and to give the complex with the same structure presented in figure 4.12. This result was confirmed by the H-NMR analysis. Using no anhydrous CH<sub>3</sub>CN it is not possible the synthesis of the Pd-complex activated. The H-NMR signals, corresponding to the two methyl groups of the activated Pd-complex, did not have a 1:1 signal ratio. It means a partial activation. The same procedure just described the H-NMR peaks correspond to a different structure (figure 4.12). Even leaving the solution under stirring for 16 hours the result does not change. Increasing the time reaction between the CH<sub>3</sub>CN and triflic-acid many other by-products form. Other experiments were conducted at higher time reaction until 172 hours. This result is in accord with the literature [38,39]. For the activation of the acetonitrile must be used the CH<sub>3</sub>CN in its anhydrous form.

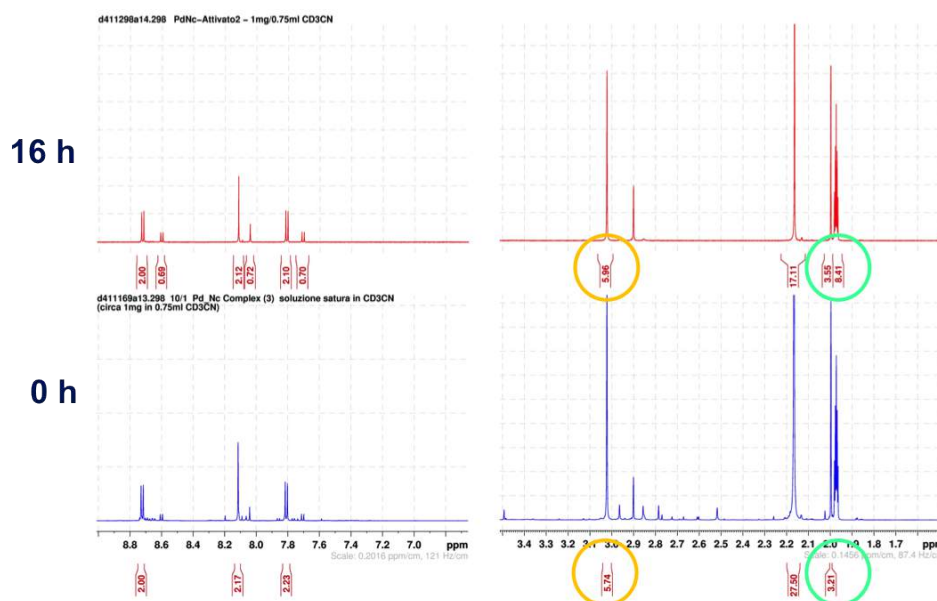


Figure 4.13: The H-NMR spectrum for the activated form of the complex using the no anhydrous CH<sub>3</sub>CN; the two signals related to the two methyl groups have a area ratio equal to 2:1

Sample	Weight	Pd amount	Average	$\sigma$
[-]	[mg]	[%w/w]	[-]	[-]
A	17.73	14.334	14.2	± 0.2
B	17.60	14.173		
C	11.39	13.969		

Figure 4.14: The ICP analysis to define the amount of Pd of the activated Pd-complex

Sample	Weight	Water Amount	Average
[-]	[mg]	[wt%]	[wt%]
A	100.6	2.32	2.39
B	96.5	2.04	
C	102.0	2.63	

Figure 4.15: The KF analysis to define the amount of water of the activated Pd-complex

#### 4.2.4 The synthesis of the dimer form of the Pd complex

The theoretical structure of the dimer in its form (figure 4.16) comes from the reaction between the PdNc-C and PdNc-A (activated form).

In figure 4.17 is presented an hypothetical scheme to explain how the catalyst works during the reaction [25]. The synthesis starts with 0.100 g of PdNc-A (0.144 mmol) that are dissolved in a flask of 25 ml with 15 ml of CH<sub>3</sub>CN.

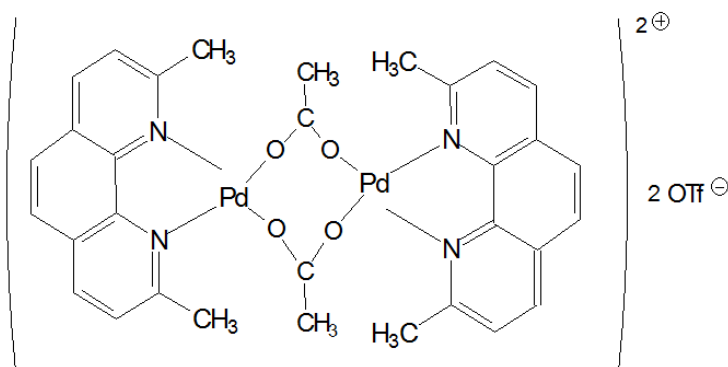


Figure 4.16: The theoretical structure of the dimer form of the PdNc complex

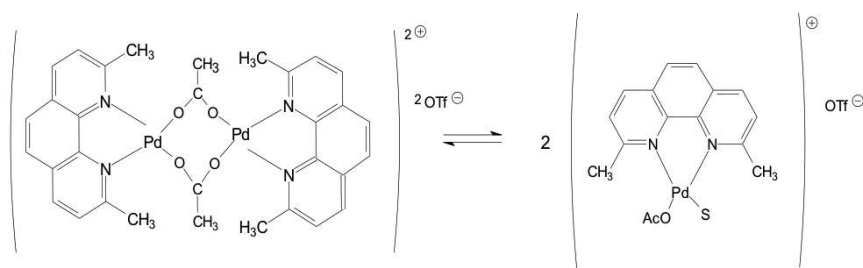


Figure 4.17: The simple scheme shows the possible behavior of the Pd complex in solution when is used as catalyst

After the complete dissolution a 0.063 g of PdNc-C (0.145 mmol) are added. The slurry changes its color from a yellow to a clear orange solution. The solution is left under stirring for 3 hours and after this time is added diethyl ether (DE) to obtain a solid precipitation. After the precipitation the solid is washed with DE (two times for 2 ml).

The synthesis was improved to produce higher amount of the catalyst as follows: 0.800 g of PdNc-A (1.128 mmol) are dissolved in a four necks flask (capacity 100 ml) with 18 ml of  $\text{CH}_3\text{CN}$  anhydrous. After the complete dissolution a 0.520 g (1.201 mmol) of PdNc-C are added. The solution is left under stirring for 3 hours and after this time is added 21 ml of DE to obtain a solid precipitation. The solution is left to decant for 15 minutes and subsequently filtered. The supernatant liquid is put in another one flask to be recovered.

At the solid 10 ml of DE are added and after a brief mixing it is filtered. The flask is washed with 5 ml of DE two times to recover the solid from the walls of the flask.

From the supernatant liquid recovered, it was possible to extract a minimum amount of solid after DE addition (10 ml), from 1 to 2% of the total amount



synthesized.

The total amount of dimer (PdNc-D) was equal to 942 mg. The NMR analysis was not useful to identify correctly the dimer. In solution, indeed, this complex gave a large amount of by-products reaching a thermodynamic equilibrium between numerous different structures. This large amount of structures gave as result a complex NMR spectrum with which was impossible to identify every single structure.

To avoid this problem and to be sure about the nature of the complex another technique was employed, the matrix assisted laser desorption-ionization (MALDI). This technique ensured a soft ionization, widely used in mass spectrometry for the organic molecules with an high molecular mass. These organic molecules, in fact, tend to be decomposed into many structures when ionized by conventional ionization methods. The results were expressed as spectrogram where on the abscissa axis appear the mass on charge values (figure 4.18). The mass on charge ( $m/z$ ) peak at 795.961 corresponds to the mass of the dimer, without the two anions derived from the triflate salt, plus 1 mol of water. The presence of this water was confirmed and estimated equal to 1.825 wt% from the KF analysis (figure 4.19). Finally the ICP

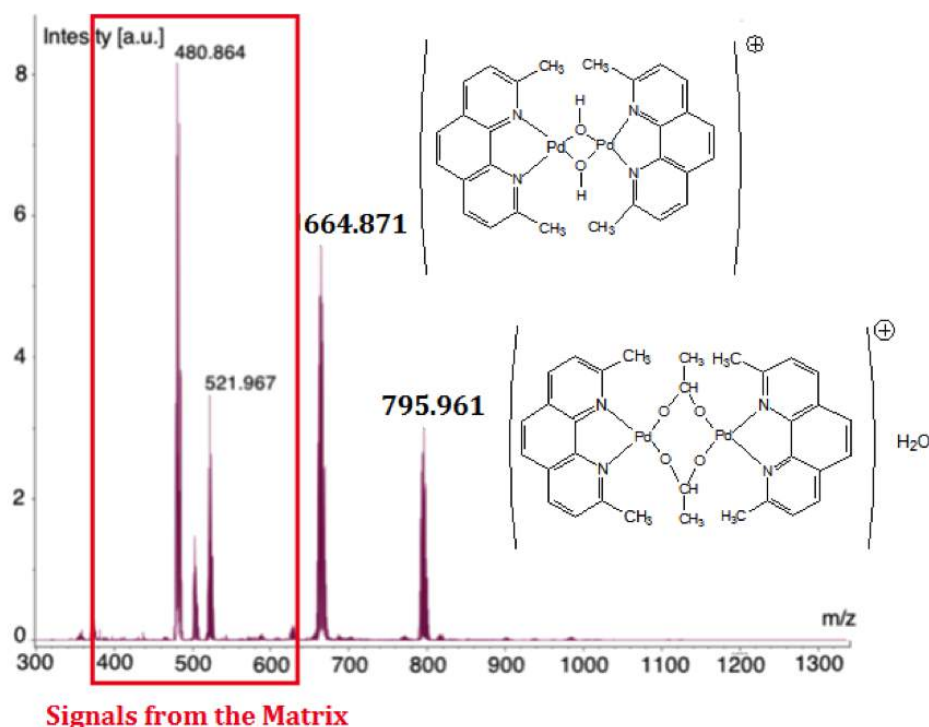


Figure 4.18: The MALDI spectrum for the dimer

(figure 4.20) analysis completed the characterization.

For the dimer yield was estimated equal to 77.5% (yield from literature

Sample	Weight	Water Amount	Average
[-]	[mg]	[wt%]	[wt%]
A	44.4	1.87	1.825
B	44.1	1.78	

Figure 4.19: The KF analysis to define the amount of water of the dimer Pd-complex

Sample	Weight	Pd amount	Average	$\sigma$
[-]	[mg]	[%w/w]	[-]	[-]
A	5.29	17.013	17.3	$\pm 0.8$
B	4.02	16.729		
C	5.48	18.248		

Figure 4.20: The ICP analysis to define the amount of Pd of the activated Pd-complex

61%) and the ICP assay equal to 89.1%.

#### 4.2.5 Considerations about the organometallic Pd complex

The work to synthesize the organometallic catalyst involved one year of research.

The synthesis of this complex was not well described in literature. Also the description of the characterization was superficial, even in the main works presented in literature [7,36,43,44].

The work developed in these months carried out with a well defined methodology for the complex synthesis. The procedure proposed offers a high yield for each of the three structures. Finally this research underlined the critical aspects that are possible to find during the approach to the synthesis.

### 4.3 The catalyst based on Au nanoparticles

It was the first catalytic system investigated.

In literature the best results with this catalyst were presented by Rodrigues *et alii* [1] in 2011. Referring on their results was based the preliminary economical evaluation. Anyway one year and half later Rodrigues published an *errata corrige* of the article. The results presented were wrong cause a bad HPLC method used to determine the DHA. The peak associated to DHA was indeed formic-acid.

Before the publication of the *errata corrige* and before to abandon the study of Au/C, a research on these mono-metallic catalysts was carried out. The

aim of the study was to obtain a catalyst with a good dispersion of the nanoparticles and an high activity, even testing different supports. In fact, it was necessary to looking for a reliable method of the catalyst synthesis starting from the best results from literature.

Rodrigues *et alii* [1] used the multi-walled carbon nanotubes (MWCNTs), but this support was not retained an efficient industrial one because too expensive. For this reason other supports were tested, mainly carbon balck and graphite (from Sigma Aldrich).

#### 4.3.1 The different methods for Au NPs synthesis

The synthesis of these catalysts was started from the literature [1,18,19]. Together with carbon black and graphite other supports were tested:

- Carbon Nanotubes (Single and Multi walled)
- Mesoporous Carbon
- Graphite Oxide (directly obtained from graphite)

The synthesis followed three methods:

- Impregnation (I)
- Double-Impregnation (DI)
- Liquid phase reductive deposition (LPRD)

The reason to follow different solutions for the synthesis was to check the easiest way to obtain the catalyst. The frist supports employed were:

- Carbon Black Nanopowder by Sigma, particles smaller than 50 nm, specific surface higher than 100 m<sup>2</sup>/g (from BET), volume of the voids not computed
- Carbon Powder, mesoporous support, specific surface 1081 m<sup>2</sup>/g, volume of the voids 0.82 cm<sup>3</sup>/g

The mesoporous carbon was synthetized by electrochemical way at Politechnic of Turin.

The three methods were applied as follow.

#### The Impregnation method

This method was rated as the worst one because the reduction of metal precursors with H<sub>2</sub>. Usually the reduction of the metal is conducted in H<sub>2</sub> atmosphere at high temperature.

The synthesis followed the subsequent steps:



Figure 4.21: The FESEM image takes from the sample with Au NPs synthesized with impregnation method; support: carbon black

- to dry the support at 100-110°C for 1 hour
- to prepare the solution of metal precursor in order to obtain the correct amount of metal on the support (defined as wt%)
- dropwise of the solution on the support
- the support, after the dropwise, is left overnight on the becker
- the day-after the compound is dried in the oven at 100-110°C for 24 hours

After the drying step in oven, the sample is put in H<sub>2</sub> static atmosphere at 350°C. The temperature was reached with steps of 50°C starting from room temperature (23 °C).

This method was employed only with the carbon black. The complicate and dangerous way to conduct the reduction and the bad results obtained suggested to abandon this way of synthesis. Gold NPs on catalyst synthesized with this method and observed at FESEM showed NPs dimensions larger than few nanometers (figure 4.21). The dimensions of the NPs were variable

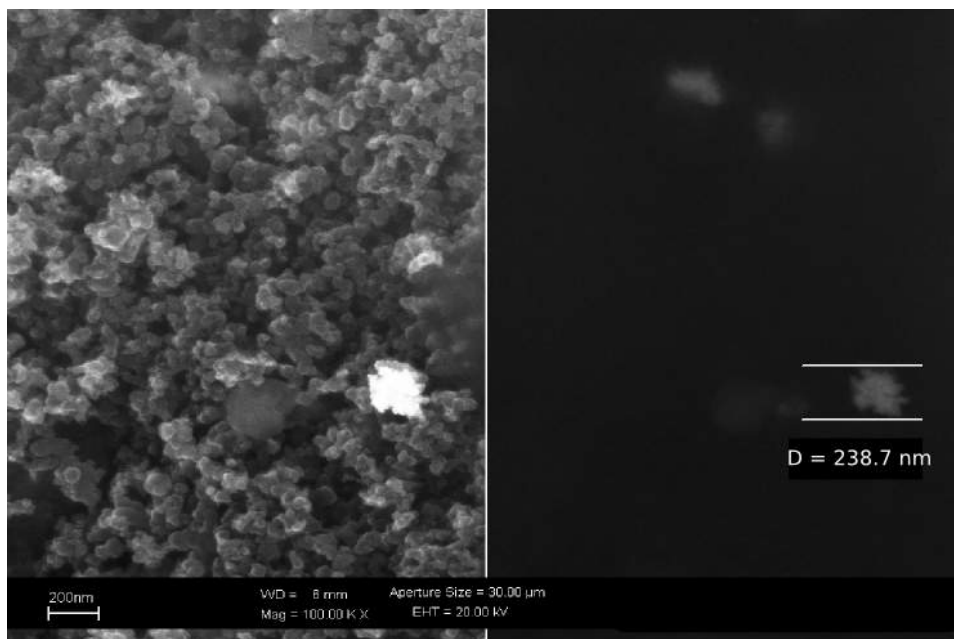


Figure 4.22: The FESEM image takes from the sample with Au NPs synthesized with double impregnation method; support: carbon black

and larger than the 10-15 nm required.

### The Double Impregnation (DI) method

The DI method is more trivial than the impregnation one. Moreover the reduction step is different. Two solutions were prepared: one with metal precursor and one with  $\text{Na}_2\text{CO}_3$  as reducing agent. During the deposition the molar ratio between the metal precursor and reducing agent was 1:4 (Appendix B). At the end of the dropwise of the two solutions on the support, was performed a thermic treatment at 110 °C. The results, presented in the figure 4.22, showed a dimension of the NPs larger than one order of magnitude respect of the wished dimension of few nano-meters. Anyway the results obtained were better than ones from the impregnation technique. The figure 4.22 suggested the Au clusters formation. Anyway NPs no smaller than 200 nm were indentified during the FESEM analysis.

### The Liquid Phase Reductive Deposition (LPRD) method

With the last method proposed, the LPRD one, the best results were obtained.

As for the impregnation and DI methods the support was dried in the oven

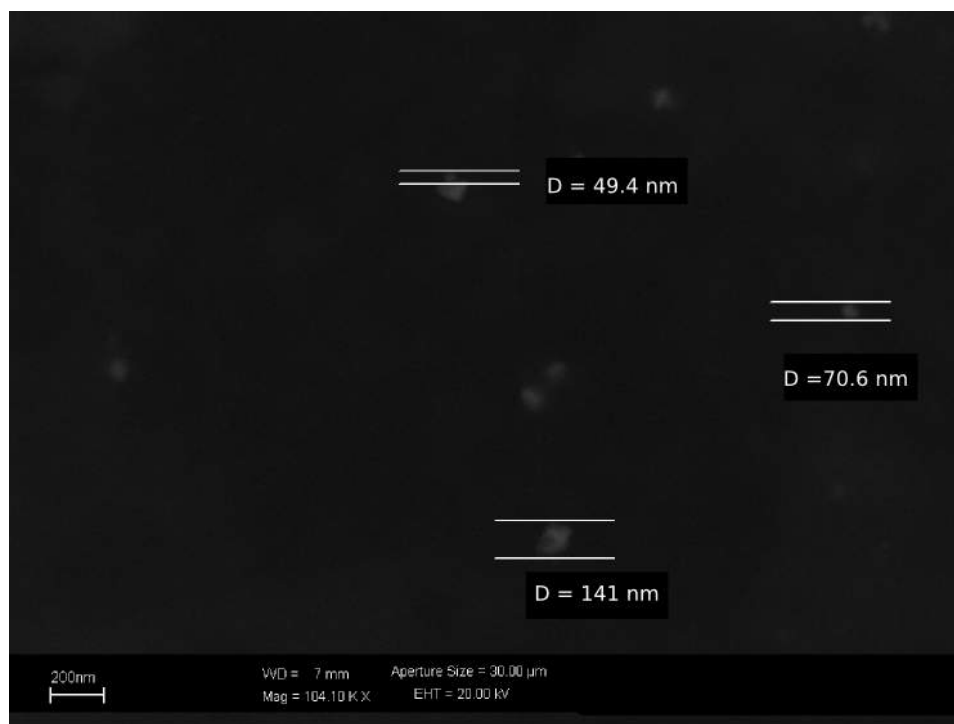


Figure 4.23: The FESEM image takes from the sample with Au NPs synthesized with LPRD method; support: carbon black

at 100-110 °C for 1 hour. Two solutions were prepared, one with the metal precursor and one with a sodium hydroxide in order to obtain the  $\text{Au}(\text{OH})_3$  (Appendix B). The two solutions were mixed together overnight. The day after the solutions were used to impregnate the support and at the end of the dropwise the support was dried in the oven. The heat treatment at 110 ° was performed to reduce the gold hydroxide to obtain Au NPs [1,2]. Because with the LPRD the NPs synthesized had the smallest dimension obtained (figure 4.23), this technique was also used on another support: a mesoporous carbon with an higher specific surface (figure 4.24). This first preliminary study indicated the LPRD method as the best technique. Anyway the dimension of the NPs, even if small, was not yet of the theoretical best size. Further studies was conducted in order to obtain the desired morphology and to give a reproducible and a simply way of synthesis for the catalyst.

#### 4.3.2 The improvement for the synthesis of the gold based catalyst

In this section will be treat the different techniques studied in order to obtain the best catalyst. Different aspects were taken into account: pH, the nature

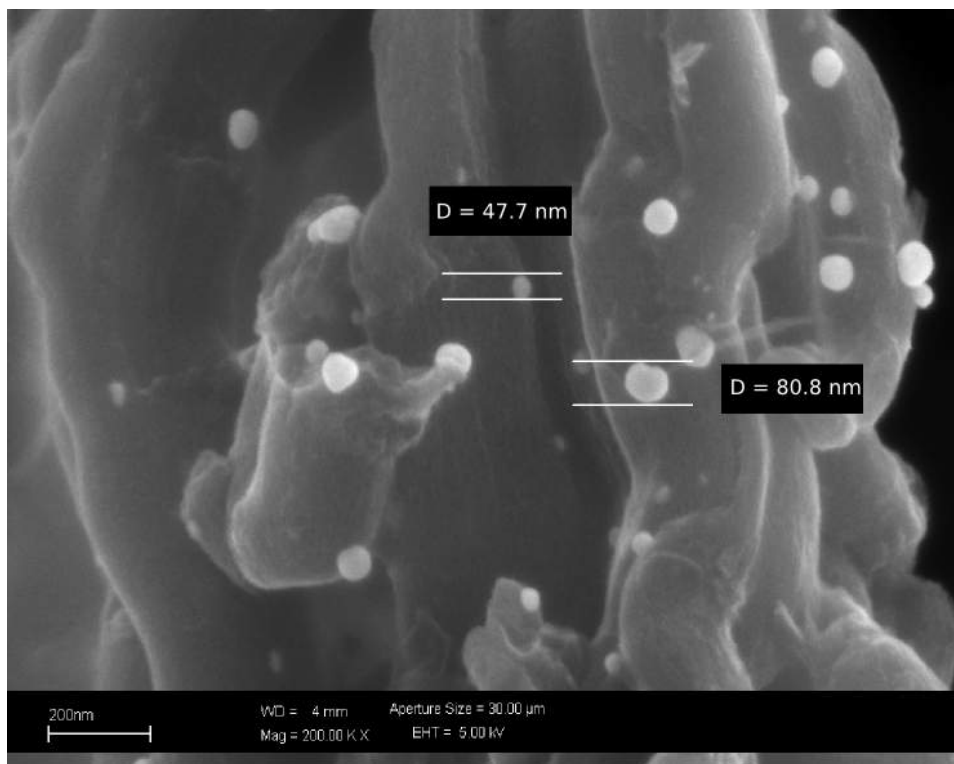


Figure 4.24: The FESEM image takes from the sample with Au NPs synthesized with LPRD method; support: mesoporous carbon

of the support and the utilisation of chemicals as surfactants.

New supports were studied with the aim to find different solutions and to investigate if the nature of the support can influenced the synthesis. The supports studied were:

- graphite
- graphite oxide (GO)
- multi-wall carbon nanotubes
- carbon black by sigma aldrich
- single-wall carbon nanotubes

the nanotubes were provided from the group of prof. Alberto Tagliaferro, Politechnic of Turin. Anyway with the discovery of the *errata-corrige* from Rodrigues *et alii* [54], the solution with the mono-metallic catalyst was abandoned and not all supports in the list were tested.

The GO was also used as support for the bi-metallic catalysts, while LPRD was the main method used for the synthesis because of the good results reached.

### **The pH control and surfactant agents**

One of the parameters that were taken into account was the pH of the solution during the metal deposition. There are different points of view in literature related to the optimal pH during the synthesis. The pH value seems to be responsible of the growth of the nanoparticles, their dimensions and distribution on the support [19]. From a point of view a faster growth seems to be the right way to obtain good dispersed NPs while, on the other hand, a slower growth seems to avoid the agglomeration. In the following synthesis, when specified, the pH was controlled during the deposition of the metals.

From experiments performed in laboratory was observed that when the value of the pH is between 5 to 7 the conditions were good to obtain the wished dimension of the NPs. Anyway not only an acid pH offered good results. Finally, to obtain the desired morphology, surfactant agents were used in order to cap the ions formed during the reaction and before the reduction of the metals to avoid the agglomeration phenomena.

### **The graphite as support**

The graphite was purchased by Sigma-Aldrich. The synthesis of the catalyst with this support was conducted with and without the pH control. Without the pH control the method was the LPRD already explained before. This synthesis conducts to the results in figure 4.25. In the same figure it is possible to observe a better distribution of bigger particles. Even if the distribution seems to be good, the dimension of the NPs results no homogeneous. The NPs dimension was still too "big" with particles with dimension from 17 to 20 nm. The same synthesis with the same support was conducted modifying the pH during the reaction. The main idea was to modify the pH in order to accelerate the reaction to avoid the NPs agglomeration. Immediately after the dropwise ending, the pH solution was brought to a basic value between 12 and 13. The modification of the pH was done by dripping a solution 1 M of NaOH. In figure 4.26 is possible to observe big agglomerations (figure 4.26), clusters of NaOH salt residual and not reacted during the synthesis. For this reason a washing step before the catalyst utilisation became necessary. On the other hand working with a pH between 12 and 13 the dimension of the particles obtained was more homogeneous with a better dispersion. To have an idea of the NPs dimension, in figure 4.27 a picture from the same sample shows some NPs diameter at higher zoom (750.00 kX).

### **The carbon as support with the pH control**

Following the good results obtained with the graphite by controlling the pH, the same way was followed with carbon by Sigma-Aldrich. The results ob-



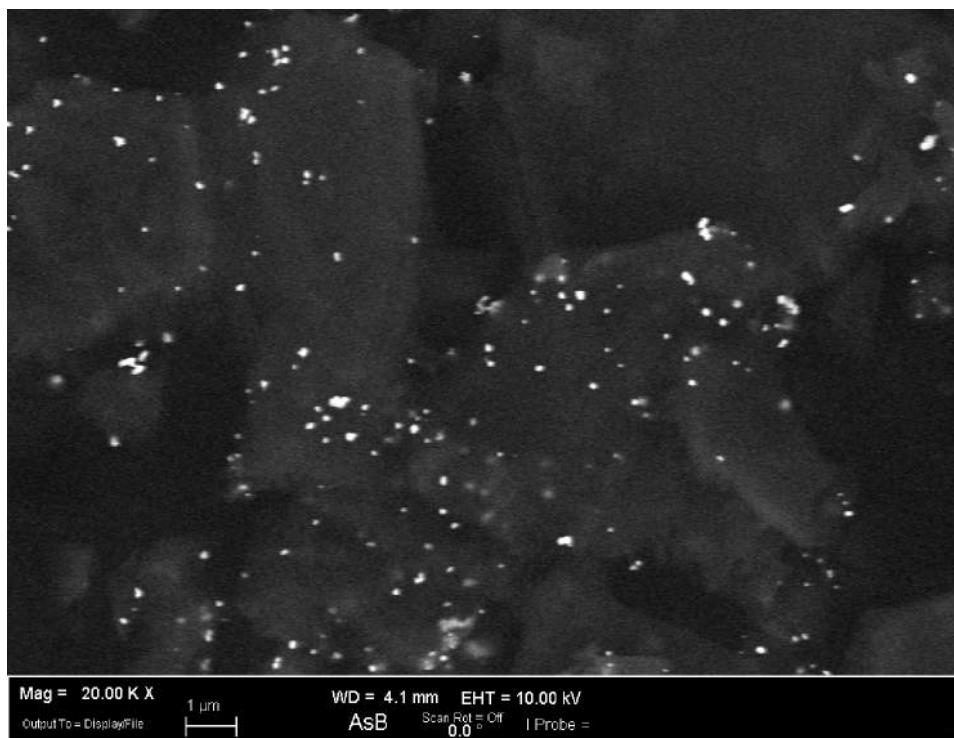


*Figure 4.25:* The FESEM image takes from the sample with Au NPs synthesized with LPRD method; support: graphite without pH control

tained with this support are reported in figures 4.28 and 4.29. Two pictures taken from the same sample but in different region to show the homogeneous NPs distribution.

Another step was realized to decorate the supports with metal NPs. Even if the goal to reach the NPs dimension lower than 15 nm was reached with a good homogeneity, another test was performed using a surfactant agent. In this section will be reported the results obtained on carbon black by Sigma using cetyltrimethylammonium bromide (CTAB) as surfactant agent. The synthesis method was always the LPRD one where an amount of 100 mM of CTAB was added to the suspension, before the dropwise of metal precursors in solution with water.

In figure 4.30 it is possible to observe the results obtained with the CTAB addition. At the limit conditions of FESEM it is possible to observe the presence of very small Au-NPs.

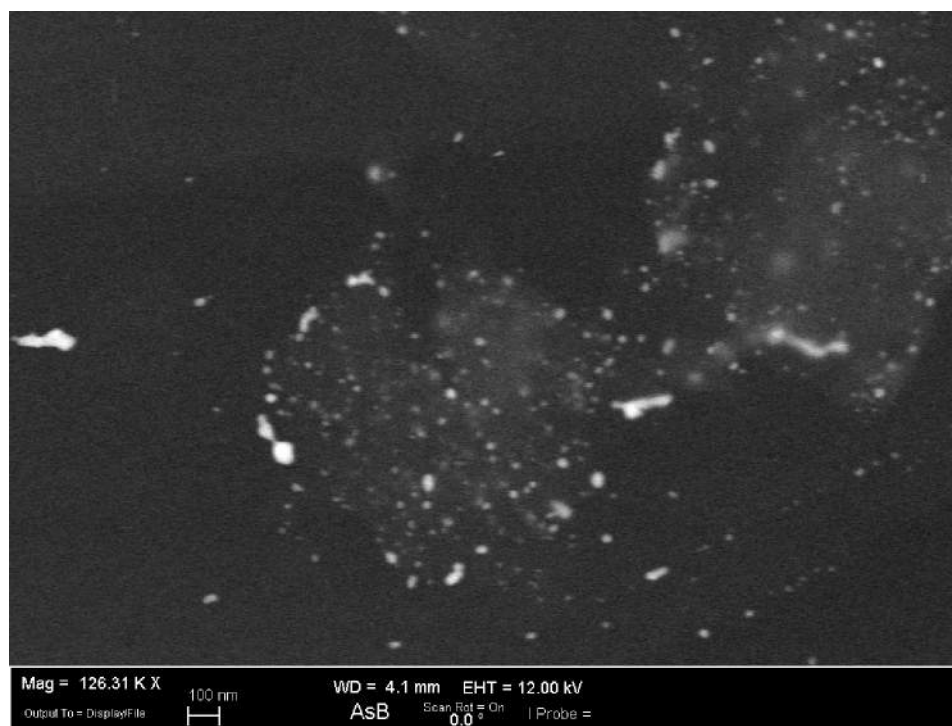


Figure 4.26: The FESEM image takes from the sample with Au NPs synthesized with LPRD method; support: graphite with pH control

#### 4.4 The bi-metallic catalysts

In the preliminary study these catalysts were not taken into account. After the publication of the *errata-corrige* by Rodrigues and co-workers, the attention moved to looking for another possible heterogeneous catalyst. Because the good results obtained, the attention was posed on the work published by Hu and co-workers (2011) [47]. In this work a bi-metallic catalyst based on Pt-Bi was employed for the selective oxidation of glycerol into DHA in stirred tank reactor. Even if the results were good the maximum yield was limited, with not a completely conversion of the glycerol.

Studying the bi-metallic catalyst, one of the idea was to improve the results of Hu and co-workers even testing new supports. Hu and co-workers, indeed, proposed a Pt/Bi ratio optimisation but keeping unchanged the nature of the support. Anyway, such as reported in literature (see chapter 1), many groups have shown the importance of the support on the catalyst's activity (conversion and selectivity). Finally different aspects were not completely clear:

- how the bi-metallic catalyst works exactly
- if it is possible to reach an higher yield by improving the catalyst

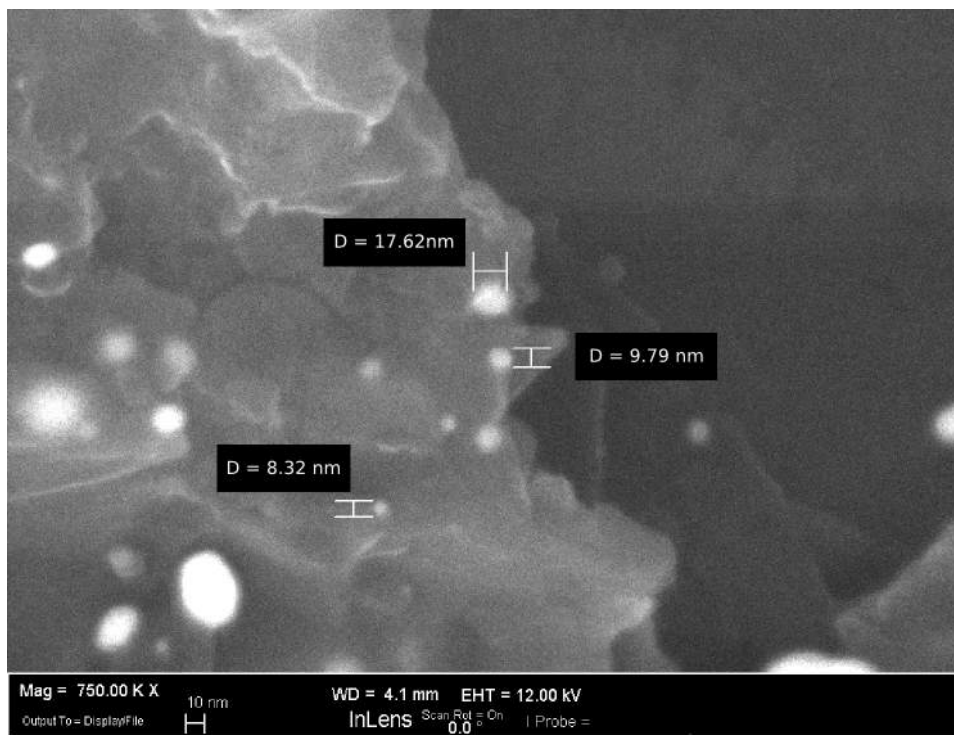


Figure 4.27: The FESEM image takes from the sample with Au NPs synthesized with LPRD method using NaOH 1 M; support: graphite with pH control

nature: the bi-metallic NPs dispersion and dimension

- what is the role of the Bi: other studies showed how the only Bi was inactive in the oxidation reactions

Because all of these reasons the idea was to pursue the following goals:

- to improve the results [14,47] working on the reactor design
- to look for a reproducible method for the catalyst synthesis, with the aim to scale-up the reaction
- to study new possible supports

#### 4.4.1 The catalysts synthesis

The graphite was chosen as support. The graphite was chosen because one of the cheapest supports available. Moreover its functionalisation became the aim of the bi-metallic catalysts development. The idea was to improve the NPs dispersion on the support reducing the clusters dimension and increasing their activity. The aim was to functionalize the support's surface to anchor the NPs seeds and to control their growth.

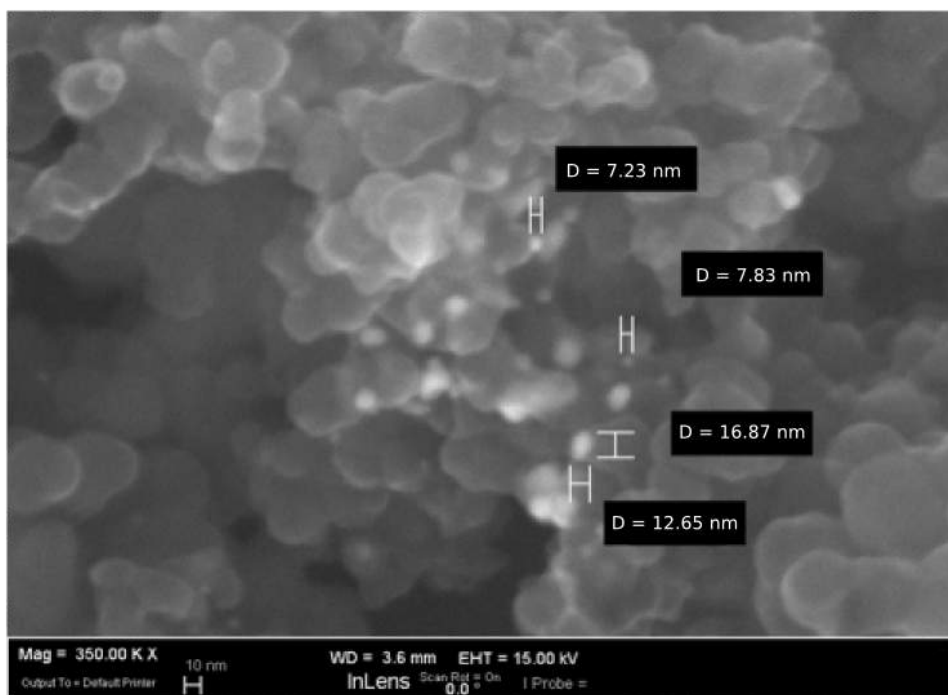


Figure 4.28: The FESEM image takes from the sample with Au NPs synthesized with LPRD method; support: carbon with pH control

#### 4.4.2 The carbonious supports and the metals deposition

The graphite was bought from Sigma-Aldrich and the GO was synthesized in laboratory. The graphite functionalisation was performed referring to the Hummers method (1958) [52] (Appendix A).

The graphite functionalisation allowed to modify the graphite morphology, obtaining different functional groups between the graphite flakes [58]: -C-OH, -C=O, -COOH. In figure 4.31 it is possible to observe a simulation about the difference from a graphite sheet and a GO one.

The Hummers method was modified during the study in order to obtain different graphite functionalisations (Appendix A).

To confirm the functionalisation of the support the X-Ray diffraction (XRD) and the X-Ray photoelectron spectroscopy (XPS) analysis were did. The XRD analysis was considered the faster way between the two analysis and permitted to check the functionalisation of the support. The characteristic peak of the graphite, indeed, shifts after the functionalisation from a value of  $26^\circ$  ( $2\theta$ ) to a value around  $10^\circ$  ( $2\theta$ ).

Anyway this method did not give any information about the nature of the functional groups on the support (figure 4.32).

As the XRD intuitively shows, the GOII, for example, was less functionalized (%Area of functional group on the surface) than the GO IV: these

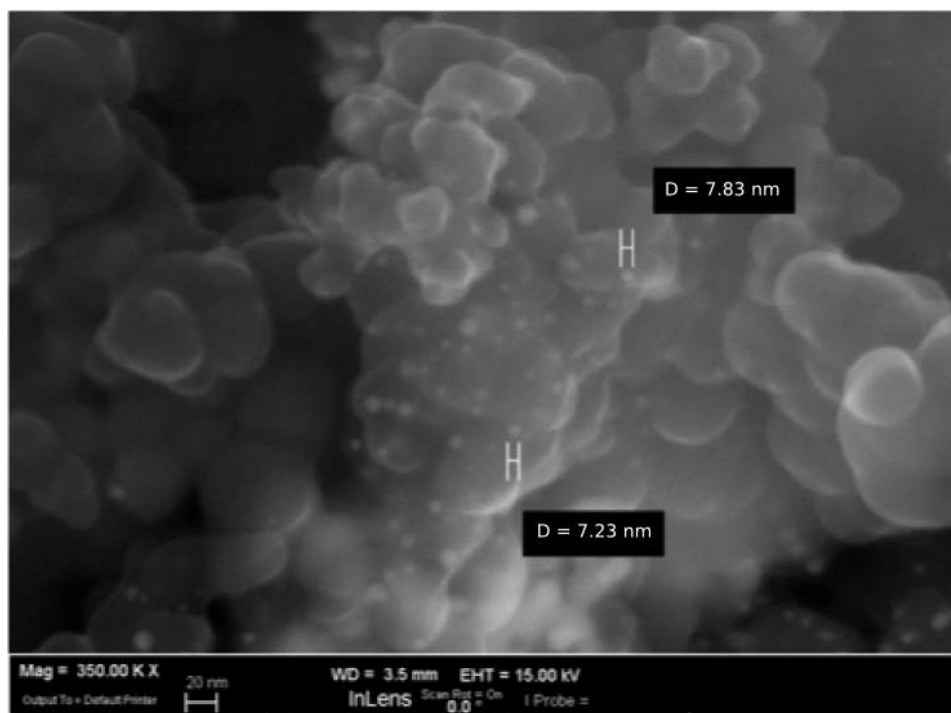


Figure 4.29: The FESEM image takes from the sample with Au NPs synthesized with LPRD method; support: carbon with pH control

qualitative informations were confirmed later by XPS analysis. In figure 4.33 the different XRD spectra of the GO are compared.

For the support less functionalized, the GO II and the GOIII, no peaks at  $10-11^\circ$  ( $2\theta$ ) appear. On the other hand the characteristic peak of the graphite, at  $26^\circ$  ( $2\theta$ ), disappears completely. In these two cases only the XPS confirmed the surface modification, describing accurately its functionalisation. In figure 4.34 the XRD analysis on GO II and the GO III XRD are compared. Together with XRD analysis the XPS offered more completely informations about the sample surface. In order to analyzed the XPS spectra and to proceed with the peaks' deconvolution the NIST database was used as main reference ([srdata.nist.gov/xps/default.aspx](http://srdata.nist.gov/xps/default.aspx)). Together with the characteristic peak of the C-C bounds other peaks appeared. These peaks were associated to -C-OH, -C=O, -COOH groups. The figures 4.35 and 4.36 show the XPS results for a graphite and a GO samples.

The XPS technique was used also for the analysis after the metal NPs deposition. It was chosen because gives the possibility to understand the nature of the NPs in their oxide form, metallic one or coupled system.

As in the case of the mono-metallic catalyst the deposition was performed with the impregnation method. The precursors of the Pt and Bi was bought from Sigma-Aldrich in form of  $\text{H}_2\text{PtCl}_6$  hydrate,  $\text{Bi}(\text{NO}_3)_3$  and  $\text{BiCl}_3$ . After

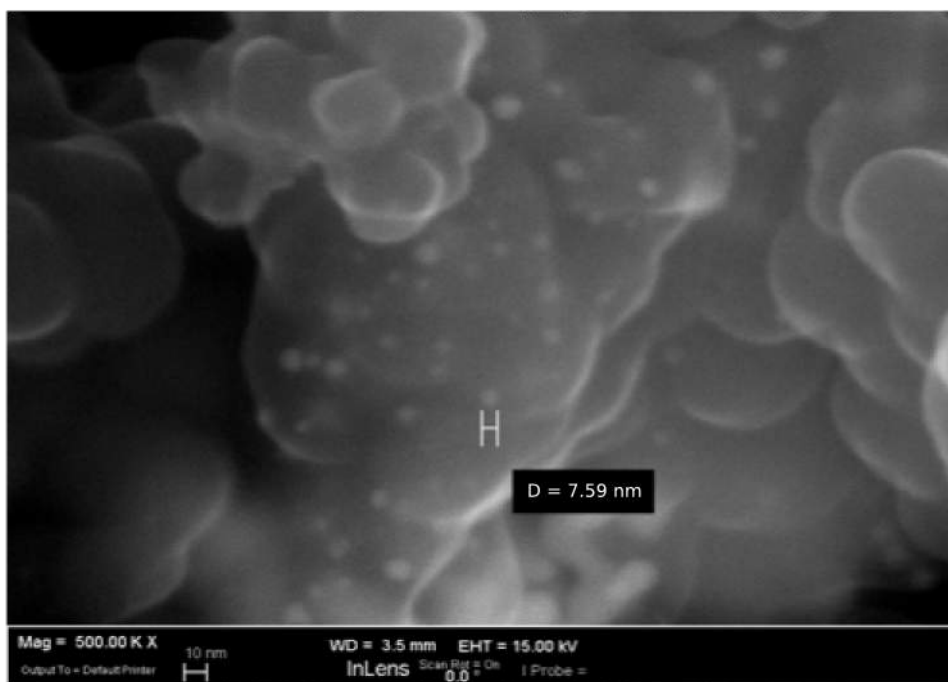


Figure 4.30: The FESEM image takes from the sample with Au NPs synthesized with LPRD method using CTAB

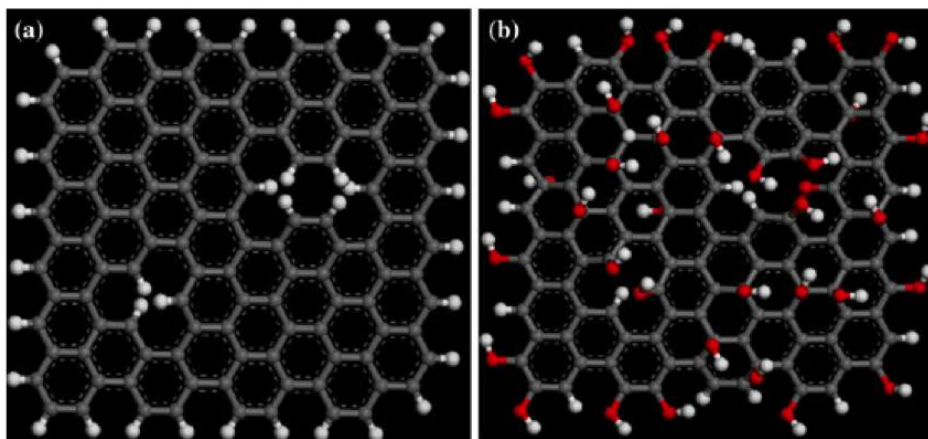


Figure 4.31: The graphite sheet (a) and a graphite oxide sheet (b)

the impregnation the reduction was carried out using  $\text{NaBH}_4$ . This method offered a fast and an easy way for the catalyst synthesis.

The catalyst was synthesized in a 250 ml flask with three necks and using a Liebig refrigerant to permit the reflux (the completely synthesis is better described in Appendix B). The impregnation was done by a dropwise of the metal precursors in solution with water, directly in the flask where the sup-

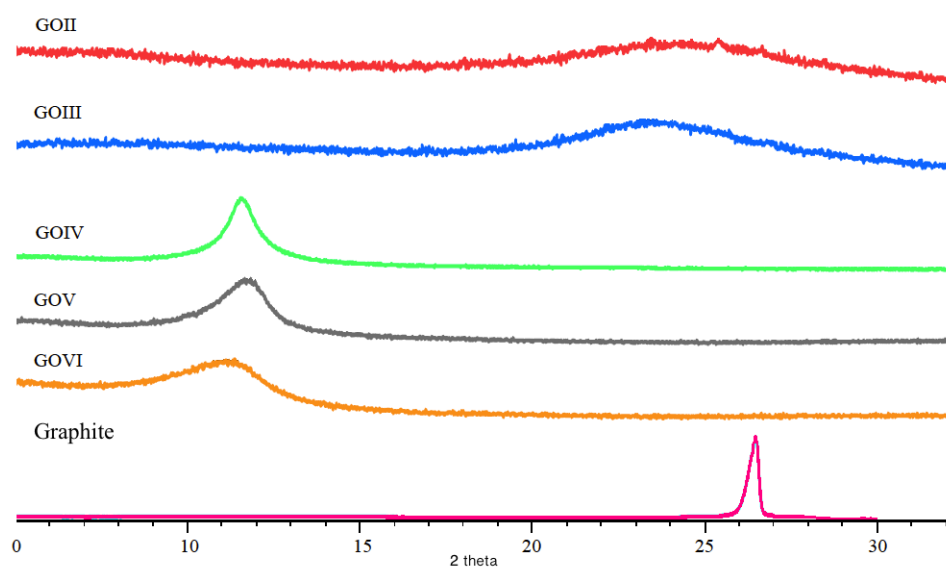


Figure 4.32: The XRD on the graphite and on the GO; the XRD shows the shift on the graphite peak

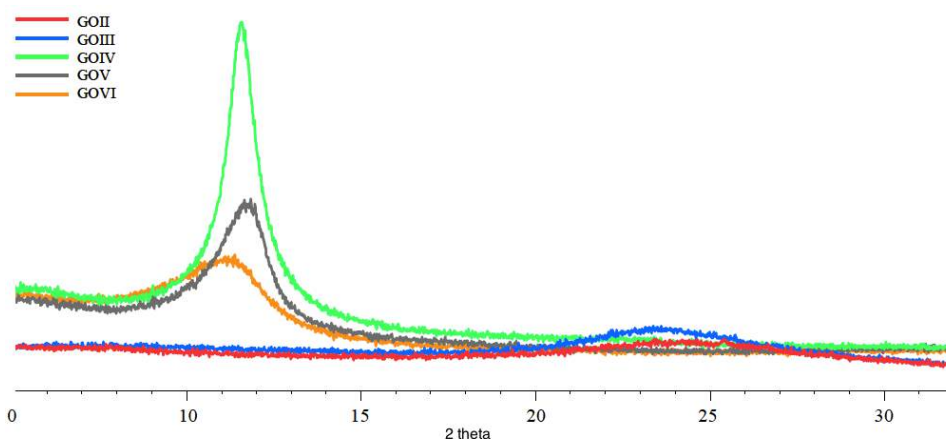


Figure 4.33: The XRD on the graphite and on the GO; the XRD shows the shift on the graphite peak

port was in solution with water: the GO is not hydrophobic like graphite. The functionalisation of the support confirmed the possibility to reach better results in terms of dispersion and nano-particles dimension. In figure 4.37 is reported the Scanning Transmission Electron Mycroscopy (STEM) image of Pt and Bi nanoparticles on graphite oxide (GO III). The complete method of synthesis, to obtain the results just presented, is accurately described in the Appendix C.

In the following chapters will be presented some results obtained with the

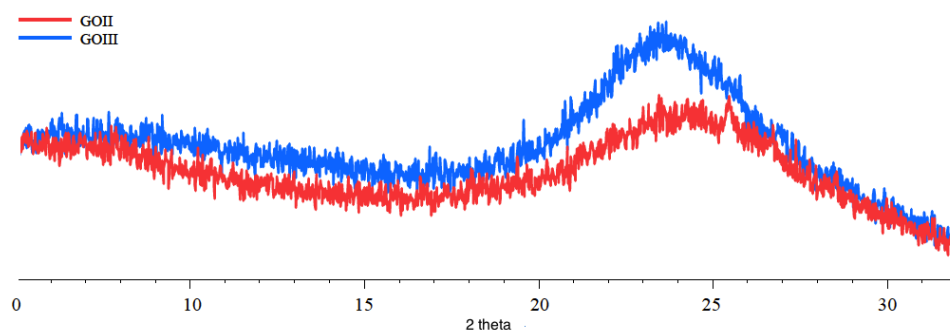


Figure 4.34: The XRD comparison between the two GO weakly functionalized

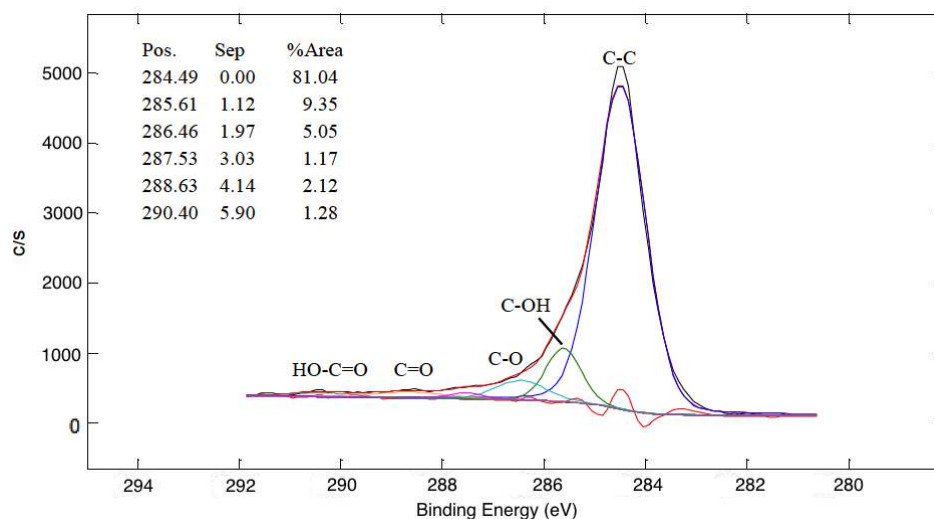


Figure 4.35: The XPS on the graphite by Sigma-Aldrich

deposition of the Pt and Bi NPs on the functionalized supports. To characterize the catalysts, together with XRD and XPS, other two techniques were used:

- Field Emission Scanning Electron Microscopy (FESEM) and STEM microscopy to define the morphology
- Energy Dispersive X-ray Analysis (EDX) analysis

#### 4.4.3 Bimetallic Pt-Bi on graphite oxide

In order to obtain different supports at different functionalisation level, some modification at the original Hummers method was performed (Appendix A). These modifications were well described in literature [94] and with them it



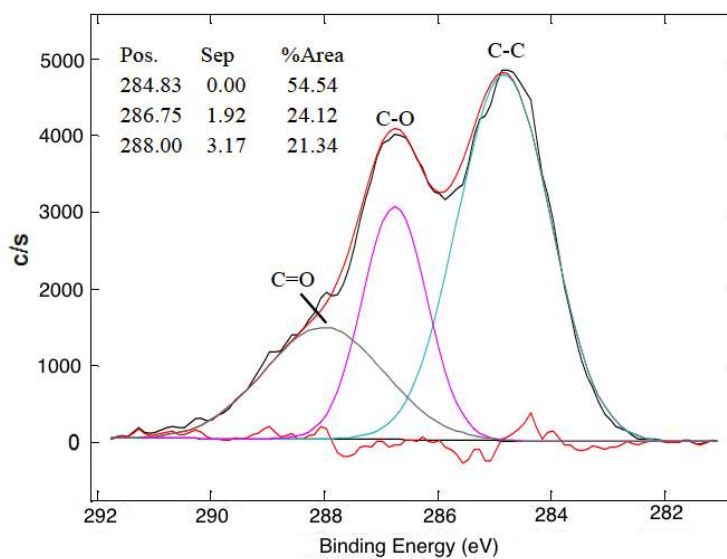


Figure 4.36: The XPS on the GO IV obtained in laboratory; see the Appendix B for the synthesis description

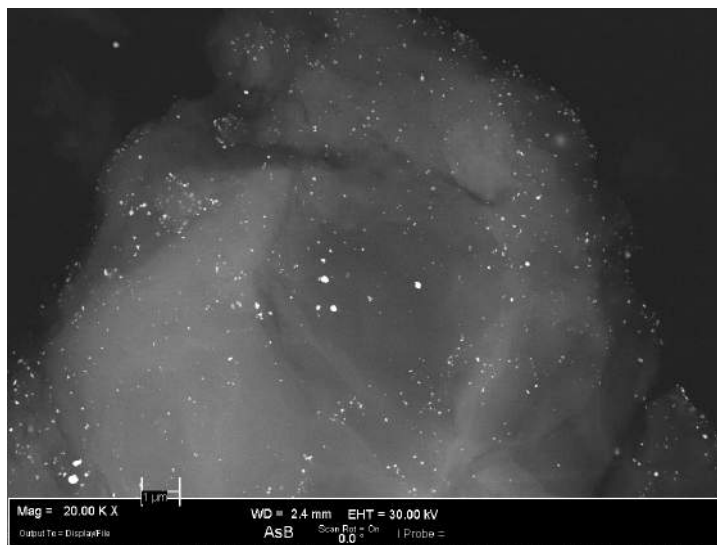


Figure 4.37: Pt Bi nanoparticles on graphite oxide; deposition using subsequent impregnation

was possible to obtain different supports. Usually the main differences that occur between the approaches can be summarized by three points:

- reaction time
- moalr ratio between reagents
- temperature

## The PtBi-based catalysts

The results obtained using graphite and GO as supports were compared with results obtained with a carbon black and graphite as supports. The reason of this choice is due to have the necessity to compare the results and to put in evidence the main differences.

The results presented in this chapter were obtained with the analysis techniques presented before. An initial analysis at microscope was important in order to have an idea of the morphology of the samples and to evaluate their dimensions.

The first results here presented are related to the deposition of the NPs on the GOII and GOIII. The only difference on this two supports synthesis is related to the molar ratio between the reagents,  $\text{H}_2\text{SO}_4$ ,  $\text{NaNO}_3$  and  $\text{KMnO}_4$ , and the graphite (see Appendix A).

The figure 4.38 is an example of the GOII decoration with particles of Pt and Bi. The figure 4.39 shows the sample of figure 4.38 from the same point of view, but placing in evidence the NPs distribution and their dimensions. Apart from the morphology no more informations about the nature of these

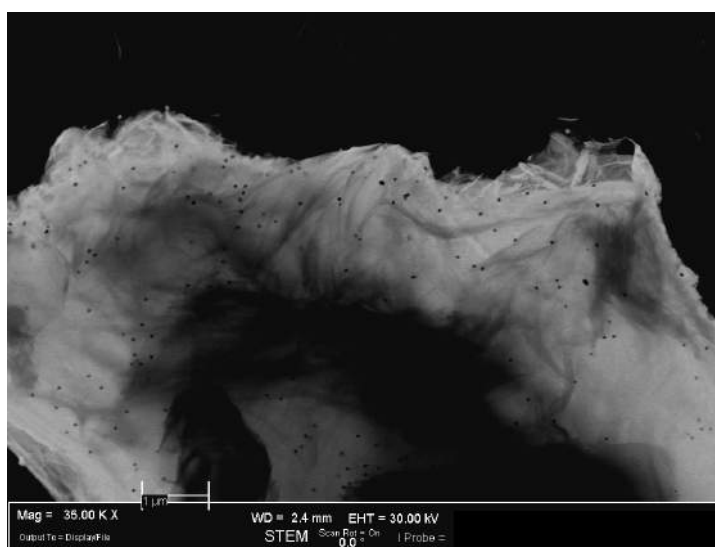


Figure 4.38: Pt Bi nanoparticles on graphite oxide (GO II) using the STEM

NPs can be collected with this technique. The XPS and EDX analysis became necessary to investigate the nature of these NPs in their mono-metallic or bi-metallic (PtBi) composition as coupled system.

Very similar results were obtained with the GOIII as showed in figure 4.40. Could be interesting to underline the importance of the coupled system PtBi one more time. Based on the literature results [4,47,50] the Bi reduce the velocity of the Pt poisoning. For this reason the presence of coupled system PtBi structure was an important goal to reach.

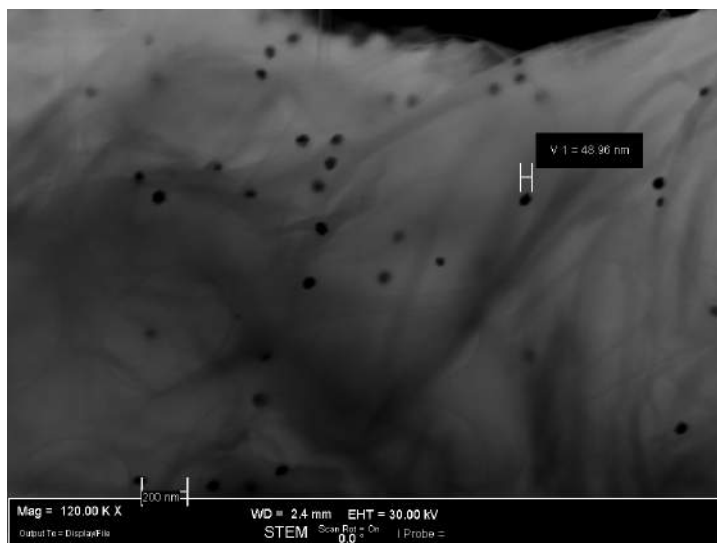


Figure 4.39: Pt Bi nanoparticles on graphite oxide (GO II) using the STEM

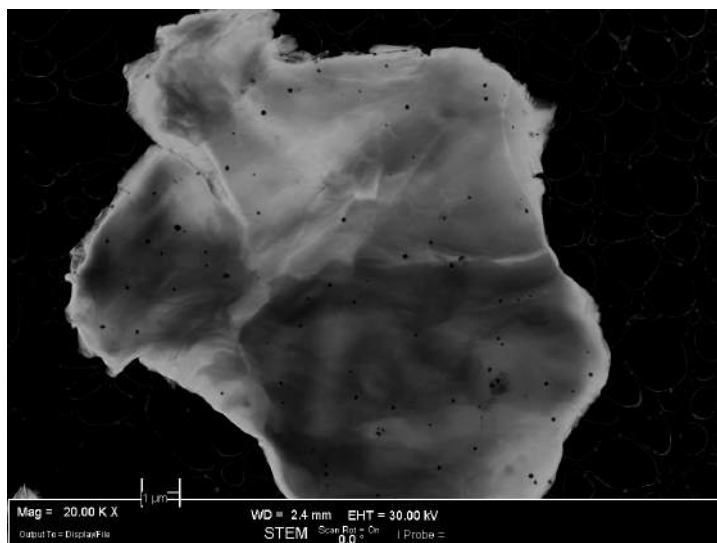


Figure 4.40: Pt Bi nanoparticles on graphite oxide (GOIII) using the STEM

#### 4.4.4 The EDX and XPS analysis

In the following three pictures (figure 4.41, 4.42 and 4.43) is presented a comparison between the graphite after the XPS analysis. The GO II and GO III were used as supports.

The XPS analysis offered the possibility to put in evidence the functional

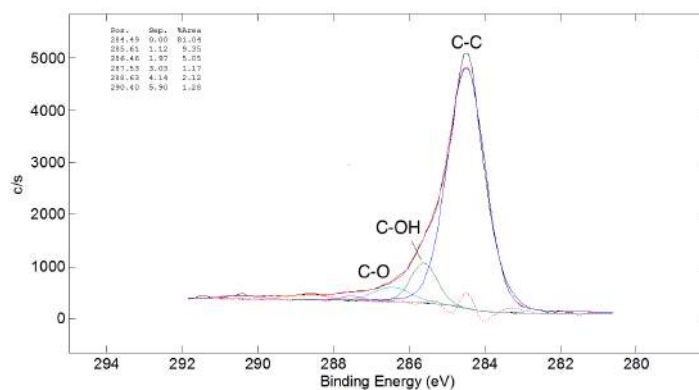


Figure 4.41: the XPS of graphite on the C binding energy range

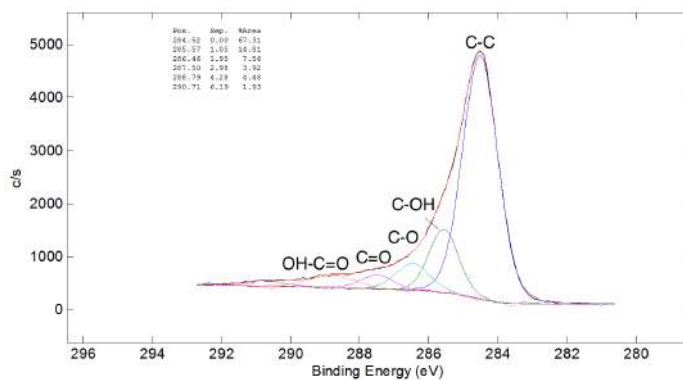


Figure 4.42: the XPS of graphite oxide GOII on the C binding energy range; were put in evidence the functional groups

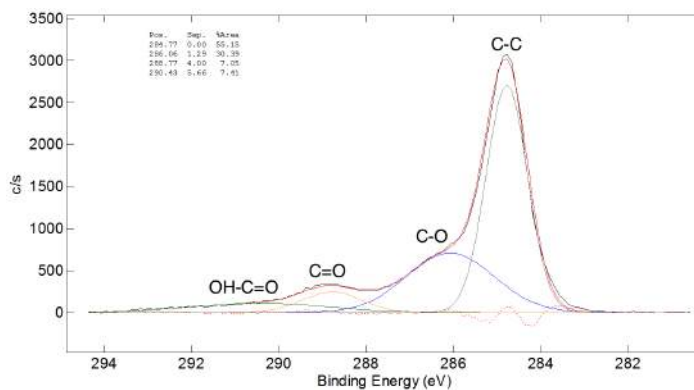


Figure 4.43: the XPS of graphite oxide GOIII on the C binding energy range, were put in evidence the functional groups

groups on the surface. In the three pictures it was possible to recognize the graphite before and after its modification (deconvolution of the peaks).

Moreover the analysis of the XPS's spectra confirmed the presence of the functional groups expected, and the % Area gave a qualitative idea of the functionalisation level.

Even after the impregnation the XPS analysis was performed. With the help of the literature were individuated the binding energy for the Pt and the Bi. In the figures 4.44, 4.45 and 4.46 the XPS spectra related to the C binding energy range are presented together with the Pt and Bi ones. First of all

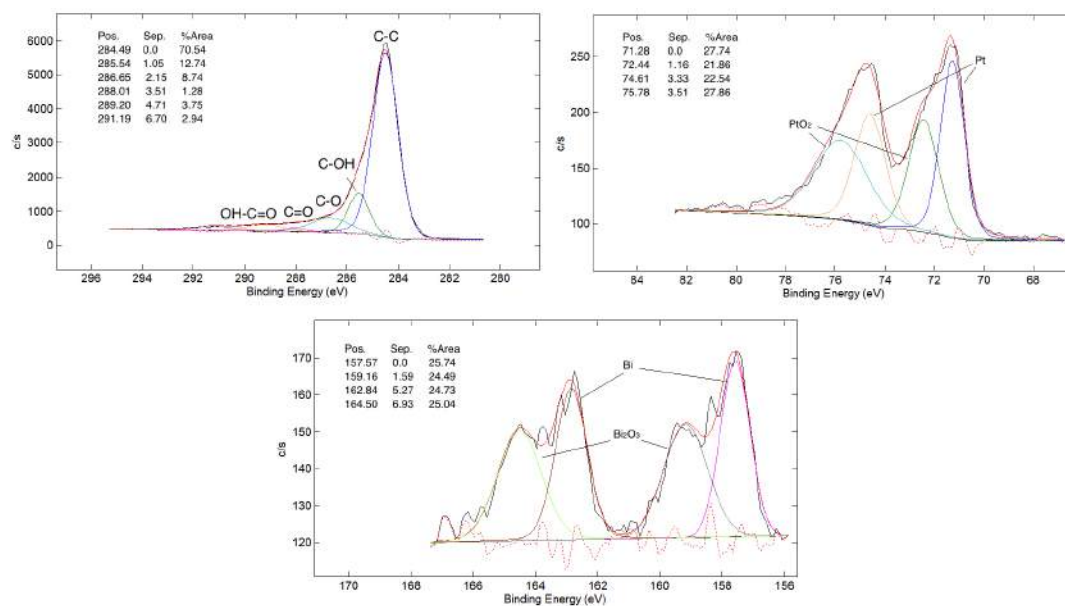


Figure 4.44: the XPS of graphite after the impregnation; together with the C binding energy are presented the Pt and the Bi binding energy ones

with the help of XPS was possible to verify the presence of two typologies of Pt, in a metal form as Pt and as PtO<sub>2</sub> (see figure 4.44). Even the Bi was presented in its oxide form and as Bi. The presence of the Pt in its metal form was a good information about the potential activity of the catalyst. The Bi as metal alone, indeed, did not showed any activity to the alcohols oxydation [47].

Another one information came from these spectra and in particular from the Bi binding energy range. A peak in the binding energy range between 157 eV and 159 eV was detected and suggested the presence of Bi/Pt as coupled system (assumption supported by NIST data base). In order to confirm the presence of the two metals in their coupled form, an EDX analysis was conducted on the same samples. The data from XPS were used together with the EDX analysis to confirm the bi-metallic structure.

In figure 4.47 an EDX analysis on the graphite sample is showed. The analysis was done in a specific spot and the spot is identified with a cross

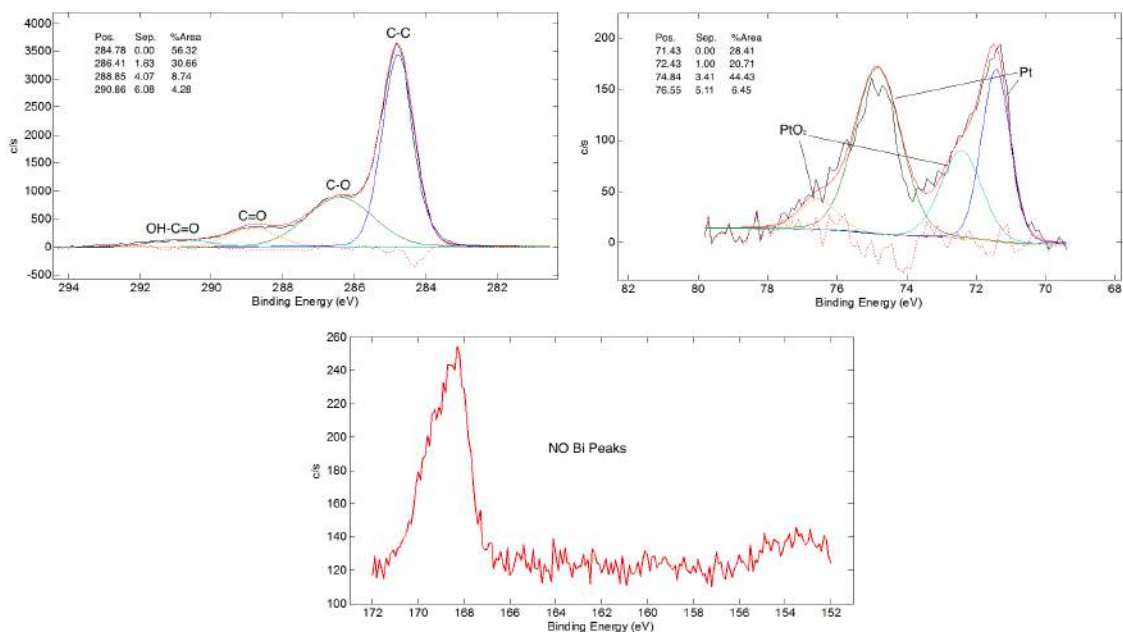


Figure 4.45: the XPS of GOII after the impregnation only with Pt metal precursor; together with the C binding energy are presented the peaks of Pt

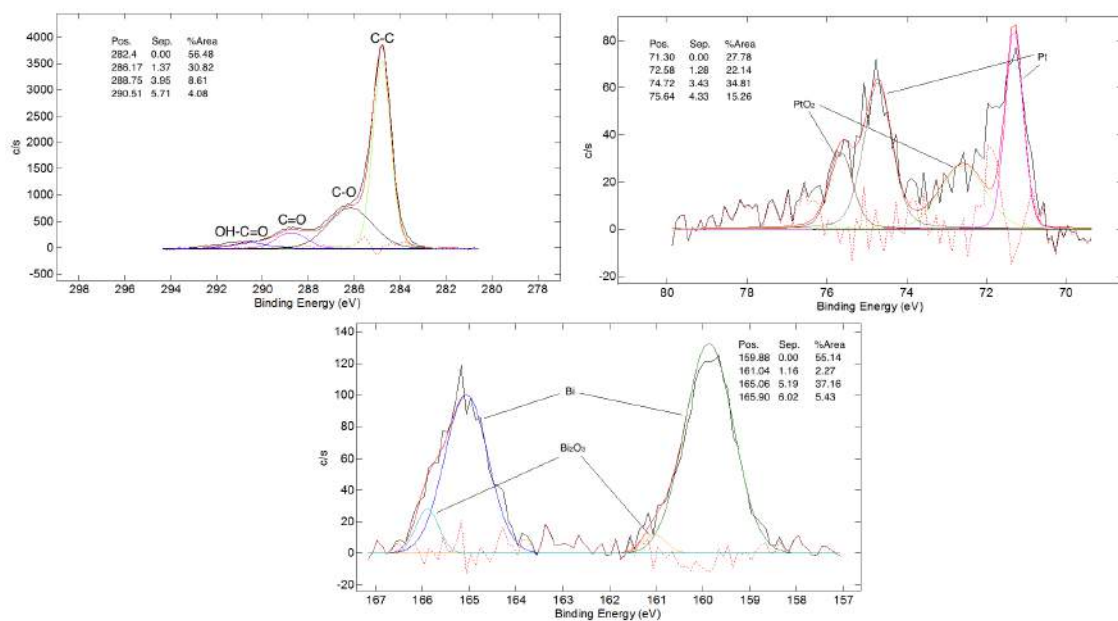


Figure 4.46: the XPS of GOIII after the impregnation; together with the C binding energy are presented the Pt and the Bi binding energy ones

and was positioned in the middle of a NPs. The analysis confirmed the

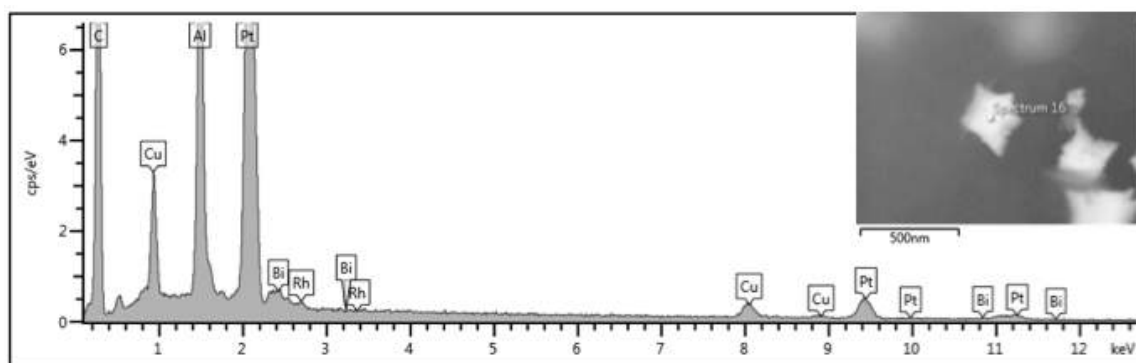


Figure 4.47: the EDX analysis on the PtBi based catalyst on graphite

presence of different species:

- C is the signal related to the graphite
- Al and Cu are the signal from the support
- Rh is a signal probably due to the presence of impurity directly from the flask used for the synthesis
- Bi and Pt signal confirm the presence, in the point selected and immediately near, of the PtBi; this signal supported the thesis about the presence of a coupled system

The same considerations about the peaks revealed from EDX analysis can be made for the other samples. In figure 4.48 and EDX analysis confirmed the absence of the Bi on the support. The EDX result was done not in a single point but on a bigger area. That one reported in the picture in the right side of the EDX spectrum showed in figure 4.48. This information was

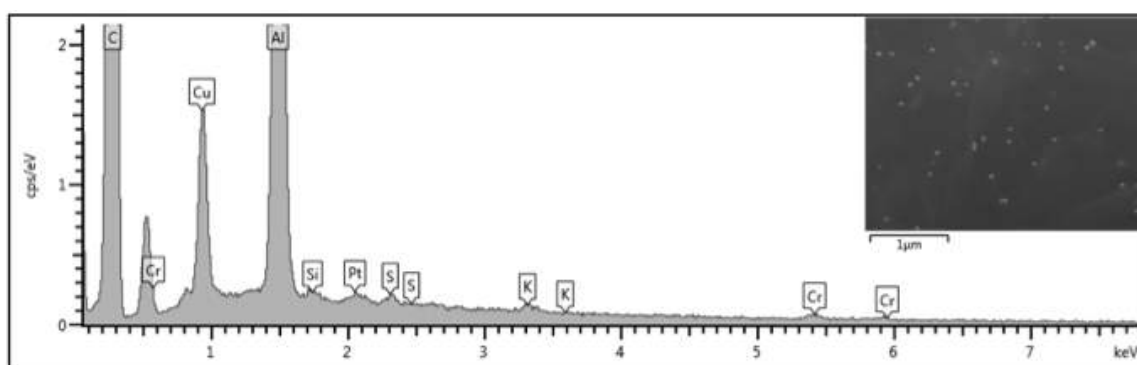


Figure 4.48: the EDX analysis on the PtBi based catalyst on GOII; this EDX analysis was a further information about the absence of the Bi on the surface

in accord with the XPS analysis that, for the eV range related to the Bi,

showed the absence of the Bi. In figure 4.49 the EDX on GOIII after the PtBi deposition. The spectrum showed one more time the presence of both metals. In figure 4.50 is reported the EDX related to the same sample on

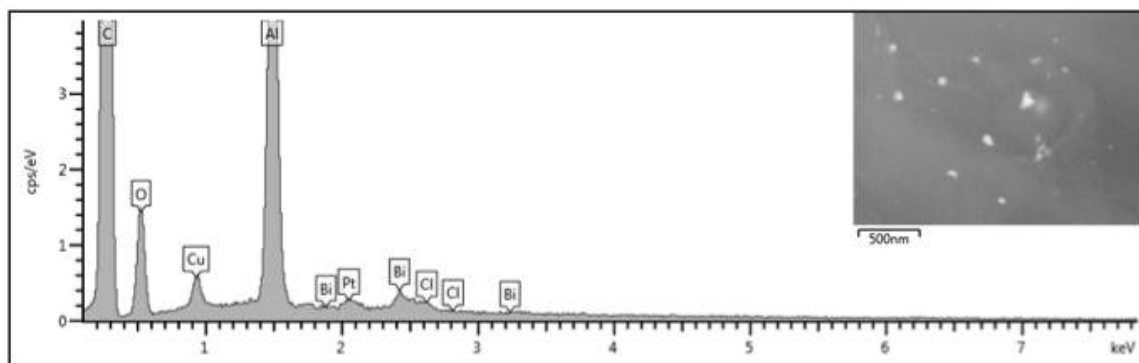


Figure 4.49: the EDX analysis on the PtBi based catalyst on GOIII; the EDX analysis was done on the entire area presented in the small window on the right side of the spectra

a single particle. This measure confirmed the presence of the Pt and Bi as coupled species as XPS signal suggested.

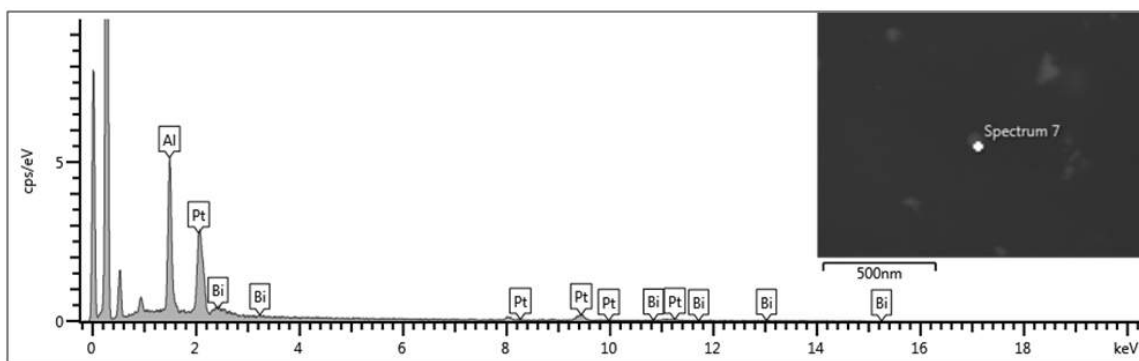


Figure 4.50: the EDX analysis on the PtBi based catalyst on GOIII; the EDX was done on the same sample of the figure 4.49 but in a punctual zone

#### 4.4.5 Further results on the GOIV, GOV and GOVI

After the good results obtained with the GO II and GO III the research moved on the direction to study the functionalisation influence on the NPs deposition. The question was simple: how a stronger functionalisation can modify the synthesis of the catalyst? In order to answer to this question three others functionalized supports were tested for the metal nanoparticles deposition. The results obtained were different.

The GO IV is the support with which was obtained the higher functionalisation (figures 4.32, 4.33). In this case the results from the NPs deposition



were worst than the results with GO II and GO III (figure 4.52). The NPs seems to be displaced on the support to form agglomerates. The method for the NPs deposition is the same for the samples on GO II and III (and described in Appendix B). Moreover on GO IV sample was difficult to find the presence of the metal particles. The reason about this result was attributed to the too high level of functionalisation. The  $\text{NaBH}_4$  used for the reduction, indeed, can easily reacts with the functional groups present on the support, reducing the possible to react with metal precursors.

A microscopy analysis on GO IV is reported in figure 4.51. Better results

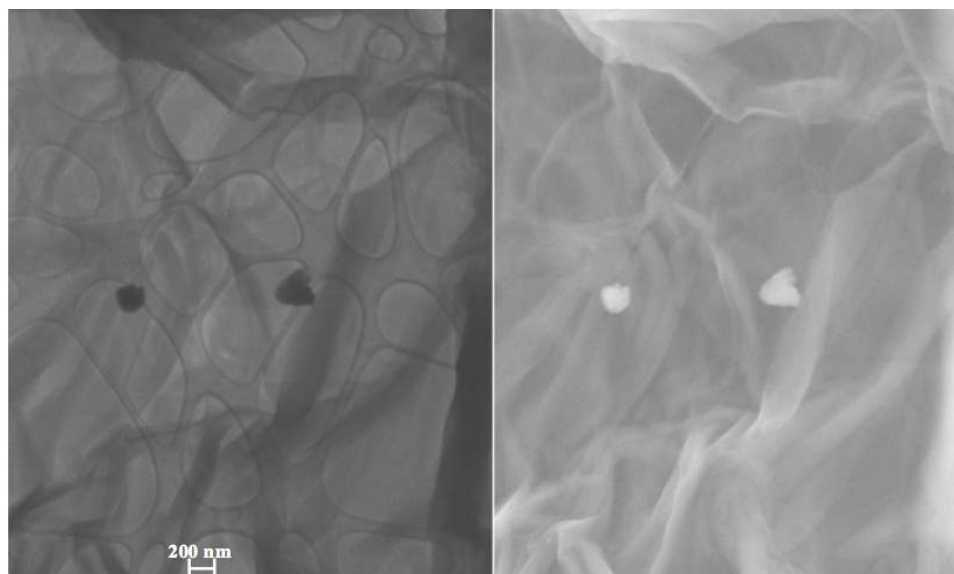


*Figure 4.51:* An image from the STEM analysis on the sample GO IV after the Pt and Bi deposition; it is possible to observe the Nps displacement on the surface

were obtained with other two supports: GO V and GO VI ( figure 4.52, 4.53 and 4.54). These supports have a lower level of functionalisation than GO IV.

With GO VI (figure 4.54) the results expected should be similar with those obtained with the GO V because the functionalisation grade was similar. On the contrary the results obtained are worst and the NPs dispersion is lower for both supports if compared with the results on GOIII, where the functionalisation was more mild. Some of these catalysts were tested (chapter 6) but more efforts are necessary to conclude the study.

#### 4.4.6 Conclusions about the bi-metallic catalysts

The aim to improve the synthesis of this bi-metallic catalyst found good results using the graphite oxide as functionalized support. The GO can be considered a good alternative to carbon black. The NPs dispersion obtained

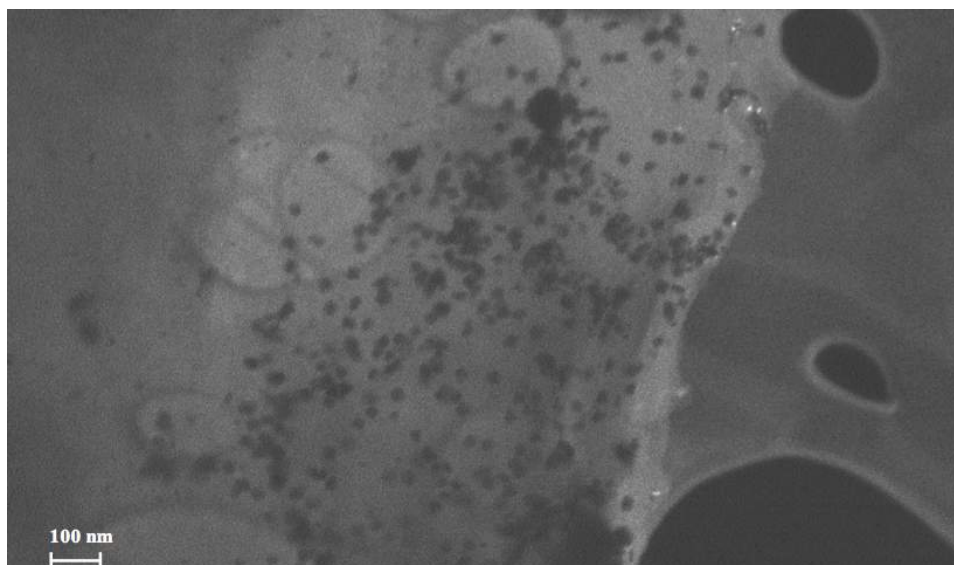


*Figure 4.52:* This image from STEM, Pt on GO V, shows the presence of the metal NPs on the surface of the functionalized support; moreover it shows how the NPs are localized on the functionalized part of the support, the finest one; the STEM permits to have an idea of the thickness of the support that it is very thin in correspondance of the functionalisation. It is possible to see, indeed, the carbon lattice of the copper grids for the FESEM microscopy through the sample

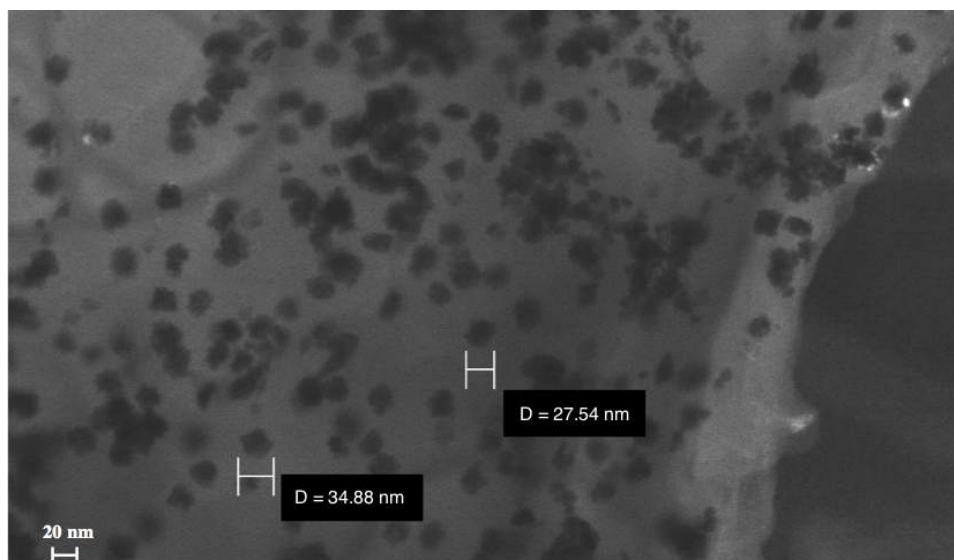


*Figure 4.53:* This image from STEM, Pt on GO V, permits to have an idea of the NPs; moreover the distribution seem to be homogeneous

with these supports is good and the dimesion of their is uniform. Moreover the results obtained show how the level of functionalisation can influence

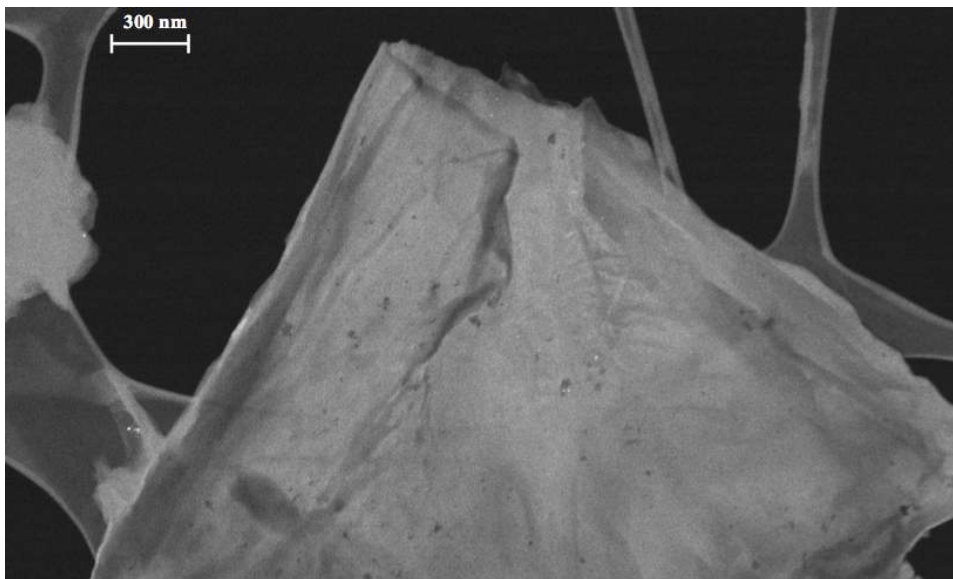


*Figure 4.54:* This image from STEM to observe the NPs of Pt on the GO VI

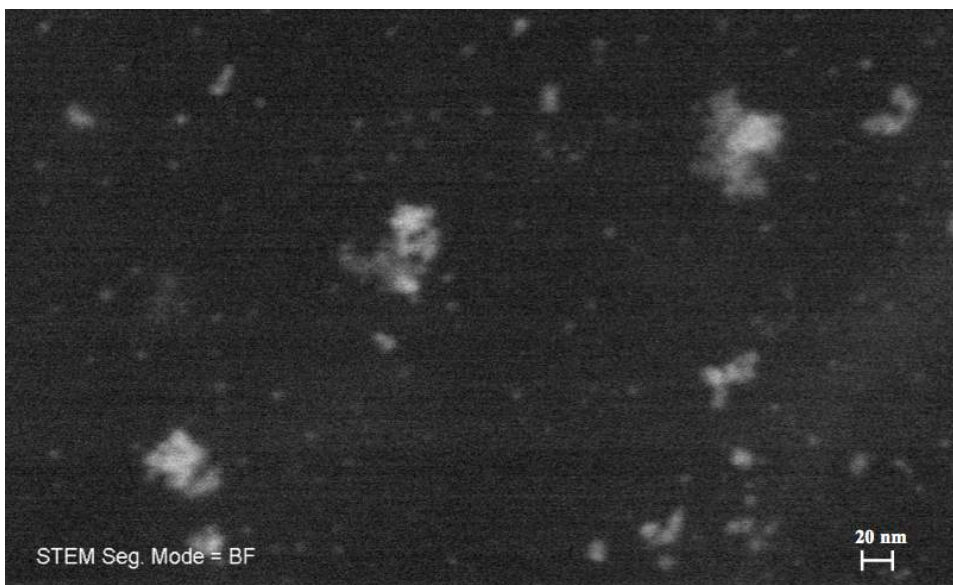


*Figure 4.55:* This image from STEM, Pt on GO VI, permits to have an idea of the NPs dimension

the dispersion and the dimension of the NPs.

The results from XPS showed the possibility to obtain three different form of the metals:

- the oxide form of the Pt and Bi
- the metal structure of the Pt

- a coupled form of the PtBi

Another important characteristic of these catalysts is its oxide nature. The GO confirmed an hydrophilic behavior and this one it is an important property considering the possibility to use the catalyst with water, reducing the possible mixing problems and mass-transfer effects.

The bi-metallic solution was studied after the bad experience with the Au catalyst and the research started in October 2013. Working in parallel with the organometallic catalyst, with which was obtained better results, the synthesis of the bi-metallic was conducted to have a second solution and for curiosity to explore a new catalytic way. Its characterization finished in October 2014 and more tests were planned for the end of this year. Some tests were started recently in order to verify the activity.

Finally it is important to underline how this catalyst was placed at disposal for other reaction where heterogeneous catalysts based on bi-metallic PtBi are under study. The reaction is the selective oxidation of glucose to D-Saccharic acid as the first step for the synthesis of Adipic Acid.

## 4.5 The tri-metallic AuPtBi catalyst

One of the catalyst tested in the reactor was one with tri-metallic nature. This catalyst was synthesized at Università degli Studi di Milano by group of prof. Prati.

Before the tests the catalyst was analyzed by FESEM (STEM) to define the particles distribution and dimension.

This catalyst presents on its surface Au, Pt and Bi as NPs (figure 6.1). The figure shows a good dispersion of the nanoparticles with dimensions even lower than 10 nm. Another picture was taken from the sample in another region (figure 6.2). This catalyst exploration shows a good homogeneity in terms of morphology.

The catalyst was supplied with the ICP characterization. The nominal value of the metal content from the ICP is the following one:  $\text{Au}_{0,6}\text{Pt}_{0,4}\text{Bi}_{1,0}/\text{C}$ .

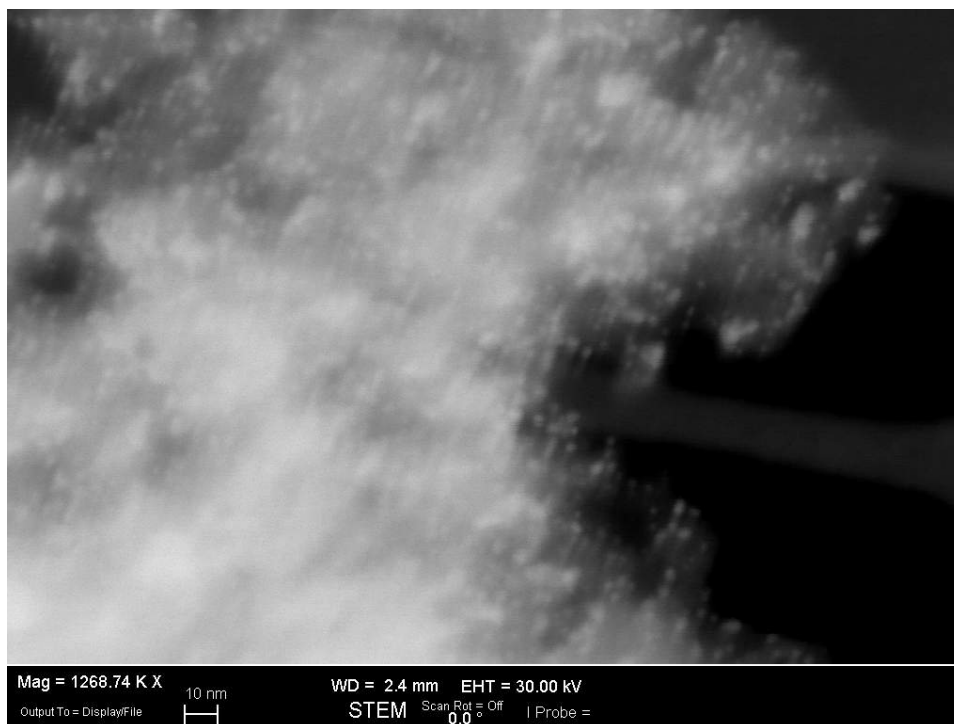


Figure 4.56: The STEM analysis on the tri-metallic catalyst



Figure 4.57: The STEM analysis on the tri-metallic catalyst

---

---

## CHAPTER 5

---

### THE ANALYTICAL METHODS

The development of a reliable analytical method became one of the principal challenge in this work. The reason was due to the absence in literature of a well described analytical method for the DHA and glycerol detection. The unique method was proposed by Hu *et alii* [46] and it was an HPLC one (not described in detail). Furthermore only one analytical method was insufficient to have a reliable way of analysis. The reason was the high number of possible by-products (figure 5.1) from the glycerol oxidation. Finally it is important to remember the error committed by Rodrigues and co-workers [54]. Their wrong analytical HPLC methodology was not able to distinguish DHA and formic acid.

For these reasons, in order to analyze the products of reaction, three ways was developed *ex novo*. The first one was a GC analysis with detector FID. The analysis was conducted with an external standard and the method required the functionalisation of the analyte with the trifluoroacetic anhydride (TFAA). Following the same method the samples were analyzed even with a GC-MS in order to confirm the analytes nature, glycerol or DHA, analyzing the mass on charge ratio.

Finally an HPLC was used. This method uses an HPX-87H column normally used for the carbohydrate and alcohols detection. The method was tuned by the departement of CRB-biology at Ivrea, Colletterto Giacosa, Bio-industry Park Silvano Fumero.

The amount of possible products suggested to check accurately the possibility to see the majority of the main molecules in order to be sure about the solidity of the analytical method.

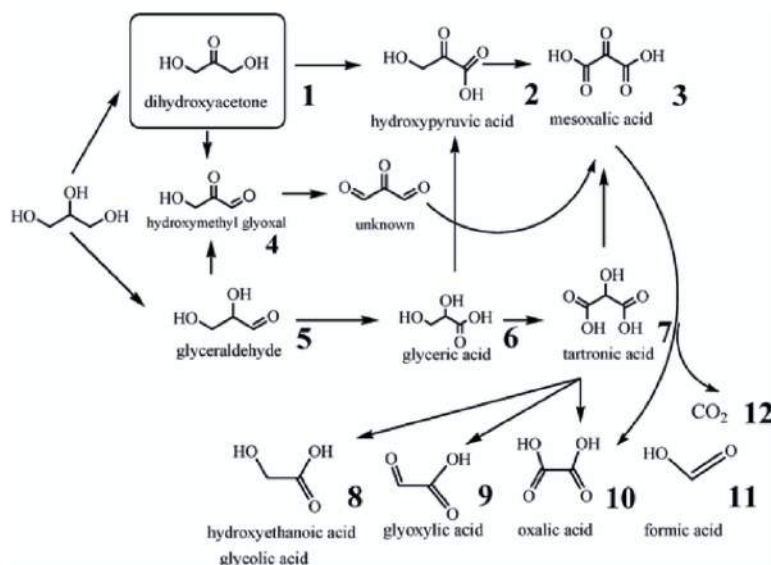


Figure 5.1: The scheme of the possible structures from the oxidation of the glycerol [60]

## 5.1 The GC-FID

This method is the main one used for this research. The method was used with an external standard.

After the filtration of the sample an amount of the solution is dried under  $N_2$  flux. This step is important to evaporate totally the solvent. After the evaporation the sample is frozen at  $-20^\circ C$  for at least three hours. The following step is the lyophilization of the sample in order to remove the amount of water still adsorbed on the sample. After the end of the lyophilization the sample is derivatized with the TFAA and, after seven hours, is ready for the analysis. It is important to underline how to reach the completely derivatization the sample with the TFAA is left at environmental temperature for a long period, between five and seven hours, to ensure the complete derivatization.

Reminding the problem about the wide amount of the possible structures from the oxidation of the glycerol the following molecules were prepared for the GC-FID analysis:

- Glycerol
- DHA
- Glyceraldehyde (GLYA)
- Glycolic Acid
- Glyceric Acid

- Hydroxypyruvic Acid

With this method only the two first molecules, the desired ones, is possible to detect. The others molecules were not detected with the same method. One of the reason is the no derivatization of the molecules in same conditions used to derivitized the glycerol and DHA.

This test confirmed the validity of the method in order to detected the two desidered molecules. In figure 5.2 a spectrum from a GC-FID analysis with the co-presence of the glycerol and DHA.

The runtime of the method is 36.3 minutes, considering the cooling down of

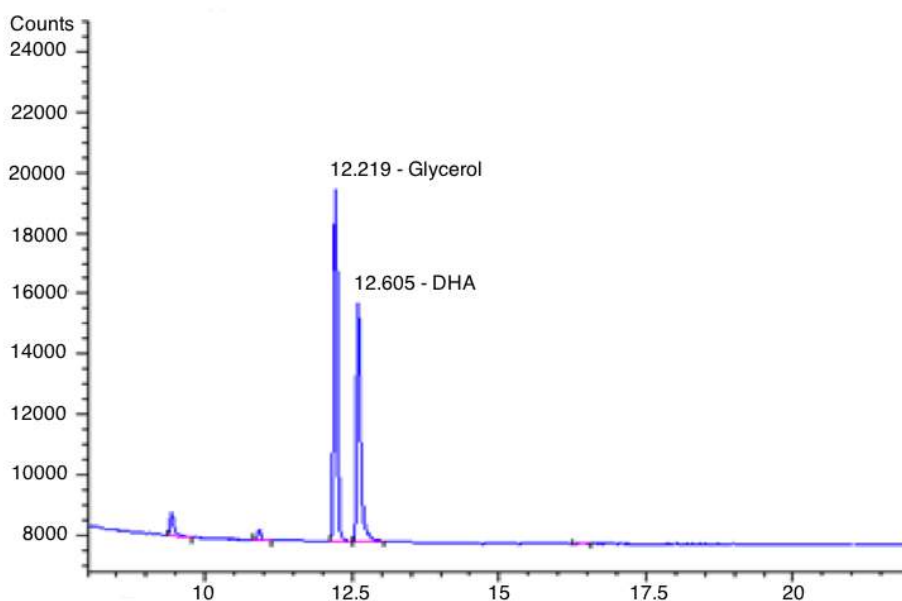


Figure 5.2: The GC-FID chromatogram with the external standard

the column to start a new analysis. There are two heating ramps during the analysis. The starting temperature is equal to 100°C. The column stays on this temperature for 4 minutes. After 4 minutes, with a rate of 10 °C/min., the temperature reach 150 °C and stays at this value for 15 minutes. After 24 minutes from the start of the analysis the second heating ramp took place. With a rate of 30 °C/min. the column reaches 220 °C.

After the first heating ramp, between the 9<sup>th</sup> and the 24<sup>th</sup> minute, the glycerol and the DHA come out. In figure 5.3 the scheme about the oven program. The GC-FID method can be summarized as follow.

- Capillary column : DB 624, 30m X 0.32mm X 1.8 m lm thickness
- Carrier gas: He
- Mode: constant pressure (11 psig and 100°C)



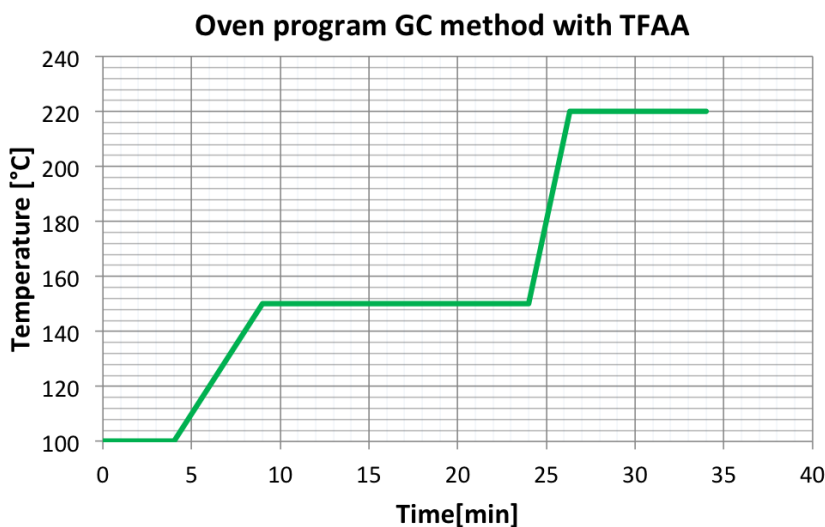


Figure 5.3: The GC-FID chromatogram with the external standard

- Oven: set at 100°C for 4 min, then heat to 170°C, with a 10degree C/min rate; hold the temperature for 15 min, then heat from 170°C to 220°C, with a 30°C/min rate; hold at 220°C for 10 min; back to 100°C and equilibration time 0.5 min
- Injector temperature equal to 220°C
- Detector FID at 240°C
- Make up flow 25 ml/min N<sub>2</sub>
- Air flux: 300 ml/min
- Hydrogen flux: 30 ml/min
- Sample preparation: each sample ( 100 mg of solution) was with N<sub>2</sub> to evaporate quite all the solvent, then freeze-dried, added by TFAA(1ml) and used for the analysis

## 5.2 The GC-MS

In order to confirm the nature of the analytes observed with the GC-FID method the same samples were analyzed also with the GC-MS. This analysis confirmed the nature of the analyte and gave the certainty of the analysis with the GC-FID. The GC-MS chromatograms for the glycerol and for the DHA are reported in the figure 5.4 and figure 5.5 respectively. Also a solu-

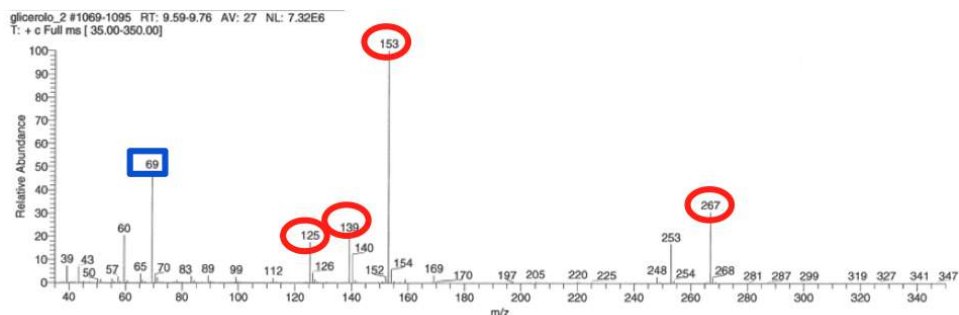


Figure 5.4: The GC-MS spectrum for a solution with pure glycerol; with the blue square is underlined the signal  $m/z$  relative to the  $\text{CF}_3$  from TFAA after the derivatization; with the red ellipsis the signal  $m/z$  related to the glycerol

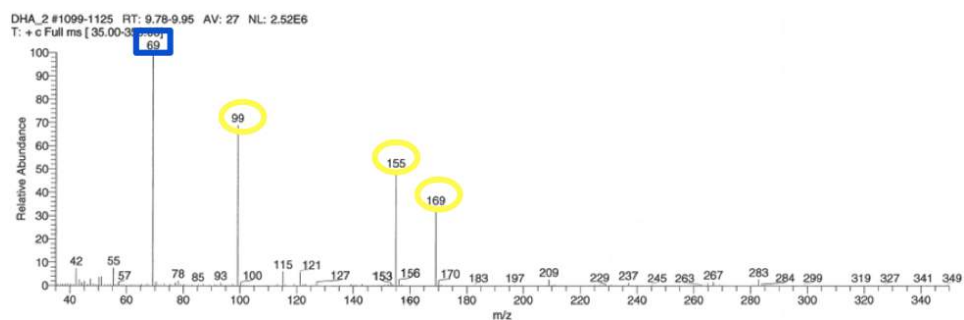


Figure 5.5: The GC-MS spectrum for a solution with pure glycerol; with the blue square is underlined the signal  $m/z$  relative to the  $\text{CF}_3$  from TFAA after the derivatization; with the yellow ellipsis the signal  $m/z$  related to the DHA

tion with DHA and glycerol was analyzed in order to verify the possibility to identify the two species separately. The GC-MS analysis validated the method and confirmed the possibility to distinguish the two molecules.

### 5.3 The HPLC methods

During the research two different HPLC methods were developed. One method was developed in order to follow the reaction synthesis of the monomer  $\text{Pd}(\text{OAc})_2$  coupled with Neocuproine. The other one was developed by the Biology department of Centro Ricerche Bracco (CRB) and is used as redundant analytical method and as support for the GC-FID analysis.

### 5.3.1 The analytical method to follow the synthesis of PdNc(OAc)<sub>2</sub> complex

This method was developed because there was the need to have the possibility to monitor the reaction in order to understand when the reaction finished. The method was prepared with a simply C18 column using as mobile phase water and CH<sub>3</sub>CN (MeOH). It is a gradient flow where the volume ratio between the two mobile phase changes during the analysis. The MeOH has a negative effect on the organometallic complex because in presence of methanol the Pd(OAc)<sub>2</sub>-Neocuproine decomposed, generating simply Pd and Neocuproine.

On the other hand the method is very efficient to monitor the Neocuproine consumption that becomes the ligand for the organometallic complex. A chromatogram in figure 5.6 shows a post run of two analysis: before the reaction only Neocuproine is present while at the end of the reaction between Neocuproine and Pd(OAc)<sub>2</sub> appears the organometallic complex signal.

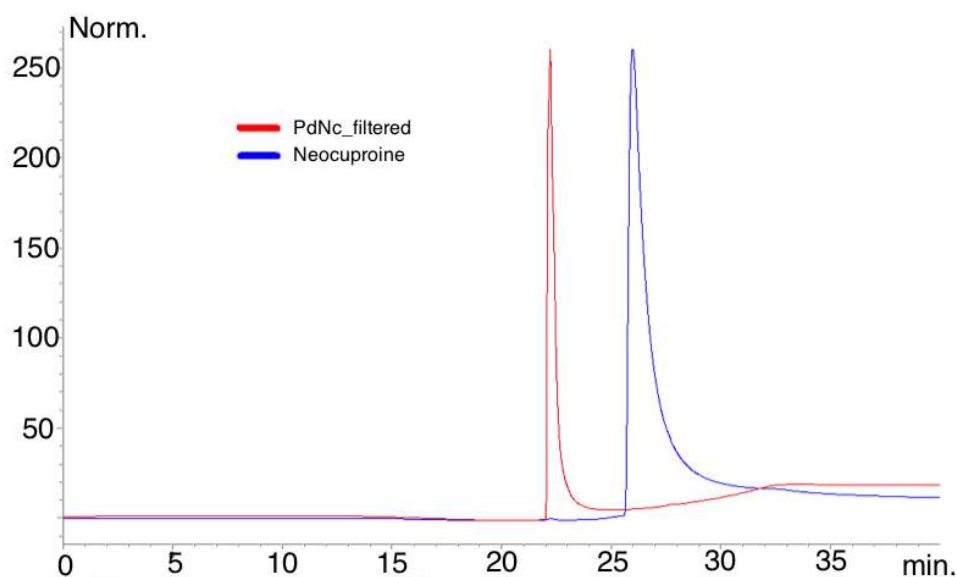


Figure 5.6: The chromatogram from the HPLC analysis at the start and at the end of PdNc(OAc)<sub>2</sub> synthesis

### 5.3.2 The HPLC-RID for the DHA detection

This particular HPLC method is based on the direct separation of the analytes on an organic acid column coupled with a refractive index detector (RID).

The HPLC analyses were carried out on an HP liquid chromatograph equipped with binary pump delivery system.

The mobile phase is composed by a solution with 65:35 water:CH<sub>3</sub>CN containing 0.5 mM H<sub>2</sub>SO<sub>4</sub>, under isocratic conditions. The flow rate used is equal to 0.5 ml/min and the column temperature is set to 25°C. Runs were monitored both with RID and with UV; even if this last detector is not helpful for the glycerol detection. The glycerol does not absorb in UV and can be seen only with RID. In figure 5.7 is reported a chromatogram from the HPLC method as an example and directly taken from a reaction solution. This method is very helpful in order to validate the GC-FID measures even if the quantitative analysis is not reliable. Like for the GC-FID analysis this method does not offer the possibility to check other compounds. The retention time of the two species, glycerol and DHA, is different (obviously) from the GC-FID analysis. In this case the DHA comes out before the glycerol (figure 5.7).

Finally it is important to underline how with this method no derivatization

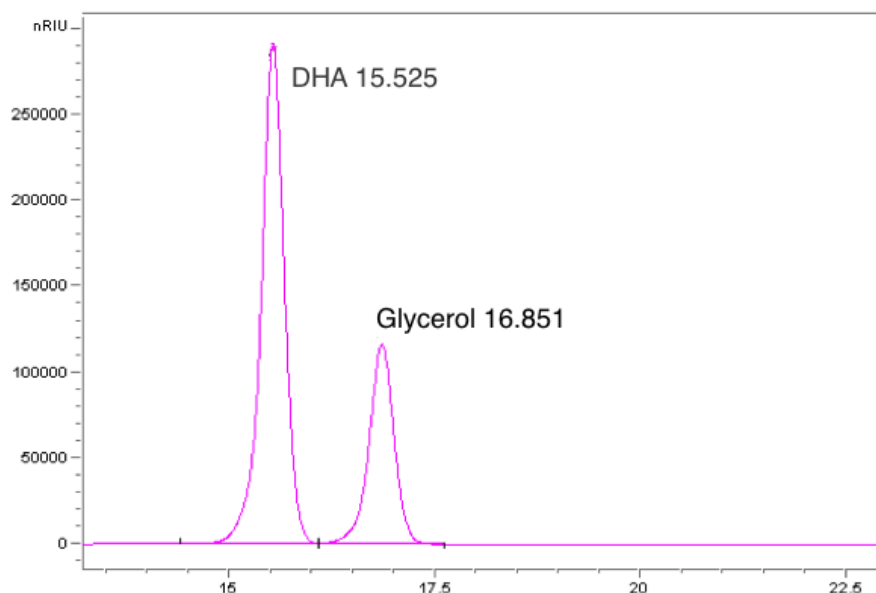


Figure 5.7: The chromatogram from the HPLC analysis from a reaction solution

is necessary. This aspect makes this HPLC method more interesting than the GC one.

### 5.3.3 The RP-HPLC for the DHA detection with UV detector

Together with the HPLC-RID another one method was developed. This method offered an higher detection sensitivity. From the obtained data, in fact, the most sensitive method resulted to be the UV detection of the

pentafluorobenzoyloxime derivative (DHA-PFBHO), obtained after a derivatization reaction of DHA with pentafluorobenzylhydroxylamine (PFBHA). The analysis follow the subsequent methodology.

A 1.66 M of DHA stock solution was prepared in water, whereas PFBHA 50 mg/ml (200 mM with a MW 249.57) was prepared in 0.1 M citrate buffer pH 4. About 60  $\mu$ l of PFBHA solution was added to 100  $\mu$ l of each sample and incubated for 30 min at room temperature (RT) to give the corresponding oxime (DHA-PFBHO). Then 600  $\mu$ l CH<sub>3</sub>CN and 240  $\mu$ l water were added before injection (25  $\mu$ l) on a 250 mm x 4.6 mm Zorbax Eclipse XDB-C8 column (particle size 5 $\mu$ m). The flow rate was 1 ml per minute (elution gradient flow) and the column works at 40°C. Elution was monitored at 215 and 263 nm. The applied elution gradient is described in the table reported in figure 5.8.

In order to increase the sensitivity, lower dilution factors were tested be-

<b>Time (min)</b>	<b>% B</b>
0	25
11	58
12	80
14	80
15	25
18	25

Figure 5.8: The RP-HPLC elution gradient

fore injection.

With this method was not possible to detect the glycerol. On the other hand not only DHA was detectable. Under these chromatographic conditions, glyceraldehyde, DHA, hydroxyacetone (HA) and pyruvic acid were well separated from each other. The retention times were around 7.49 min, 7.82 min, 10.49 min and 5.73 min respectively. HA was tested as internal standard, it gave two peaks, although area values were consistent and well reproducible. On the other hand Pyruvic acid gave a poor peak, not exactly quantifiable, however it did not interfere with DHA detection.

Detection at 263 nm gave a cleaner baseline, however sensitivity was clearly much higher (11 times) at 215 nm (figures 5.9 and 5.10).

Due to the complete derivatization and minimal sample manipulation, no internal standard based quantification was employed, but HA was used as a coderivatized internal standard.

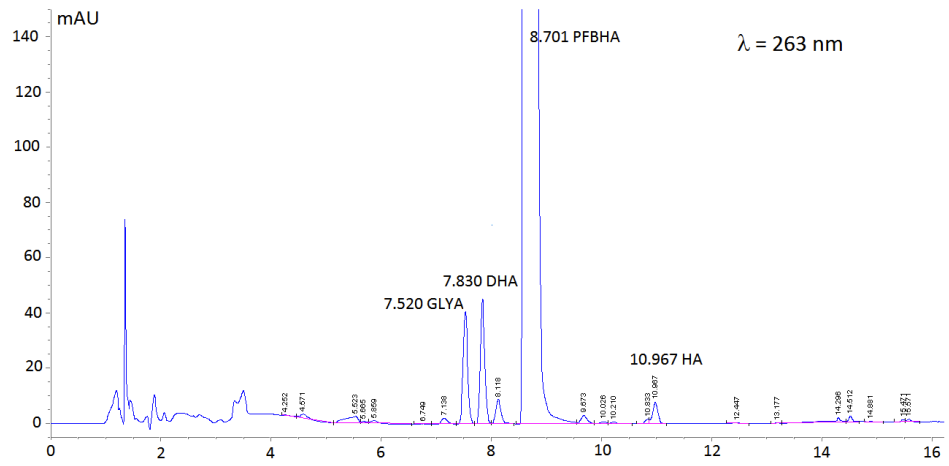


Figure 5.9: The RP-HPLC analysis, on the abscissa the retention time [min]; UV detector at 263 nm

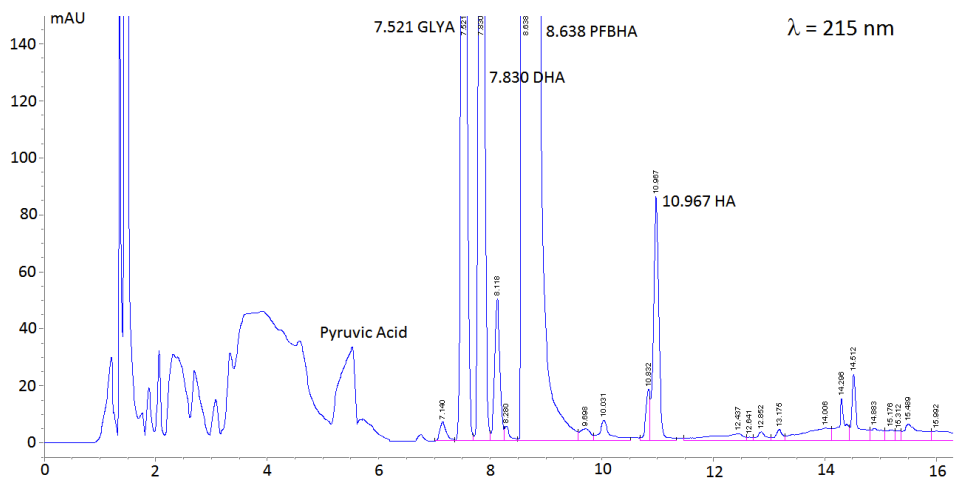


Figure 5.10: The RP-HPLC analysis, on the abscissa the retention time [min]; UV detector at 215 nm

---

---

# CHAPTER 6

---

## EXPERIMENTAL RESULTS

In this chapter will be presented results obtained during glycerol oxidation tests using the catalysts developed. The reaction is syntetically described in figure 6.1.

Before starting with the experiments it was necessary to configure the



*Figure 6.1:* The selective oxidation of glycerol to obtain the DHA

reactor in a suitable way. Batch reactor was equipped with a tube to blow oxygen, a cooling loop to control the temperature and an impeller to mix the solution. The impeller has a particular design. It has a caved structure and during the rotation it creates a sub-pressure to allow gases to be re-mixed with liquids (figures 6.2 and 6.3). The described set-up was developed with the purpose of overcoming any kind of mass-transfer effects, in particular those relative to gas-liquid mixing.

During the reactions same tube used for blowing the gas (into the reactor) allowed to sample without opening of the reactor. The following catalysts were tested:

- Pd complexes (more tests are in programm)
- Au based on carbon (tests completed)
- Pt-Bi on graphite oxide (more tests are in programm)
- Tri-metallic catalyst (tests completed)

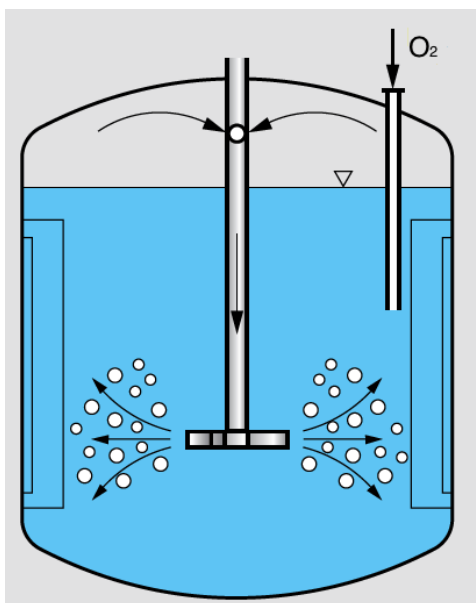


*Figure 6.2:* The scheme represents how the impeller works coupled with the oxygen tube; this is not the best solution for a real reactor, but is one of the best solution for a kinetic study

Water was solvent for reactions with heterogeneous catalysts, and water, CH<sub>3</sub>CN and a solution with both of them were solvent with organometallic catalysts. For this reason a study on solubility of these three solvents was performed. In water the glycerol and the DHA are both soluble. On the other hand the glycerol solubility changes when using CH<sub>3</sub>CN:water (10:1 v/v) solutions (figure 6.4). Tests regarding the glycerol and DHA solubility were done using concentration we applied for the reaction (1 M). These tests underlined an important aspect: working with a volume ratio 10:1 CH<sub>3</sub>CN:water, it was not possible to estimate the glycerol conversion during the reaction because the glycerol resulted not completely in solution. In these conditions, during the reaction, a sampling resulted not representative of the reaction volume. This aspect was taken into account during the experiments. The composition of the solution was crucial also for the oxygen solubility (figures 6.5 and 6.6). Oxygen shows a different behavior into the water and into the CH<sub>3</sub>CN. In CH<sub>3</sub>CN the O<sub>2</sub> is from 8 to 9 times more soluble than in pure water [31]. This parameter was used to evaluate the Henry constant at different temperatures and pressures in order to estimate the moles of oxygen into the liquid phase.

The Henry constant is reported in equation 6.1.

$$C = k_{H,pc}(T)P \quad (6.1)$$

where  $C$  is the concentration of the gas (mol/l),  $P$  is the pressure of the gas and  $k_{H,pc}$  is the Henry's constant, function of the temperature ( $T$ ). In order





Figure 6.3: The interior of the reactor; it is possible to observe the holed impeller, the cooling loop on the right side and the pipe for the gas injection

to estimate the  $k_{H,pc}$  the Van't Hoff was employed (see relation 6.2) [31].

$$k_{H,pc}(T) = k_{H,pc}(T^-) e^{(-Const.(\frac{1}{T} - \frac{1}{T^-}))} \quad (6.2)$$

Where the *Const.* is a gas-dependent constant.

Figures 6.5 and 6.6 report moles of oxygen at different pressures and for four different temperatures, used also during the experiments.

This study about oxygen solubility suggested how  $\text{CH}_3\text{CN}$  is a better solvent than pure water for the terminal oxydant. Anyway, working in the range of temperatures and pressures studied, the maximum amount of  $\text{O}_2$  into the liquid varies from 0.01 to 0.04 M or 0.05 to 0.25 M for water and  $\text{CH}_3\text{CN}$ , respectively. At these conditions moles of  $\text{O}_2$  are lower than the

Solution (H <sub>2</sub> O:CH <sub>3</sub> CN)	DHA	Glycerol
100:0	Yes	Yes
75:25	Yes	Yes
50:50	Yes	Yes
25:75	Yes (slow)	Incomplete
1:10	Yes (slow)	Incomplete

Figure 6.4: This table shows the results obtained at different volume ratios of water and CH<sub>3</sub>CN prepared to test the solubility of the glycerol and DHA (1.0 M) before to start the experiments

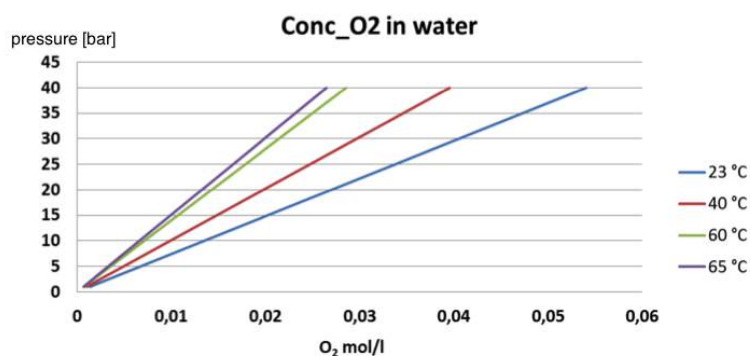


Figure 6.5: The solubility of O<sub>2</sub> in water solution and different temperatures

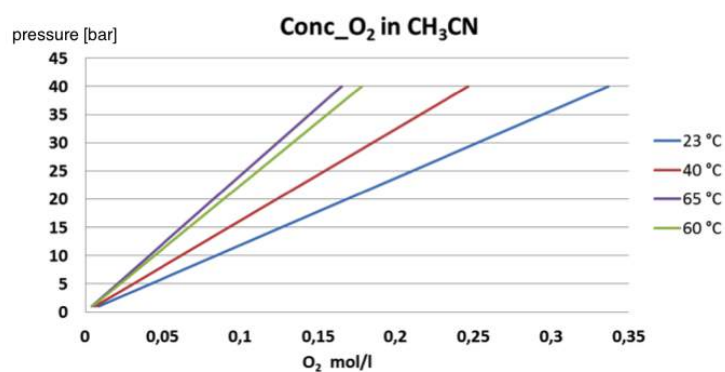


Figure 6.6: The solubility of O<sub>2</sub> in CH<sub>3</sub>CN solution and different temperatures

moles of glycerol. This sub-stoichiometric conditions (figure 6.1) did not considered because, working with a batch reactor, even if the moles of O<sub>2</sub> are insufficient into the solution, there is a big provision of oxygen in the gas phase over the liquid. To evaluate this oxygen provision was not sufficient to apply the perfect gas law:

$$PV = nRT \quad (6.3)$$

The pressure and temperature are too high to use the hypothesis of the ideal gas. For this reason the theorem of the corresponding states was used [57]. This equation (6.4), involving use of the compressibility factor of the gas (equation 6.4), allowed to assume that the oxygen moles are sufficient for the reaction.

$$\zeta = \frac{VP_r}{nRT_r} \quad (6.4)$$

Where  $\zeta$  is the compressibility factor that is function on the gas-phase. Moles of O<sub>2</sub> in the gas phase are ten time higher respect to value required from the stochiometry.

With these thermodynamic considerations and before starting experiments, a standardized form to collect data was created: temperature, pressure, molar ratio, pH (before and after the reaction), solvent, sampling and nature of the catalyst. A *fac-simile* of the table is reported in figure 6.7.

Kind of reaction:

Operator:

DATE	CATALYST	REACTION SOLUTION	CONDITIONS	Note	TIME [h]	MEASURES	SAMPLES			
							N°	P(bar)	T(°C)	time
			T <sub>set</sub> = [°C] P <sub>set</sub> = [bar]	Degass O <sub>2</sub> T = 60 [s]; 50 l/h	t <sub>in</sub> = -  t <sub>fin</sub> =  Δ = -	pH <sub>in</sub> = 11-12 P <sub>in</sub> = - [bar]  pH <sub>fin</sub> = 11-12 P <sub>fin</sub> = - [bar]	I	-	-	15.30
							II	-	-	16.44
							III	-	-	18.00
							IV			
							V			
							VI			
							VII			
							VIII			
							IX			
	PdNc(1) monomer	Cat= 27 mg Cocat (CH <sub>3</sub> COONa)= 49 mg Gly = 10 g  Sol. (1:10, H <sub>2</sub> O: CH <sub>3</sub> CN)  110 ml	T <sub>set</sub> = [°C] P <sub>set</sub> = [bar]		t <sub>in</sub> =  t <sub>fin</sub> =  Δ =	pH <sub>in</sub> = - P <sub>in</sub> = - [bar]  pH <sub>fin</sub> = 7 P <sub>fin</sub> = - [bar]	I	2.9	26	16.20
							II			
							III			
							IV			
							V			
							VI			
							VII			
							VIII			
							IX			

NOTES:

Figure 6.7: The form to collect data from the laboratory experiments

## 6.1 The Pd complexes as catalyst

Based on literature [3, 7, 32, 36, 43] a set of experiments using different forms (monomer and dimer ones) of the catalyst were planned.

We used the same approach of Painter and colleagues for setting experimentation plan up [Selective Catalytic Oxidation of Glycerol to Dihydroxyacetone; Ron M.Painter, David M. Pearson and Robert M. Waymouth; *Angewandte Chemie (International Edition)*; 2010; ref.7]. A general mechanism of reaction is showed in figure 6.8. In this scheme the dimeric complex of Pd results active as 1 and 4.

Furthmore in this article the catalytic oxidation of glycerol was tested in different ways. The table in figure 6.9 summarizes the most interesting experimental results obtained by Waymouth and co-workers. With 5 mol% palladium (2.5 mol% structure in figure 6.10) and 3.0 equivalents of benzoquinone (BQ) in acetonitrile at room temperature proceeded with 97% conversion in 24 hours and 96% selectivity for DHA. The nature of the solvent has a significant influence in the rate of reaction: in 7:1 CH<sub>3</sub>CN/water solution (v/v) complete conversion of glycerol was observed in 3 hours, with BQ as terminal oxydant. When the reaction was conducted in dimethylsulfoxide, the oxidation was complete within 15 minutes with complete selectivity for DHA. The selective oxidation of glycerol was readily performed on a 10 mmol scale in wet CH<sub>3</sub>CN, oxidation of 0.92 g (10 mmol) of glycerol afforded DHA in 92% yield after chromatography, or 58% yield after crystallization of the product as its dimer.

The selective oxidation of glycerol can also be significantly carry aerobically out. The oxidation of glycerol in wet CH<sub>3</sub>CN under flask of O<sub>2</sub> with 10 mol% Pd (1 mmol scale) afforded the isolated DHA in 69% yield; on a larger scale (10 mmol glycerol), under a continuous stream of air (semi-batch). Attempts to perform the aerobic oxidation of glycerol at lower catalyst concentrations led to high selectivity for DHA, but low conversions: using 5 mol % palladium under a flask of air afforded only 47% conversion after 24 hours in CH<sub>3</sub>CN/water. Competitive oxydative decomposition of the catalyst is a likely cause of the lower conversions and yields. The high conversions of glycerol into DHA resulted under aerobic conditions, but only at relatively high palladium cocentrations [7].

Based on these informations the first tests were planned.

First of all the aim of the research was to improve some reaction's conditions:

- reducing (or avoinding) solvents like DMSO or CH<sub>3</sub>CN
- working with an high value of molar ratio (MR, equation 6.5) to reduce the amount of the catalyst; the amount of catalyst employed by Waymouth *et alii* was not reliable for industrial application
- optimising the reaction without terminal oxydant such as benzoquinone

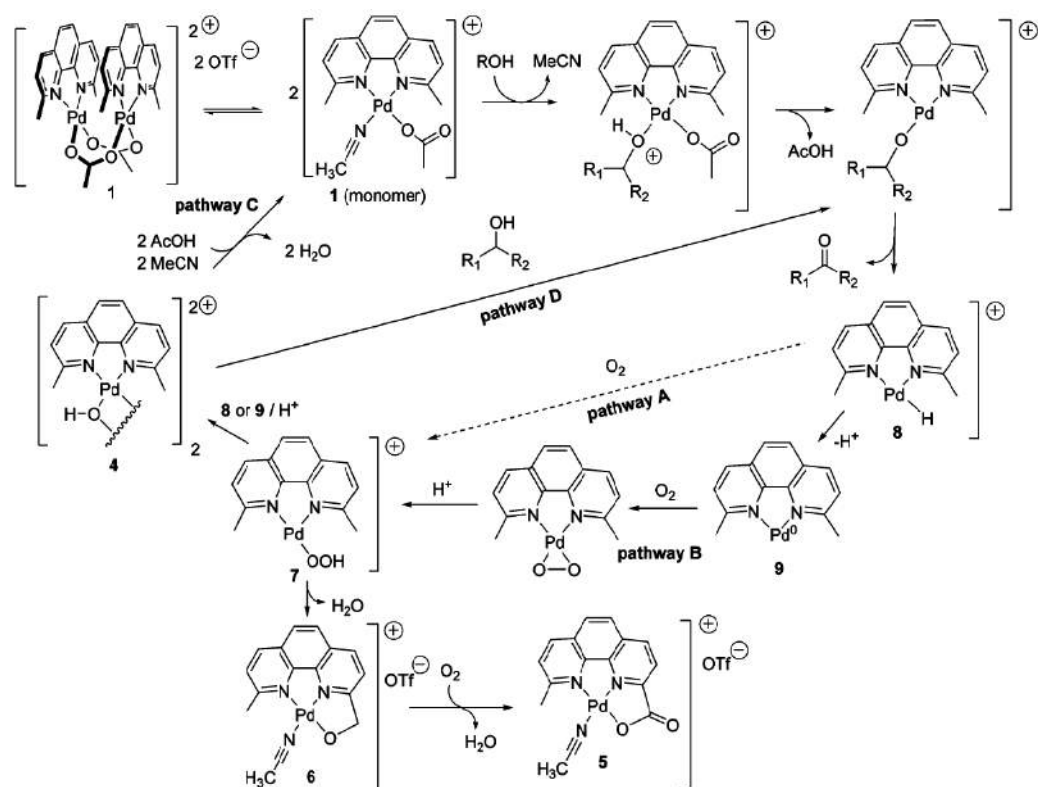


Figure 6.8: The reaction mechanism proposed by Waymouth and co-workers

N°	Solvent	MR	Ox.	Time	$\zeta$	$\sigma$	$\psi$
[-]	[-]	[Gly/cat.]	[-]	[h]	[%]	[%]	[%]
1	CH <sub>3</sub> CN:H <sub>2</sub> O (10:1)	10	O <sub>2</sub>	4	95	/	69
5	CH <sub>3</sub> CN:H <sub>2</sub> O (10:1)	10	air	18	/	/	73
2	DMSO	20	air	24	47	80	/
3	CH <sub>3</sub> CN	20	benzoquinone	24	97	99	/
4	CH <sub>3</sub> CN:H <sub>2</sub> O (7:1)	20	benzoquinone	3	97	99	/

Figure 6.9: The table summarized some operational conditions using the dimer form of the Pd catalyst

(BQ)

- reducing the time of the reaction

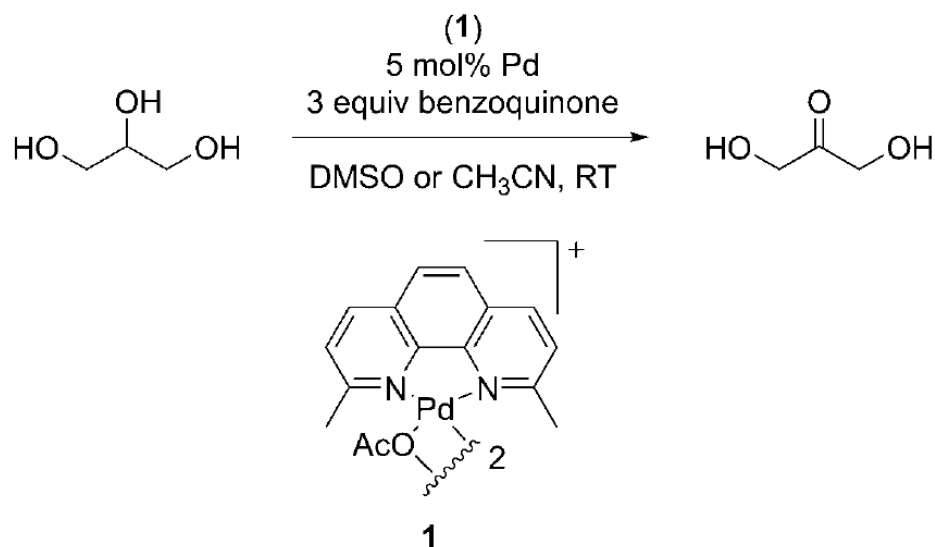


Figure 6.10: The reaction scheme from the literature [7]

$$MR = \frac{\text{Glycerol}_{moles}}{\text{catalyst}_{moles}} \quad (6.5)$$

each point was studied for optimising the glycerol conversion and the DHA yield.

The monomeric activity of 1, as proposed in the scheme in figure 6.9, also suggested to conduct tests with PdNc-C. The first reactions were conducted at low pressure of oxygen (from 3 to 3.5 bar) and reducing the MR from 10 (literature conditions) to 1600. The only parameter varied was the temperature. The samples were analyzed by GC-FID (chapter 5, section 5.1) and the amount of the analytes was computed by a calibration curve. The reaction solution was sampled only at the end of the reaction. First results obtained can be summarized in a graph of DHA yield (figure 6.11). The different values of yield between the reaction conducted at 20 °C and 65 °C was too low and they were considered into the range of the measurement uncertainty.

Because the very low DHA yield values pressure was increased from 3 to 10 bar of pure oxygen. The conditions were not mild anymore. Temperature was maintained set at 40°C. At this step three different conditions were applied changing the nature of solvent solution. A CH<sub>3</sub>CN:water (10:1) solution, CH<sub>3</sub>CN:water (1:1) solution and pure water were used as solvents. Results about these three reactions are reported in figure 6.12. Bold numbers underline the most relevant results:

- conversion of the glycerol at the end of the reaction
- yield to DHA by GC-FID analysis

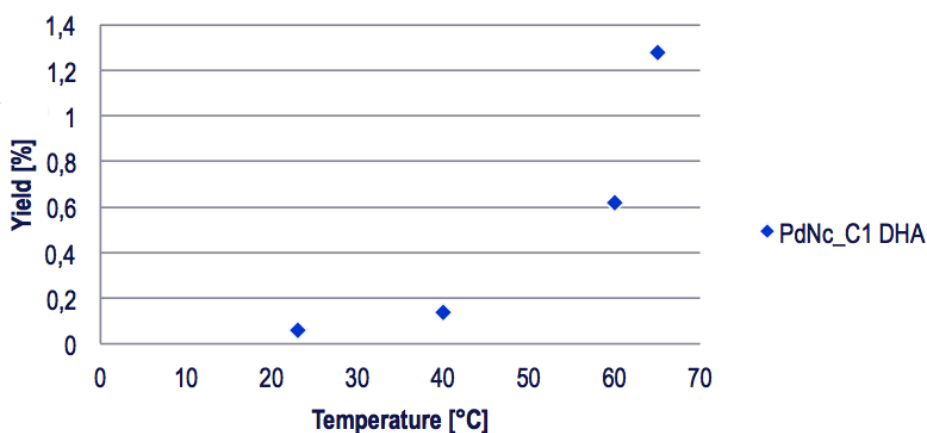


Figure 6.11: The graph about the yield evaluation for the DHA at different temperatures

Maintaining the MR equal to 1600, the pressure increasing from 3 to 10 bar does not lead an higher value of DHA at the end of the reaction. Moreover the change of the solution composition, reducing the amount of  $\text{CH}_3\text{CN}$ , brings also to a low glycerol conversion. The conversion level at the end of the reaction using only pure water is higher than the other one with  $\text{CH}_3\text{CN}$ :water (1:1) (figure 6.12). This result must be verified because it was not in accord with the other results.

Because the low yield obtained the reaction conditions were modified once more. Then molar ratio (MR) was modified reducing the value from 1600 to 160 and subsequently to 16 (quite the same value used by Waymouth and co-workers).

Temperature and oxygen pressure were modified passing from  $40^\circ\text{C}$  to  $60^\circ\text{C}$  and from 10 to 30 bar respectively. The experimental data were summarized in figure 6.13. They were reported as DHA yield and final glycerol conversion. The results from these set of experiments shows an higher glycerol conversion in the case of an higher amount of  $\text{CH}_3\text{CN}$ . The conversion in pure water (dagger markers) results lower.

Moreover from the results in figure 6.13 it is possible to evidence dependence of the yield from the solvent mixture. An high amount of  $\text{CH}_3\text{CN}$  produces an high yield. These results became the starting point for a further study using the PdNc-C as catalyst.

Already from these initial experiments it was observed the formation of inactive compound at the end of the reaction deposited at the bottom of the reactor. The decomposition observed was in accord with the literature.

Solution	time	$\zeta$	$\psi$
[CH <sub>3</sub> CN:H <sub>2</sub> O]	[min]	GC [%]	GC [%]
<b>10:1</b>	0	-	0
	60	-	0,83
	120	-	1,53
	180	-	0,62
	246	-	<b>1,04</b>
	324	<b>97</b>	<b>1,88</b>
<b>Pure water</b>	0	0	0
	26	10,26	0,57
	63	20,56	0,31
	123	23,24	0,49
	185	21	0,58
	244	<b>23,04</b>	<b>0,82</b>
<b>1:1</b>	0	0	0
	12	9,9	0,7
	67	12,8	1,06
	188	15,1	1,59
	248	<b>12,1</b>	<b>1,37</b>

Figure 6.12: Results about conversion of glycerol and yield to DHA for three reaction at 10 bar of O<sub>2</sub>, 40°C, MR = 1600 and in different solutions of CH<sub>3</sub>CN; the analysis were done with the GC-FID and subsequently confirmed by HPLC-RID

## 6.2 The best results with Organometallic complexes and a study about the decomposition

After the first tests, further studies were conducted on the monomer PdNc-C. These studies were based on the influence of:

- molar ratio (MR)



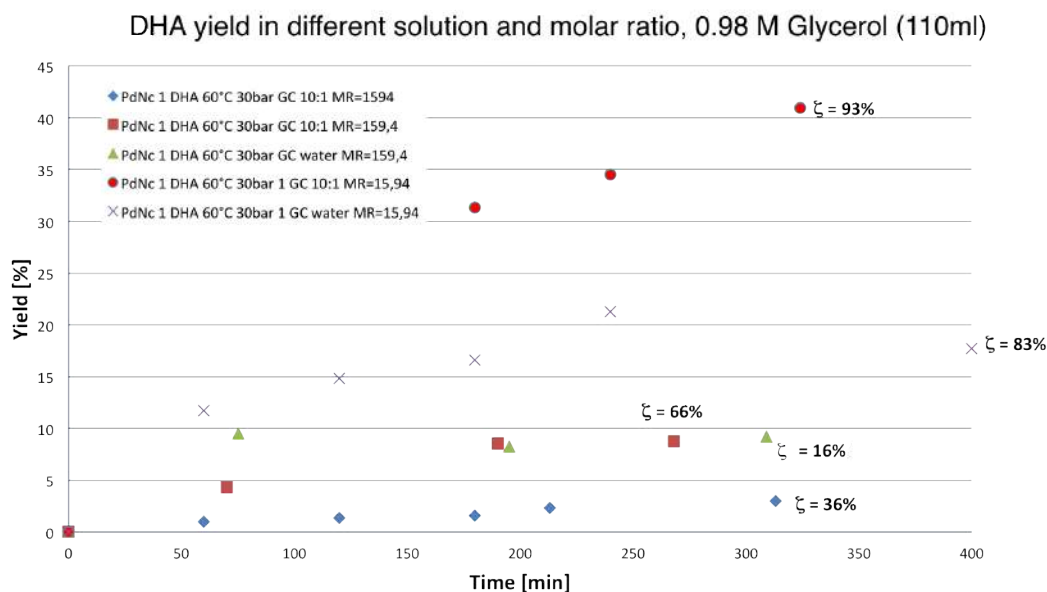


Figure 6.13: Results from reactions at 60 Celsius degree and 30 bar, for different solution of acetonitrile to water and different molar ratio glycerol to catalyst; for every test is reported the value of the glycerol conversion ( $\zeta$ ) computed at the end of the reaction

- solvent composition
- temperature (40°C and 60°C)

The influence of the MR was studied starting from 16 until 1600 passing from 160. Maintaining constant the temperature (60°C), the oxygen pressure (30 bar) and the solution (10:1; CH<sub>3</sub>CN:Water) the MR variation showed interesting results (figure 6.14). In this figure the glycerol conversion is reported only for the final samples. The reason was mainly due to the partial solubility of the glycerol in CH<sub>3</sub>CN:Water (10:1) as already explained before in this chapter.

Comparing the results for MR=16 and 1600 the conversion appears comparable. With a conversion level equal to 65.92% the experiment conducted at MR=160 is different. Anyway this conversion value was evaluated after 260 minutes from the start of the reaction, while the other two conversion levels are referred to 340 and 400 minutes, respectively.

Finally, even if the conversion level is comparable, the DHA yield resulted to have a strong dependency from the MR. An higher DHA yield was obtained with an higher MR value. The maximum yield obtained with PdNc-C is equal to 42%.

The same experiments were conducted using only pure water as solvent. In figure 6.15 is reported the glycerol conversion for the two different values of MR. In this experiments it was possible to monitor the glycerol conversion

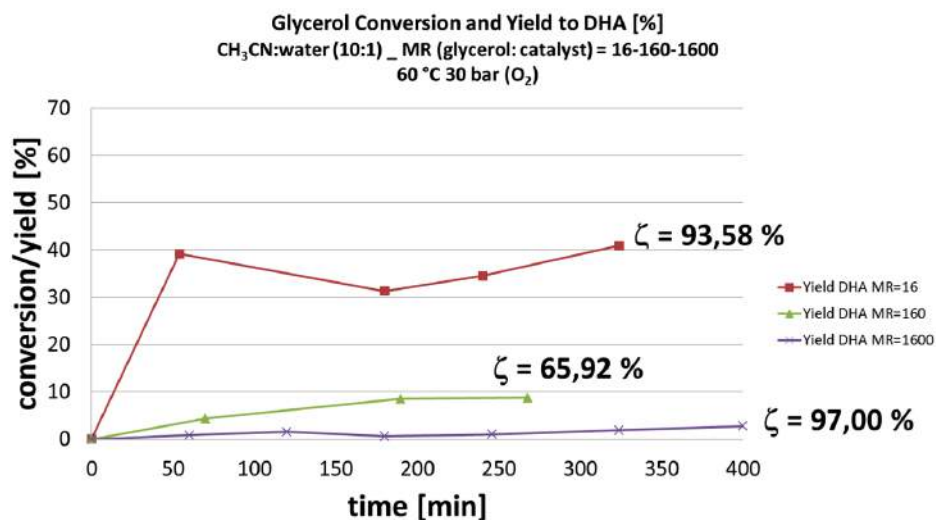


Figure 6.14: Glycerol conversion and DHA Yield at 60°C, 30 bar of oxygen at MR=16,160,1600, CH<sub>3</sub>CN:water (10:1) used as solvent

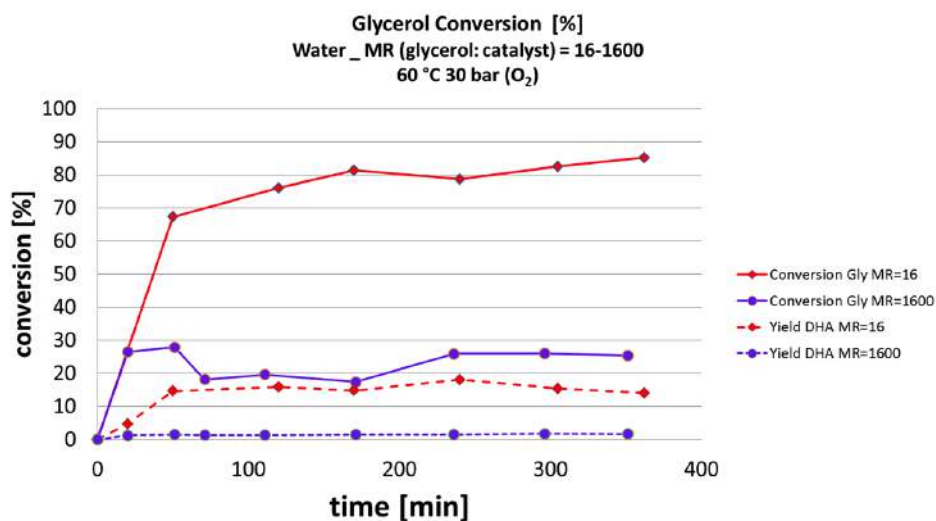


Figure 6.15: Glycerol conversion and DHA yield at 60°C, 30 bar of oxygen at MR=16,1600; pure water used as solvent

at different times cause its complete solubility in water. The conversion of glycerol results higher for an MR=16. For the two curves the reaction seems to reach a *plateau* after the first 100 minutes.

Even for the DHA yield the data showed a strongly dependence from the MR. As before it was possible to observe how the yield is strongly influenced by MR. Anyway the maximum yield never overcame the 20%. Using only the pure water the monomer PdNc-C as catalyst does not show a good ac-

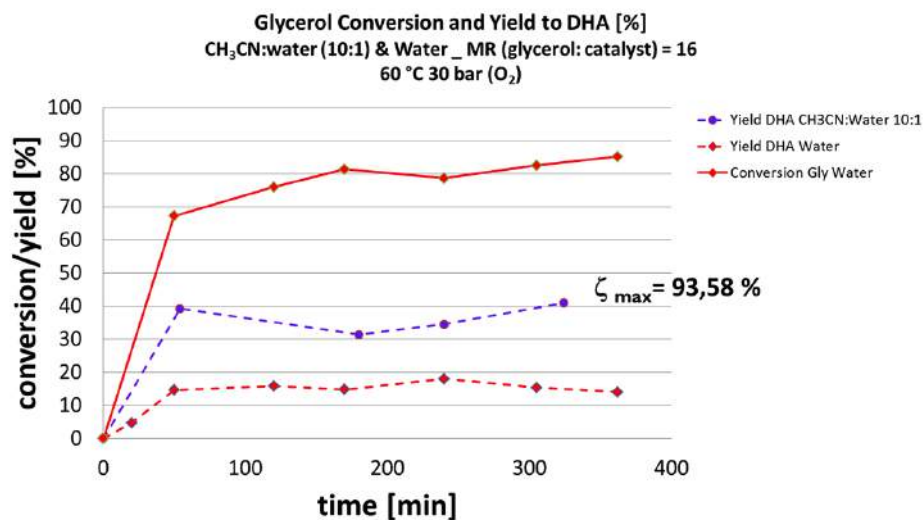


Figure 6.16: Glycerol conversion and DHA yield at 60°C, 30 bar of oxygen at MR=16; pure water and  $\text{CH}_3\text{CN}:\text{water (10:1)}$  were used as solvent

tivity, even working at an high value of MR.

Comparison between tests conducted using  $\text{CH}_3\text{CN}:\text{Water (10:1)}$  and pure water is showed in figure 6.16. First of all the glycerol conversion at the end of the reaction resulted comparable (93.58% versus 85%). The main difference is the DHA yield. The solvent containing  $\text{CH}_3\text{CN}$  showed a yield two times higher respect the maximum yield in water. This data confirmed a dependence to the solvent. The PdNc-C in its monomeric form resulted to have an higer selectivity in presence of acetonitrile. This behavior is concordant with the mechanism proposed by Waymouth and co-workers and reported in figure 6.9. On the other hand the catalyst activity to the glycerol conversion is not influenced with  $\text{CH}_3\text{CN}$ .

Another important comparison was performed between two reactions conducted at two different temperatures and oxigen pressures (figure 6.17).

A *plateau* seemed to be reached more rapidly while the yield results comparable.

Finally some experiments was conducted varying the temperature, from 60°C to 40°C, and the oxygen pressure, from 30 bar to 10 bar. The interesting results were obtained comparing two different homogeneous mixtures, pure water and  $\text{CH}_3\text{CN}:\text{water}$  (figure 6.18). Beacuse the complete solubility of the glycerol in both homogeneous mixtures it was possible to report the conversion and the yield trend of the two experiments. Even varying the thermodynamic conditions these experiments showed two important aspects:

- glycerol conversion is higher in a pure solvent than in a mixture ( $\text{CH}_3\text{CN}:\text{Water 1:1}$ )

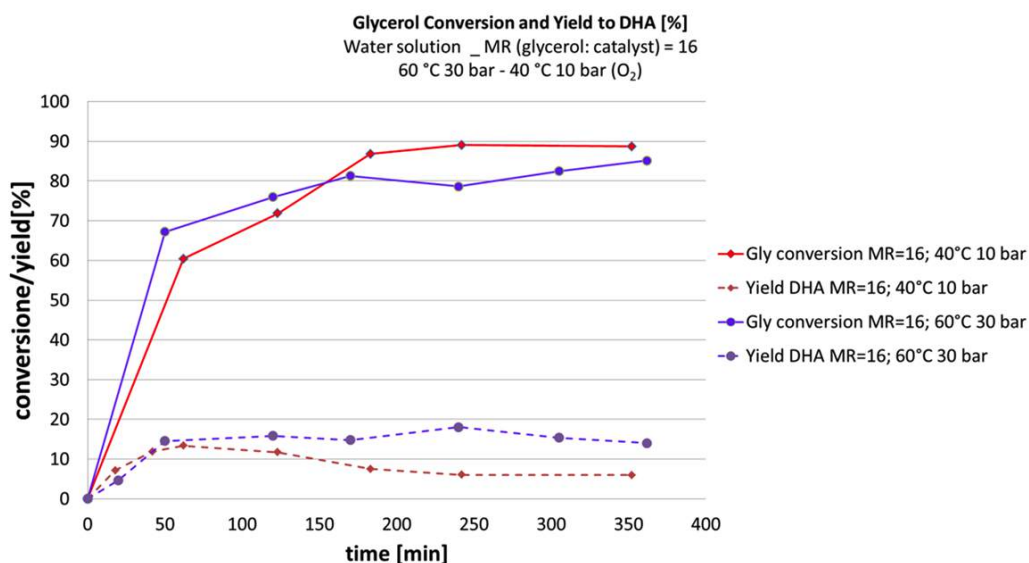


Figure 6.17: Glycerol conversion and DHA yield compared; two reactions at 40°C, 10 bar and 60°C, 30 bar of oxygen; MR=16; pure water used as solvent

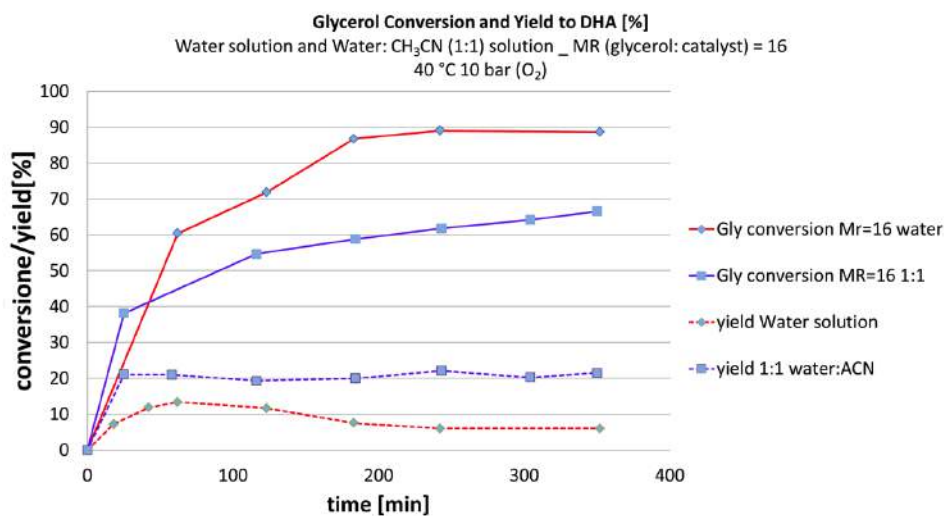


Figure 6.18: Glycerol conversion and DHA yield at 40°C, 10 bar of oxygen at MR=16,160,1600; pure water and CH<sub>3</sub>CN:water (1:1) were used as solvent

- strong dependence of the DHA yield to the presence of CH<sub>3</sub>CN

There is another possible interpretation of results. In figure 6.19 is reported a graphic about the so called regeneration factor (RF). This factor was evaluated as ratio between the moles of glycerol converted (at the end of the reaction) and the moles of catalyst employed. This factor described the catalyst behavior during the reaction. If the value is high the catalyst

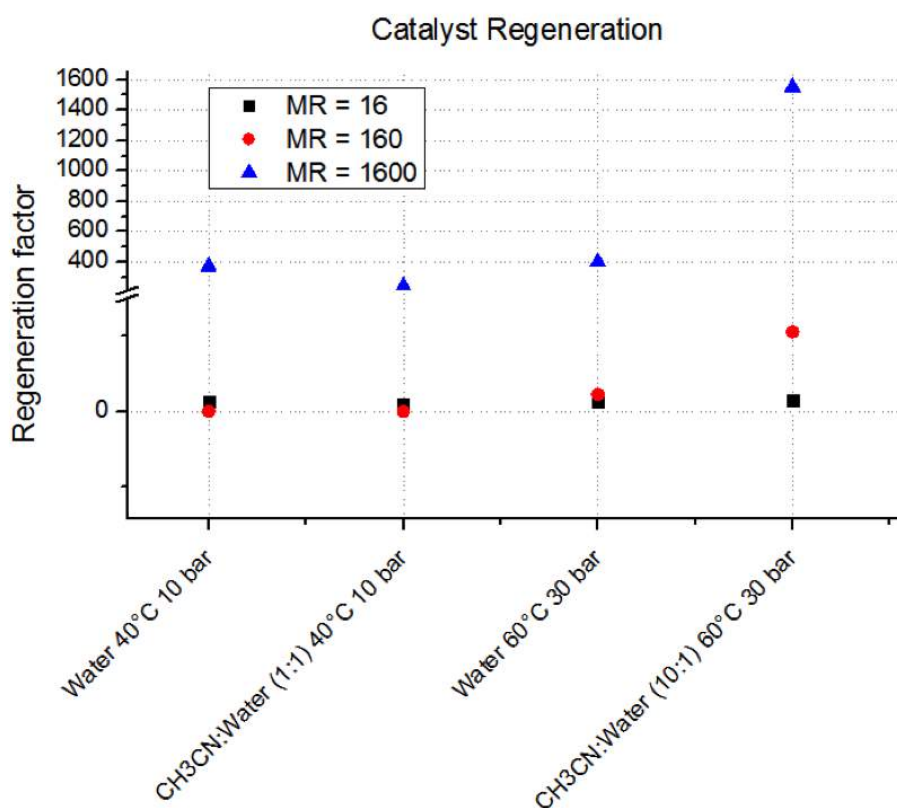


Figure 6.19: The regeneration factor

decomposition occurs slowly. It is possible to observe how at high values of MR the regeneration factor is two order of magnitude higher than the RF for low values of MR. Moreover at high values of MR thermodynamic conditions and the solvent play an important role in the catalyst regeneration. Even the dimer was tested in order to verify its activity and with the aim to compare them with the results obtained from the monomer. Figure 6.20 reports a comparison between the final conversions obtained from three different reaction mixtures conducted with monomer and dimer. Finally the results obtained with the PdNc-C (monomer) were compared with the data using the dimer. Figure 6.21 shows a comparison between three different reactions using the monomer and the dimer form of the catalyst.

### 6.2.1 Conclusions

It is possible to underline many results from these experiments. The strong dependence of the glycerol conversion from the catalyst amount (low value of MR) confirmed the expectation. The catalyst shows a variable activity in the glycerol conversion modifying

Conditions	Catalyst $\zeta_{\max}$ [%]	
	Monomer	Dimer
60°C 30 bar; MR= 16 CH <sub>3</sub> CN:Water (10:1)	85,0	91,9
60°C 30 bar; MR= 16 Water	85,2 Plateu = 170 min	95,91 Plateu = 90 min
60°C 30 bar; MR= 160 CH <sub>3</sub> CN:Water (10:1)	65,9	70,5

Figure 6.20: A comparison about the glycerol conversion with monomer and dimer for three different solutions

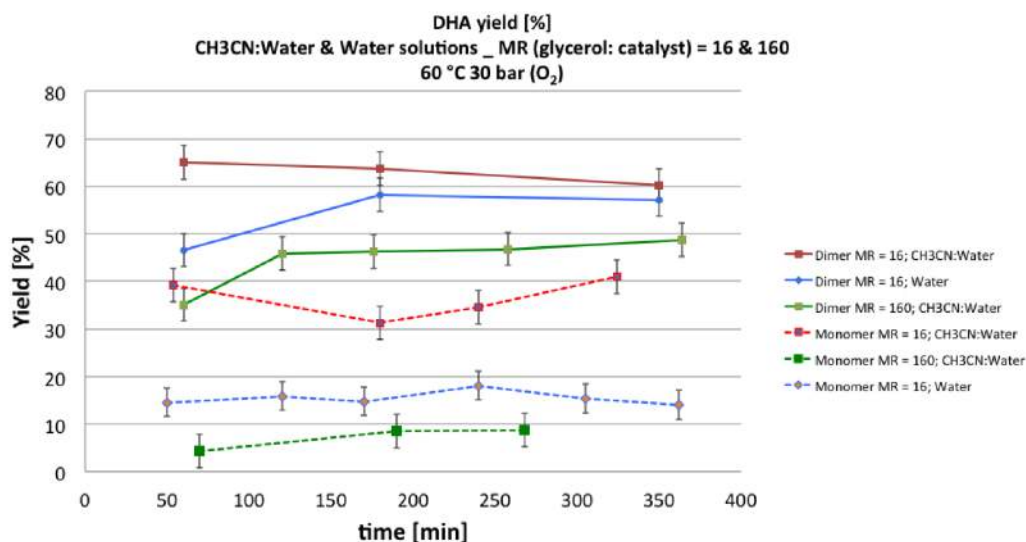


Figure 6.21: The DHA yield compared using three different solvents and the organometallic catalyst in its monomeric and dimeric form; the error bars are tuned with the instrumental error

the thermodynamic parameters as temperature and pressure. Finally even the solvent influences the DHA yield. The yield, in fact, results to be not directly function of the conversion level (figure 6.18) but of the nature of the solvent.

Some experiments conducted with simply acetate form of Pd ( $\text{Pd}(\text{OAc})_2$ ) confirmed absence of activity of the metal without the ligand (Neocuproine). The activity is not only link to the Pd, but even to the organic molecule (Neocuproine) with which Pd forms the organometallic complex. Maybe the selectivity of this catalyst is due to the chelate effect that Neocuproine has with the glycerol.

Even the catalyst decomposition was observed and studied in accord with the literature [32,44]. The NMR analysis (figure 6.22) of the catalyst at the end of the reaction showed the only presence of the Neocuproine as molecule not coordinated with Pd. The NMR of the PdNc-C and PdNc-A were taken as reference spectra for the comparison.

For each experiment conducted with PdNc-C, during the sample preparation and before the GC analysis, a solid precipitate was observed at the bottom of the reactor. The powder sampling at the end of the reaction was analyzed. The H-NMR analysis confirmed that the decomposition occurs during the reaction (figure 6.22). In this powder a heterogeneous mixture of glycerol, DHA and Neocuproine is present. No signs about the starting structure of the catalyst were present. The EDX (figure 6.23) on the same sample shows even the presence of Pd that it is clearly not coupled with the Neocuproine in an organometallic structure.

### 6.3 The results from mono-metallic catalyst

The heterogeneous catalyst based on Au was firstly tested [1,2]. No results came from these tests and the reason is well explained in the *errata corrigée* [*Corrigendum* to “Enhancement of the selectivity to di-hydroxyacetone in glycerol oxidation using gold nanoparticles supported on carbon nanotubes”, Elodie G.Rodrigues, Manuel F.R. Pereira, Juan J.Delgado, Xiaowei Chen, José J.M.Orfao; Catalysis Communication, 2013; ref. 54] about the works with gold. In this publication Rodrigues declared that the HPLC method used for the analysis was bad for the detection of the DHA and that the DHA produced with gold on MWCNTs catalysts was actually formic acid, a product of third oxidation starting from glycerol. No presence of DHA was actually detected. This event is one of the causes that led to develop a solid analytical system for the analysis (GC-FID, GC-MS and HPLC).

Anyway many tests were done with this kind of catalyst at the beginning. The experimental conditions and results were reported in figure 6.25. The completely absence of DHA into the solution at the end of the reaction confirmed the inactivity of the catalyst for the selective conversion of the glycerol to DHA.

Figure 6.24 presents a GC-FID from a reaction with the mono-metallic catalyst based on Au NPs, without DHA peaks.

### 6.4 The experiments with the bi-metallic catalysts

The catalyst based on bi-metallic NPs (PtBi/GO, chapter 3) were tested into the reactor. Many further tests have been planned, but first results helped us to focus the attention on some aspects (figures 6.26 and 6.27).

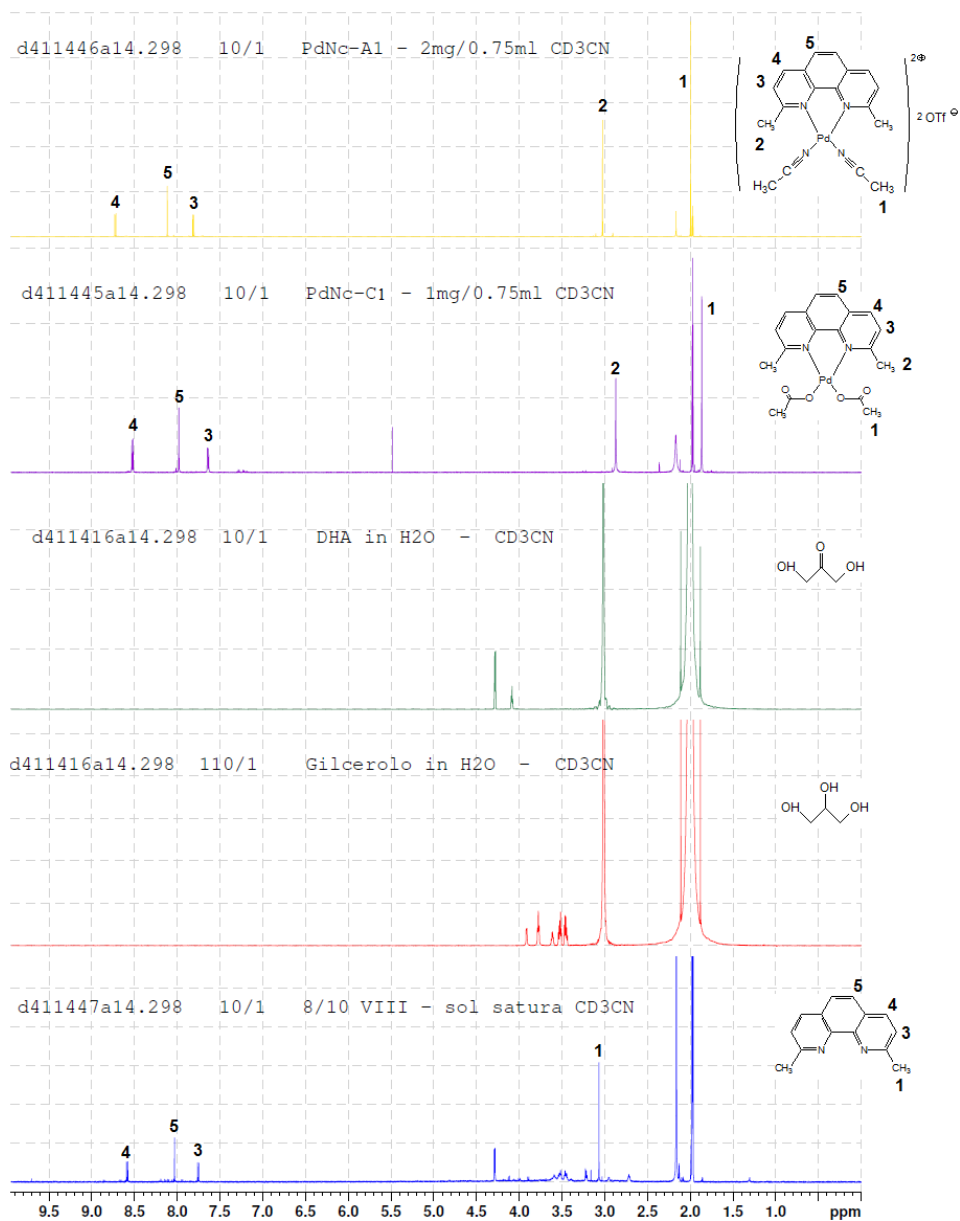


Figure 6.22: In this H-NMR the spectrum at the bottom represents the analysis of the powder recovered from the reactor; the spectrum is compared with the signal of the catalyst and with the DAH and glycerol ones

The thermodynamic conditions, temperature and pressure, were maintained equal to the reactions with the organometallic catalyst (60°C and 30 bar). The general assumption was to check the most active catalyst in strong conditions. Because of poisoning of the Pt at high concentration of O<sub>2</sub> it was clear that these conditions can not be the best ones for the catalyst.



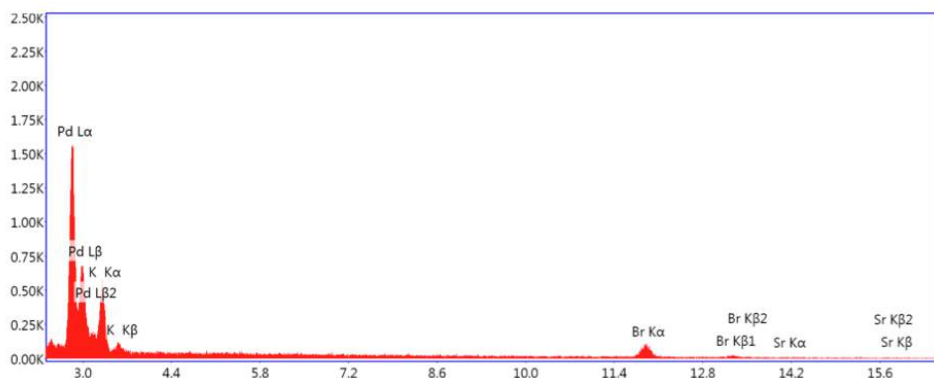


Figure 6.23: The EDX on the powder recovered from the reactor at the end of the reaction

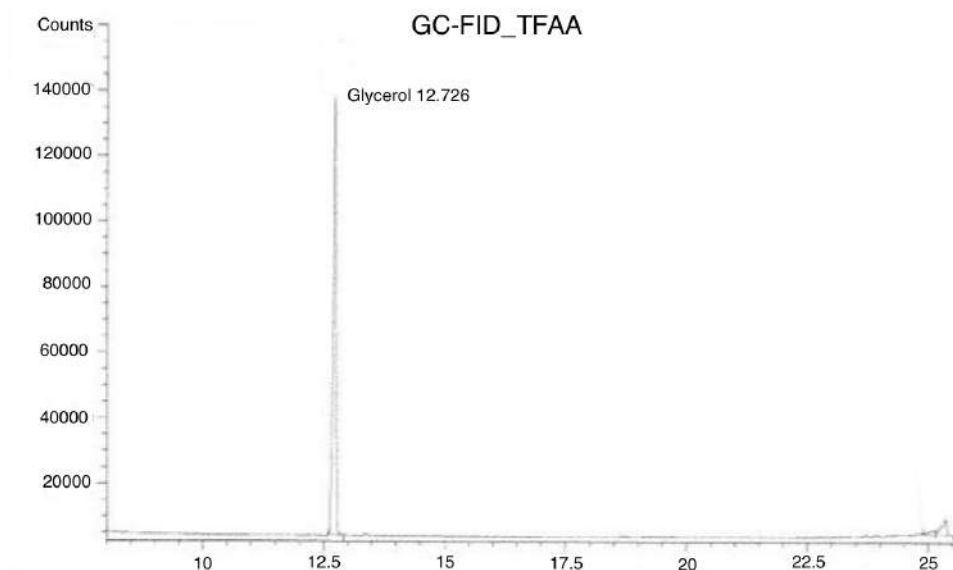


Figure 6.24: The GC-FID chromatograph obtained analyzing the samples from the reactions with gold on carbon catalysts

The pH, instead, was set to 4.5-5.5 in accord with the literature [4,47] that suggested an acid environment to obtain an high Pt acitivity.

The molar ratio reported in figures 6.26 and 6.27 is referred to the ratio between the glycerol and the moles of Pt, considered the active species.

The catalysts in these reaction conditions did not show selectivity for the DHA. On the other hand the glycerol conversion occured even in not mild conditions, showing a good activity (33.6% with PtBi on GOIII) even with a small amount of Pt (only 0.5% versus the 3.0 %) as reported in literature by Kimura and Garcia [4,47,72-75]. A milder environment could reduce the Pt poisoning augmenting its activity.

Data	Catalyst	Solution	Conditioned	Molar Ratio	[h]	Conv. to DHA
16/04	Au (1wt%) on graphite LPRD-s (0.181 g)	300 ml H <sub>2</sub> O 3.63g glycerol 2.7 g NaOH	Temp. 60°C Pressure (O <sub>2</sub> ) 3 bar	Gly/Au ≈ 4200	3	0%
22/05	Au (1wt%) Carbon σ LPRD-s (0.184 g)	300 ml H <sub>2</sub> O 3.63g glycerol 2.7 g NaOH	Temp. 60°C Pressure (O <sub>2</sub> ) 7.4 bar	Gly/Au ≈ 4200	3	0%
24/05	Au (1wt%) MWNTs LPRD-s (0.143 g)	300 ml H <sub>2</sub> O 3.63g glycerol 2.7 g NaOH	Temp. 60°C Pressure (O <sub>2</sub> ) 7.4 bar	Gly/Au ≈ 4200	3	0%
9/09	Au (1wt%) on carbon	200 ml H <sub>2</sub> O NaOH 2.7 g glicerolo 129 mg  Buffer SolutionpH=7	Temp. 60°C Pressure (O <sub>2</sub> ) 3.5 bar	Gly/Au ≈ 4200	48	0%

Figure 6.25: The table shows some significant example did with the Au catalyst; in the last column the results about the selectivity to DHA at the end of the reaction are equal to 0%



Catalyst	Solution	Conditions	$\zeta_{\text{max}}$ [%]	$\sigma$ DHA [%]
PtBi on GO III  Pt 0,5, Bi 0,65 wt%	T = 60 °C P = 30 bar  pH <sub>in</sub> -pH <sub>fin</sub> = 5.5 – 5.0 Reaction Time = 241 min	Water solution 110 ml  Glycerol 0.1 M  Molar Ratio (Gly/cat) = 46.5	33.25	0
Pt on GO V  Pt 7 wt%	T = 60 °C P = 30 bar  pH <sub>in</sub> -pH <sub>fin</sub> = 5.0 – 5.0 Reaction Time = 300 min	Water solution 110 ml  Glycerol 0.1 M  Molar Ratio (Gly/cat) = 46.5	21,07	0

Figure 6.26: The tests conducted with bi-metallic PtBi catalysts on GOIII and GOV

Moreover the strong reaction conditions were considered the reason of the no DHA production, in favor of production of over-oxidation. New tests at milder conditions will confirm this hypothesis.

Even the presence of the Bi and the functionalisation of the support suggested to play an important role. A comparison between two different catalysts, with and without Bi, showed different glycerol conversion level (figure

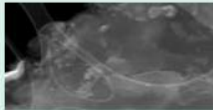

Catalyst	Solution	Conditions	$\zeta_{\text{max}}$ [%]	$\sigma$ DHA [%]
PtBi on Graphite 	T = 60 °C P = 30 bar pH <sub>in</sub> -pH <sub>fin</sub> = 5.5 – 4.5 Reaction Time = 300 min	Water solution 110 ml Glycerol 0.1 M Molar Ratio (Gly/cat) = 46.5	0	0
Pt 0,75, Bi 1,18 wt% Pt on GOVI 	T = 60 °C P = 30 bar pH <sub>in</sub> -pH <sub>fin</sub> = 5.5 – 5.0 Reaction Time = 300 min	Water solution 110 ml Glycerol 0.1 M Molar Ratio (Gly/cat) = 46.5	1,6	0
Pt 3,8 wt%				

Figure 6.27: The tests conducted with bi-metallic PtBi catalysts on graphite and GOVI

5.25). The two catalysts compared are the bi-metallic PtBi on GOIII and the mono-metallic Pt on GOV. The two supports had different functionalisation degrees, GOV was more functionalized (see chapter 3). The Pt amount was higher for the mono-metallic catalyst (7wt% versus 0.5%). An higher activity was observed for the bi-metallic/GOIII catalyst. The trend for the glycerol conversion is reported in figure 6.28. Presence of the Bi increased the catalyst activity at strong conditions (33.6% versus 21.07%). This result was in accord with the hypothesis proposed by Hu and co-workers in 2011 [47]: Bi protects the Pt by poisoning with increase of catalyst activity. Moreover the higher conversion obtained with bi-metallic is in accord with other results from literature [14,46]. A similar behavior was observed testing the Pt on GOVI with a very low conversion level (1.6%) with no selectivity.

The different activity may be due also to the support. To confirm this hypothesis, another test was performed (see figure 6.27) at the same conditions (60°C and 30 bar) using graphite (from Sigma-Aldrich) as support. A bi-metallic catalyst 0.75%Pt - 1.18%Bi was prepared. This catalyst did not show any activity.

To complete the preliminary screening on these catalyst, also the functionalized support was tested. The metal free GO IV (the support with the higher functionalisation level) resulted no-active at the same conditions. Even the selectivity results not good the screening on the activity of these catalyst is not yet completed. Furthermore this bi-metallic catalyst is waiting for other application in other activities of the colleagues that are working in my department.

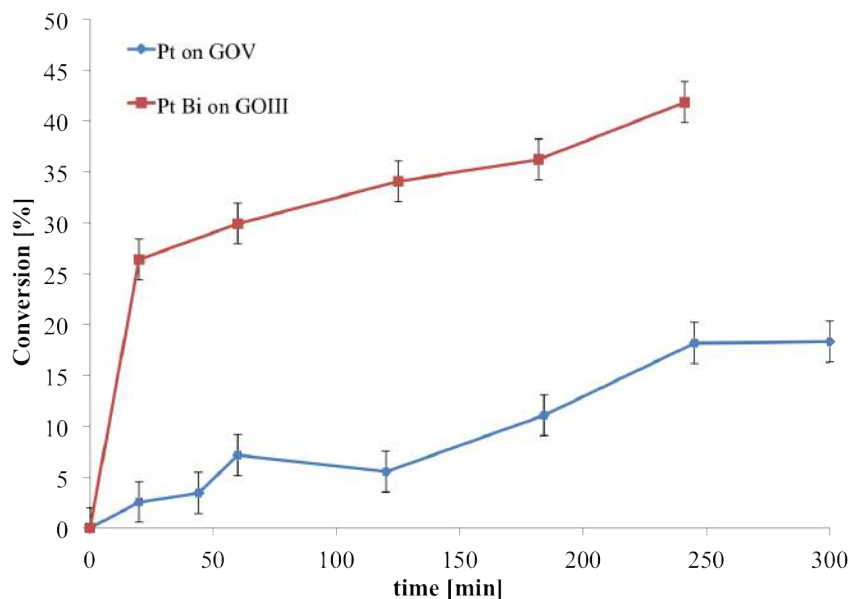


Figure 6.28: The conversion of the glycerol

## 6.5 The experiments with the tri-metallic catalyst

During second part of Ph.D. course, a brief collaboration with Department of Chemistry of the University of Milan started. After a meeting with prof. Prati and her group, we decided to test a tri-metallic catalyst with Au, Pt and Bi as recovering metal [19] based on an active carbon.

This catalyst was used for the oxidation of the alcohols.

The catalyst was synthesized at University of Milan and characterized in Polytechnic of Turin (FESEM, catalyst morphology) and in Ivrea at CRB-Imaging (ICP).

The catalyst was tested into the reactor following the literature results [14]. Three tests were performed and are here summarized in a table (figure 6.29).

Even if the catalyst shows an activity (different and function of the pH), no presence of DHA suggested to abandon for the moment this catalyst as possible solution for the selective oxidation of the glycerol. One of the main reason is the hard way of synthesis of these tri-metallic catalysts. We do not have sufficient data in order to abandon definitively this catalytic system in the future.

Catalyst	Solution	Molar Ratio	Conditions	$\zeta_{\max}$	$\sigma$ to DHA
[mg]	[-]	[Gly./Au]	[-]	[%]	[%]
102	H <sub>2</sub> O pH = 7	7000	P = 30 bar T = 60°C 0.1 M Gly	29,4	0
100	H <sub>2</sub> O pH = 9 1 eq NaOH	7000	P = 30 bar T = 60°C 0.1 M Gly	40,7	0
102	H <sub>2</sub> O pH = 1 1 eq HCl	7000	P = 30 bar T = 60°C 0.1 M Gly	4,2	0

Figure 6.29: Results from the tests into the batch reactor at different pH

---

---

# CHAPTER 7

---

## CONCLUSIONS

Starting with the aim to develop a catalyst and to propose a real reliable solution to produce DHA from glycerol many difficulties were founded, but many new discoveries and experiences came out from this research.

The first results come from the study of the mono-metallic Au NPs based catalyst on carbonious supports, carbon black, graphite and graphite oxide. Three different techniques for the synthesis were explored:

- Impregnation
- Double Impregnation (DI)
- Liquid Phase Reductive Deposition (LPRD)

very good results in terms of NPs distribution and dimension (between 8 to 20 nm) were obtained improving the LPRD method. The LPRD and its improvement resulted to be simply to reply and easy to do in order to obtain the required morphology for this catalyst.

On the other hand the catalyst shows its no activity for the selective oxidation to DHA and this result was in accord with the *errata corrige* published from Rodrigues and co-workers.

About the error committed by Rodrigues *et alii*, this fail suggested to pay more attention on the development of a solid analytical method in order to study the synthesis of DHA (see chapter 4). This step of the research evolved in a three analytical methods for the analysis of the samples.

The second step was to work with bi-metallic catalysts looking for new supports as graphite oxide. With this new kind of support very good results were obtained.

A new study, after the experience with the catalysts based on Au, on bi-metallic catalyst started. The study on this catalyst started with the purpose of improving results presented in literature [47]. Even with Au, graphite

oxide was studied as support (not present in this monograph) and the results obtained with Au stimulated the research on this way. Many efforts were made and the results presented in chapter 3 were very interesting. Graphite oxide as support has proved its functionality as a possible new cheap one. It showed a hydrophilic behavior, very good because it is usually employed with polar solvents like water. The NPs distribution is homogeneous, their dimensions are uniform (from 20 to 40 nm) and the metals show three different forms (see chapter 4, XPS analysis):

- metallic
- oxide form ( $\text{PtO}_2$  and  $\text{Bi}_2\text{O}_3$ )
- metals coupled: the main objective of the synthesis

The study required many months to be developed and first results from glycerol oxidation are present. Some promising results suggested to perform new tests. The bi-metallic catalysts supported on GO, have found a new application, thanks to their high activity and selectivity with a low amount of metals, on the selective oxidation of glucose into D-Saccharic acid, as starting material for the adipic acid synthesis.

Finally the heart of this research and the aim of this work, the study of the Pd complex. The work done on this catalyst led to important results not still present in literature. First of all was developed a complete and accurate methodology for the synthesis and the analysis of all Pd complexes, there is no similar studies in literature and these results could help for new research on this field. From the monomer (Palladium Acetate Neocuproine, PdNc-C) passing through its activated form (PdNc-A) and the dimer synthesis (PdNc-D) different analytical techniques were developed.

The thin layer chromatography (TLC), High Pressure Liquid Chromatography (HPLC), Nuclear Magnetic Resonance (NMR), Inductively Coupled Plasma (ICP), Karl-Fischer (KF) and Matrix Assisted Laser Desorption-Ionisation (MALDI) are all the techniques developed for a complete characterization of the catalysts. In accord with the literature the results with organometallic catalysts (monomer and dimer) showed a good conversion and selectivity even if the problems related to the decomposition are still.

The Palladium complex in its monomeric form was tested in this work for the first time for the selective oxidation to DHA. Even if its synthesis is very simple and the yield appears high, the decomposition is not a negligible problem (even considering the high cost of the Palladium). The NMR analysis of the powder recovered at the end of the reaction suggests the decomposition of the catalyst in its precursors, Neocuproine and Pd. The catalyst needed to be studied in order to avoid its decomposition.

The dimer was synthesized in the month of October 2014 and tests on it were planned for the November-December 2014.

Nowadays the results obtained are not sufficient to think to scale-up the reaction, but they have augmented the knowledge about the activity of this catalyst. In the future some supports for this catalyst will be studied and also methods to recover the catalyst at the end of the reaction.

So it is possible to conclude that the research conducted until now has put in evidence the main critical aspects for this particular reaction and on the main catalysts that the literature proposes without a clear knowledge about possible problems.

From an economical point of view the results on the organometallic catalysts are not so bad starting from the idea that glycerol is a waste low-cost indeed, while DHA has an high cost, about 15 Euro per kilo. It is true that is not yet possible to scale-up the reaction, but this work can be considered as one of the first explorative research to investigate the real possibility to realize the synthesis of the DHA starting from a waste material as glycerol. Finally results clear how the entire work collected different way of catalytical reaction for the selective oxidation of the glycerol and study some aspects. These results will presented in a final meeting at the Research Center of Bracco Imaging S.p.A., January 2015.



---

---

# CHAPTER 8

---

## APPENDIX A

In this Appendix will be described all the synthesis: graphite oxide, LPRD for NPs deposition, organometallic complexes.

### 8.1 The Graphite Oxide (GO): classical method

Different typologies of graphite oxide was synthetized as supports for nanoparticles.

the graphite oxide was studied as a new support looking for to verify the following hypotesis:

- the functionalisation of the surface to help the NPs dispersion
- reducing the Nps dimension and to avoid the coalescence of the nanoparticles in bigger clusters

The GO synthesis follows the Hummers method (1958). In some cases the method was modified in order to observe different functionalisation: different molar ratio between reagents and support is an exmaple.

When in the book is reported original method the name is referred to the method describe by Hummers and co-workers in the original publication [49,52].

The graphite (1 g) is put in a becher with 10 g of  $\text{KNO}_3$  (with the possibility to use the  $\text{NaNO}_3$  obtaining the same results). The becher is put in an ice bath with salt (in order to create the eutettic solution). To check the temperature during the reaction is used a Hg-thermometer directly into the becher. Once the temperature of  $5^\circ\text{C}$  is reached 230 ml of sulfuric acid are added. When the temperature is stable the ice bath is take off.

The temperature is maintained at  $35^\circ\text{C}$  for at least 30 minutes and an equal

amount of water (230 ml) is gradually added. During this step the temperature is maintained at 98 °C.

The solution is left under stirring. Once the temperature reached the environmental one the solid is separated from the liquid (centrifugation). The solid is left in a de-mineralized (DM) water for all night long: the solid precipitates at the bottom of the becher. The day after the water is get off and the support is heated to 50 °C. At this temperature a solution 3.0% (v/v) of H<sub>2</sub>O<sub>2</sub> is added (100 ml): this step is necessary in order to permit the reaction of the amount of reagents not reacted. It is important to control the addition of the H<sub>2</sub>O<sub>2</sub> because a fast addition can be dangerous (fast uncontrolled reactions).

The solution obtained is left under stirring for 15 minutes while the solid deposites at the bottom.

The solid obtained is filtered and dried in the oven for one night (between 110°C and 150°C). With this classical method was did the synthesis of the GO III but other synthesis will be describe in the next section 8.2.

## 8.2 The Graphite Oxide (GO): the modified methods

Some modifications were made on the classical method. The first one is the modification on the molar ratio between the reagents and the substrate. For the GO and GOII synthesis, each reagent was reducing in ratio 1 to 10. This simply modification was did in order to explore the level of functionalisation at different ratio.

In another one case the reaction time is modified: this is the case of the GOIV.

The synthesis of GOIV can be summarized as follows (important: here is summarized the synthesis normally used fo 2 g of support, but it can be scaled easily).

- To weigh 2 g of the support
- To dry the graphite in the oven at 105-110 °C
- To prepare an ice bath necessary during the reaction to control the temperature (initially working temperature about 5°C)
- Mixing of 155 ml of H<sub>2</sub>SO<sub>4</sub> (Molar Ratio = 4.8 H<sub>2</sub>SO<sub>4</sub>:support) with the graphite for 1 hour
- Addition of XNO<sub>3</sub> (X=Na or K) = 6.5 g (Molar Ratio = 0.46 XNO<sub>3</sub>:support)
- Addition of KMnO<sub>4</sub> = 6 g (Molar Ratio = 0.23 KMnO<sub>4</sub>:support): this step must did paying attention cause the manganates development



*Figure 8.1:* This picture was taken during the reaction and 2 hours mixing (after water addition at 98°C)

- the ice bath is taken off and the temperature is set to 35°C and maintained for 30 minutes at least
- After 30 minutes 306 ml of water DM are added and the temperature increases until 98°C and is maintained for 2 hours (until the color of the solution changes color from dark grey to clear orange); in figure 8.1 is possible to observe the final color of the solution
- After 2 hours the solution is left to cool down (environmental temperature)
- The solid is separated by centrifugation
- The solid is washed by DM water. The solution is left overnight to permit the precipitation of the solid at the bottom of the becher
- The solution is heated at 50°C and a 3.0% (v/v) of H<sub>2</sub>O<sub>2</sub> (65 ml) is added (by drop-wise): this step is necessary to permit the complete reaction of the un-reacted species
- At the end of the drop-wise the solution is left under stirring at 50 °C for 15 minutes.
- The solid is centrifugated
- The product obtained is dry in the oven at 105-110 °C

In another one synthesis, the GO V was synthesized with a simply variation of the molar ratio between the catalyst and the oxidant agent, the  $\text{KMnO}_4$ . This ratio varied from 0.23 to 0.34. Moreover at the end of the reaction no  $\text{H}_2\text{O}_2$  was added. Apart from these two modification on the procedure for the synthesis, was followed the same route used for the GO IV one. Finally, for the synthesis of the GO VI, the classical method from Hummers was modified. In this synthesis the classical method was modified as follow [49]:

- The solution is not only sulfuric acid but an amount of phosphoric was also used ( $\text{H}_2\text{SO}_4:\text{HPO}_3$ , 9:1 v/v)
- No  $\text{H}_2\text{O}_2$  was added at the end of the reaction
- Only the  $\text{KMnO}_4$  is used as oxidant (no nitrates utilisation;  $\text{XNO}_3$ ,  $\text{X} = \text{Na}$  or  $\text{K}$ )

Apart from these three differences respect the classical method the synthesis followed the receipt described below:

- To weigh 2 g of graphite
- To dry the graphite in the oven at 105-110 °C for 1 h
- To prepare an ice bath necessary during the reaction to control the temperature (initially working temperature about 5°C)
- Mixing of 230 ml of  $\text{H}_2\text{SO}_4$ :  $\text{HPO}_3$  (9:1 v/v) (Molar Ratio = 7.1  $\text{H}_2\text{SO}_4$ :support) with the graphite for 1 hour
- Addition of  $\text{KMnO}_4 = 15$  g (Molar Ratio = 0.57  $\text{KMnO}_4$ :support): this step must did paying attention cause the manganates development
- the ice bath is taken off and the temperature is set to 35°C and maintained for 30 minutes at least
- After 30 minutes 460 ml of water DM are added and the temperature increases until 98°C and is maintained for 2 hours (until the color of the solution changes color from dark grey to clear orange)
- After 2 hours the solution is left to cool down (environmental temperature)
- The solid is separated by centrifugation
- The solid is washed by DM water. The solution is left overnight to permit the precipitation of the solid at the bottom of the becher
- The solid is centrifugated
- The product obtained is dry in the oven at 80-100 °C

---

---

# CHAPTER 9

---

## APPENDIX B

In this Appendix is presented the complete description about the synthesis of the heterogeneous catalysts. For the characterisation it is necessary to refer to the dedicated Chapters.

### 9.1 The gold mono-metallic catalyst

In this section will be describe the synthesis way for the mono-metallic synthesis.

Every synthesis was conducted in a flask in a system as that reported in figure 9.1.

Such as explained in Chapter 4, three methods were used for the synthesis of the mono-metallic catalyst: Impregnation, Double Impregnation and Liquid Phase Reductive Deposition (LPRD).

In this section will be summarized rapidly the three methods. For some of them (DI and LPRD) the method was modified in accord with the considerations reported in Chapter 4. Anyway even with these modification (pH, surfactants, *et caetera*) there are some steps that remains unchanged and are reported below.

The first method described is the Impregnation one. The synthesis can be summarized as follow:

- drying of the support in the oven (100-110°C) for 1 hour at least
- dropwise of the support with the metal solution (X wt%)
- mixing overnight
- drying of the sample in the oven (100-110°C) for 24 hours

After the impregnation the gold is reduced in H<sub>2</sub> atmosphere at 350 °C. The temperature is reached with heating steps 50°C (static atmosphere).

The second method is the Double Impregnation (DI) one. The impregnation is double because the support is impregnated subsequently with the solutions of chloroauric and Na<sub>2</sub>CO<sub>3</sub> (1:4 molar ratio between the Au and Na<sub>2</sub>CO<sub>3</sub>). The NaCO<sub>3</sub> for the metal precursors reduction.

- drying of the support in the oven (100-110°C) for 1 hour at least
- the support is put into a sonicator (this solution was preferred to the magnetic stirrer)
- subsequently dropwise of the two solutions
- at the end of the impregnation the sample is left into the sonicator for 90 minutes
- at the end of the sonication the sample is removed from the sonicator and dried into the oven at 100-110 °C for a night.

The liquid phase reductive deposition (LPRD) gave the best results. Also in this case the method can be summarized as follow.

- drying of the support in the oven (100-110°C) for 1 hour at least
- preparation of two solution; one with the metal precursor and one with the NaOH (1:4 molar ratio between the Au and NaOH)
- the two solutions are mixed together and left overnight under stirring and repaired from the light (dark chamber)
- dropwise of the solutions mixed
- at the end of the sonication the sample is removed from the sonicator and dried into the oven at 100-110 °C for a night.

These three method were the start point for the synthesis of the mono-metallic catalysts. The modification of these methods in order to improve the quality of the nanoparticles (NPs) dispersion have been described in the Chapter 3.

## 9.2 The Pt-Bi bi-metallic catalysts

As metal pre-cursor were used the H<sub>2</sub>PtCl<sub>6</sub> hexaidrate, the Bi(NO)<sub>3</sub> or the BiCl<sub>3</sub>. The reduction agent used is the NaBH<sub>4</sub>. The same technique can be used for different supports. Also the HNO<sub>3</sub> was used during the reaction when Bi(NO)<sub>3</sub> was used as Bi precursor.

The synthesis is conducted in a flask with three necks. A magnetica stirrer is

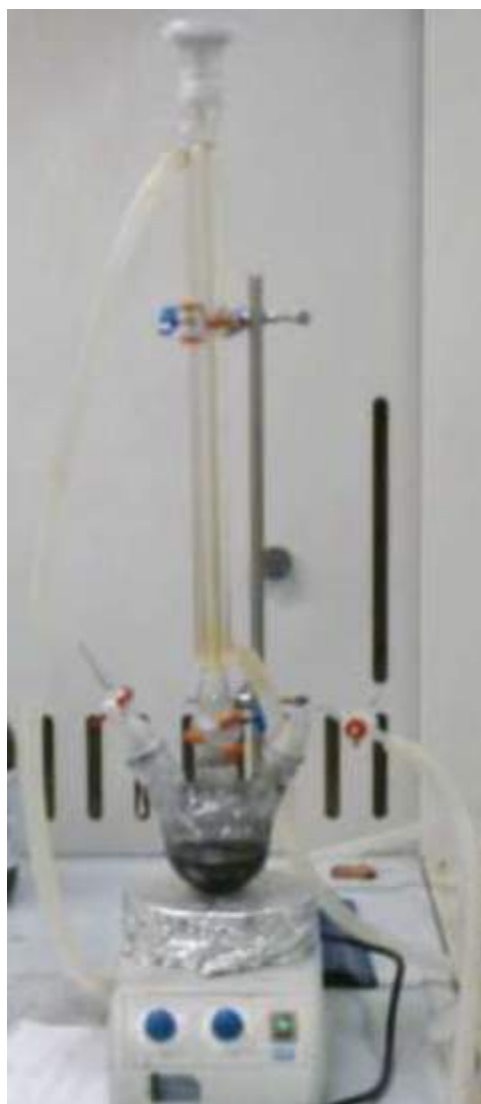


*Figure 9.1:* This picture was taken during the reaction and 2 hours mixing (after water addition at 98°C)

used to mix the solution during the metal impregnation. A Liebig refrigerant is used to permit the reflux (simply water is used with the refrigerant). One of the three necks is used for the N<sub>2</sub> flux. The N<sub>2</sub> is necessary to create a inert atmosphere and to avoid the Bi oxidation during the metal impregnation. The third neck is used as inlet.

The synthesis can be described as follow per points.

- an amount of support is dried in the oven at 110°C for 1 h at least
- when the Bi(NO)<sub>3</sub> is used as precursor it is necessary to prepare a

solution 0.012 M of  $\text{HNO}_3$ . This solution is used in every step of the synthesis. It has the task to avoid the Bi oxide formation and to make easier the  $\text{Bi}(\text{NO})_3$  dissolution

- The support is posed into the flask and the  $\text{Bi}(\text{NO})_3$  in solution is put together
- Degas with  $\text{N}_2$  for few minutes
- A solution of  $\text{NaBH}_4$  is dropped into the flask (molar ratio 10:1 between  $\text{NaBH}_4$  and  $\text{Bi}(\text{NO})_3$ ) and the solution is left under stirring overnight
- The day after a solution with Pt precursor is put into the flask; the solution is left under stirring for 5 hours
- The solid is centrifuged and dried into the oven at 105-110 °C for 2 hours
- The dried solid is washed with water several time to remove the unreacted species (salts)
- The washed solid is dried into the oven for 1 hour (at least)

The synthesis is same using the  $\text{BiCl}_3$  as precursor. The only difference is the solution of  $\text{HNO}_3$  0.012 M that it is not necessary in this case.



---

---

# CHAPTER 10

---

## APPENDIX C

### 10.1 A brief introduction to DFT calculation

In this Appendix will be presented the computational approach to the reaction studied [45,46].

At the start of the research one of the main idea was to approach the problem from experimental and theoretical point of view. The idea was to model the reaction between the glycerol,  $O_2$  and mono-metal nanoparticles (NPs). The reason of this idea was born when many groups in literature started to look for an explanation about the mechanisms that control the selective oxidation of the glycerol in presence of Au nanoparticles. It is important to underline how nowadays the mechanism is not clear yet. Only some mechanisms, like that one in figure 10.1, are proposed in literature.

The study was conducted using the free software Quantum Espresso and

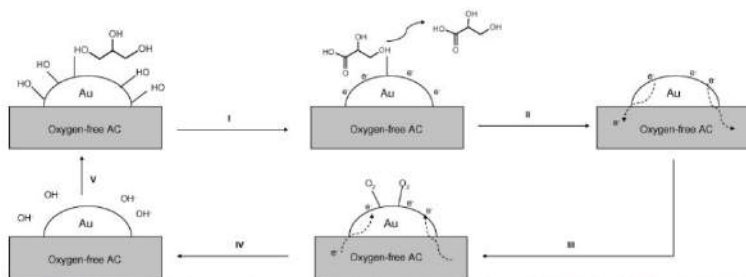


Figure 10.1: One of the proposed mechanism of reaction presented in literature

with a support of two clusters sited in Politechnic of Turin: Zefiro, thanks to the collaboration with prof. Gaingcarlo Cicero (Department of Applied Sciences), and Casper, the new high computing laboratory (HPC) coordinated by the group of prof. Nicolò Nepote.

I followed the setup of the software at HPC and together with prof. Giancarlo Cicero I obtained the possibility to conduct some simulations on the two clusters.

The computational approach to the problem was did only for one year when the catalyst based on Au-NPs was retained the best solution for the reaction. The approach was abandoned when the *errata-corrige* of Rodrigues' paper (2011 and 2012 respectively) was published and the experimental results did not give any results for the DHA.

When the idea of the mono-metallic catalyst was abandoned the time to develop a completed model on bi- and tri-metallic NPs was not sufficient and not compatible with the experimental work in laboratory. Anyway was considered interesting to report something about the work done.

## 10.2 Quantum Espresso and the approach to the model

The main problems linked to the computational approach is the nature of the simulation. In order to reproduce the mechanism of a generic reaction the *ab initio* theory was chosen. This kind of simulation required to solve the Schroedinger equations (the Hamiltonian time independent) for entire chemical system. To solve these equations it very difficult in particular when the system is bigger than an hydrogen-like one (a simply system with one proton and one electron). For this reason it is necessary to solve the problem using a cluster; many computers, able to communicate with each other and with the capability to process many data.

The simulations permit to evaluate the energy of the entire system in order to build the potential energy surface (PES). Studying the PES it is possible to identify the minimal energy paths from a configuration of the system to another one. This kind of approach offers the possibility to better understand how the reaction took place. To perform this calculus Quantum Espresso uses the Nudged Elastic Band (NEB) theory where it is necessary to know the minimal energy for each configuration theorized.

So to build this PES it is necessary to study the different possible configuration of the system and, for each one, to evaluate the free energy for that configuration. Cause different interacting structures each other it not possible to study directly the entire system. The first important step is to evaluate the energy for each singular structure whil the second one is to build the interacting system. The algebraic difference between the two energies permit to evaluate is the energy of the real system studied.

In figure 10.2 is presented a scheme followed to solve the Hamiltonian. Following this approach the different structure were built. In figure 10.3 it is possible to observe two molecules, the glycerol and the DHA. The sec-

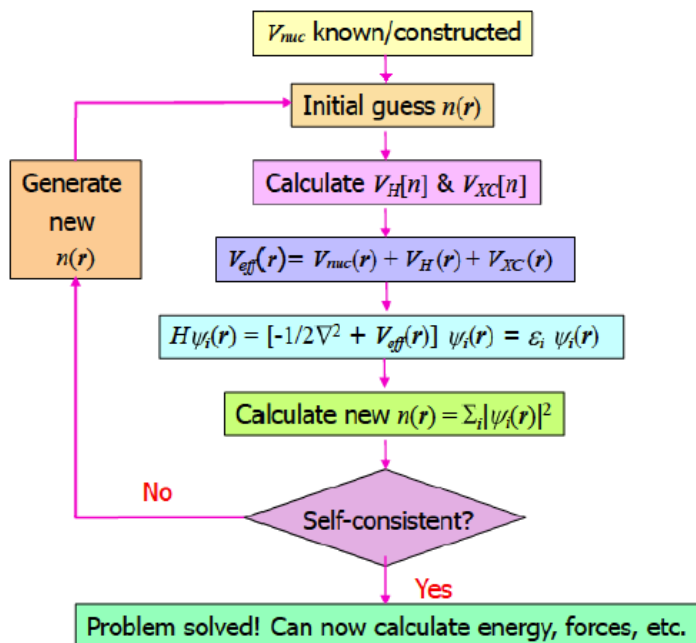


Figure 10.2: This scheme summarized how the simulation took place to solve the Schroedinger equations

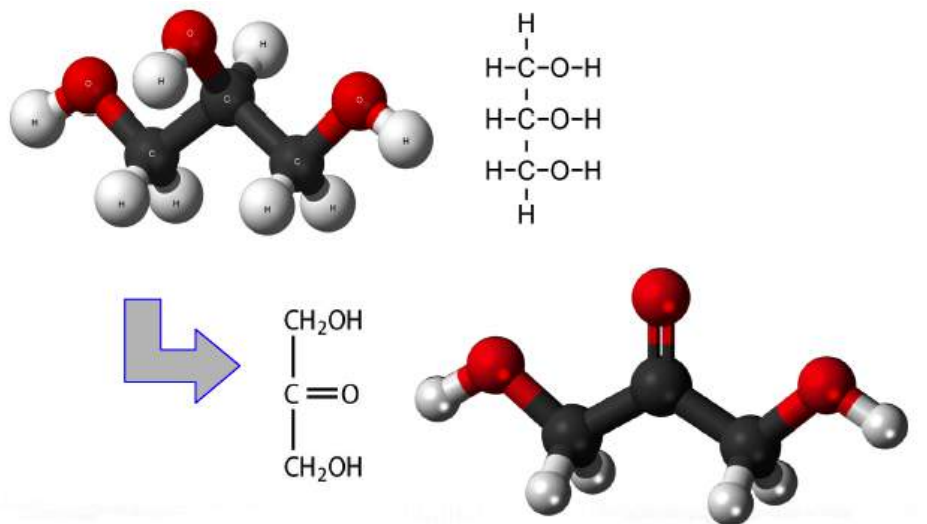


Figure 10.3: The glycerol and DHA molecules; the two structures correspond to the two configurations calculated with software Quantum Espresso

ond step was to build the nanoparticle. Ignoring the lattice constant for the Au nanoparticles was necessary to calculate the minimum of energy between two gold atoms. Starting from knowledge about the structure of the Au lat-

tice, body cubic central (bcc), the computation, using self consistent field (SCF), permitted to evaluate the lattice constant and to build the structure as reported in figures 10.4 and 10.5. After these calculation the system can

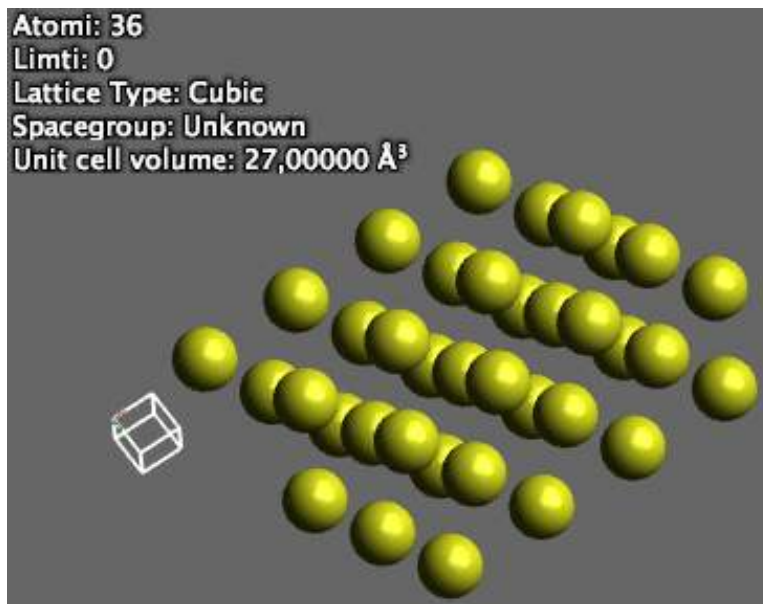


Figure 10.4: The computed crystal for gold atoms

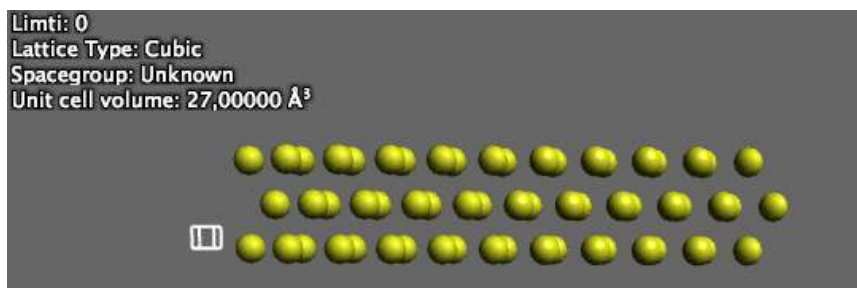


Figure 10.5: The computed crystal for gold atoms from the top; it is possible to recognized the hexagonal lattice typical for the bcc crystals, Au(111)

be built. It is important to underline how, even using two cluster, the time to do this work occupied a lot of months. The reason of this big computational cost is depends on the number of nodes that work together.

The system that was analyzed is reported in the figure 10.6 together with the code wrote to solve the Hamiltonian of the system. The computational approach to the problem was stopped at this point. The reason is due to the inefficient behavior of the gold nanoparticles for the selective oxidation of the glycerol to DHA. The experimental research was stopped and together the theoretical study.

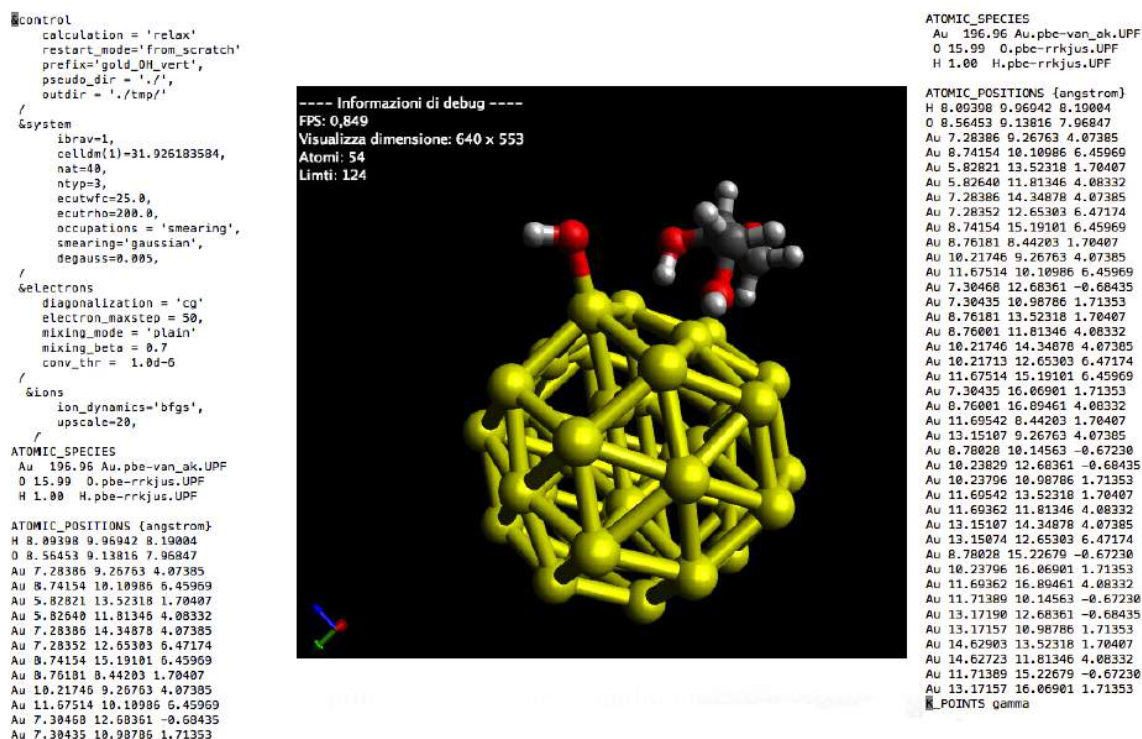


Figure 10.6: The system for which the Hamiltonian is solved; in this system it is possible to recognize glycerol, the Au nanoparticles and the -OH functional group, in accord with one of the model proposed as main mechanism of glycerol de-protonation

At this point the question could be: why no model was build for the bi- or tri-metallic catalysts and for the organometallic one? The reasons are different for the two catalysts.

For the bi- and tri-metallic catalysts the reason is the lack of a cluster computational time to solve the systems (normally a simulation runs out in one week) and the difficulties to build an efficient model to describe a coupled system. Considering that the theoretical approach was conducted in the free time, in parallel with the laboratory activity, the opportunity to study these complex systems was abandoned (the results obtained until now are not sufficient to say something about the reaction mechanism).

For the organo-metallic catalyst the reason lies in the software. Quantum Espresso was developed to solve problem linked to a periodic systems (crystal lattice, super-conductivity, quantum optics, *et caetera*). The software approximates the potential with plane waves (PWs): periodical functions that fit the periodic system like crystals. In the case of the organo-metallic catalyst not a real periodic system exist. To solve this kind of problem the PWs solution is not efficient and the calculus sometime does not reach the convergence and cannot be solved. On the other hand exist other soft-

wares used to solve these kind of problems; Gaussian and Vasp are some examples. These software, however, are developed using not the PWs but Gaussian functions to approximate the potential that is localized starting from the center of the atoms. But these software are not freeware and there was not the possibility to purchase them.

### 10.3 Conclusions about the DFT calculation

The theoretical approach was considered a good possibility with which could be possible to explain some catalytic phenomena.

Considering a no previous experience with this technique and the results obtained it is possible to do only some considerations about.

First of all the difficulty to study coupled system where a crystal (or a periodic structures) reacts together with an organic molecule. The functions used to approximate the potential, to write the Hamiltonian, have different nature: plane-waves or Gaussian functions. Nowadays does not exist a software able to treat these mixed systems, with the necessity of a big computational effort (a modern cluster it is necessary).

The study about the computational approach to the reaction showed an important thing: the necessity to create a database with the different chemical species that take part to the reaction. Exist different types of approximation to solve the computational problems link to the looking for the minimum of the free energy for a chemical system. Before to start to simulate a reaction it is necessary to do many tests to optimize the calculations. The computational work in this thesis stopped with the optimisation of the gold nanoclusters, the glycerol and the DHA structures. This optimisation required from seven to eight months using the hardware resources available.

Finally during these+ three years I have had the possibility to participate to different classes and Summer School and to discuss with other people about the applicability of this computational approach to the real problems. Nowadays this science requires many efforts to become an aid for the experimental research. The potential is high but it is possible to use this technique only for some specific problems.

---

## BIBLIOGRAPHY

1. Enhancement of the selectivity to dihydroxyacetone in glycerol oxidation using gold nanoparticles supported on carbon nanotubes; Elodie G. Rodrigues, Manuel F.R. Pereira, Juan J. Delgado, Xiaowei Chen, José J.M. Orfao; 2011
2. Gold supported on carbon nanotubes for the selective oxidation of glycerol; Elodie G. Rodrigues, Sonia A.C. Carabineiro, Juan J. Delgado et al.; Journal of Catalysis; 2011
3. Pd nanoparticles as catalyst for green and sustainable oxidation of functionalized alcohols in aqueous media; Maria Mifsud, Ksenia V. Parkhomenko, Isabel W.C.E. Arends and Roger A. Sheldon; Tetrahedron, 2009
4. Selective catalytic oxidation of glycerol: perspectives for high value chemicals; Benjamin Katryniok, Hiroshi Kimura, Elzbieta Skrzynska et al. ; Green Chemistry; 2011
5. Influence of activated carbon surface chemistry on the activity of Au/C catalysts in glycerol oxidation; Elodie G. Rodrigues, Manuel F.R. Pereira, Xiaowei Chen et al. ; Journal of Catalysis
6. Glycerol oxidation with gold supported on carbon xerogels: tuning selectivities by varying mesopore sizes; Elodie G. Rodrigues, Manuel F.R. Pereira, Jose J.M. Orfao; 2011
7. Selective Catalytic Oxidation of Glycerol to Dihydroxyacetone; Ron M. Painter, David M. Pearson and Robert M. Waymouth; Angewandte Chemie (International Edition); 2010
8. One-pot electrocatalytic oxidation of glycerol to DHA; Rosaria Ciriminna, Giovanni Palmisano, Cristina Della Pina, Michele Rossi e Mario Pagliaro; Science Direct-Tetrahedron Letters; July 2006
9. On the origin of the catalytic activity of gold nanoparticles for the low-temperature CO oxidation; N. Lopez, T.V.W. Janssens, B.S. Clausen et al. ; Journal of Catalysis; 2004

10. Study of the solubility and the metastable zone of the 1,3-dihydroxyacetone for the drowing-out process; Y. Zhu, D. Youssef, C. Porte, A. Rannou, M.P. Delplancke-Ogletree, B. Loi Mi Lung-Somarriba; *Journal of Crystal Growth*; 2003
11. On the interpretation of metastable zone width in anti-solvent crystallization; K.Sangwal; *InterScience*; 2010
12. Separation of 1,3-propandeiol from glycerol and glucose using a ZSM-5 zeolite membrane; Shiguang Li, Vu A. Tuan, John L. Falconer, Richard D. Noble; *Journal of Membrane Science*; 2000
13. Glycerol removal from biodiesel using membrane separation technology; Jehad Saleh, André Y. Tremblay, Marc A. Dubé; *Fuel*; 2010
14. Pd and Pt catalysts modified by alloying with Au in the selective oxidation of alcohols; Nikolaos Dimitratos, Alberto Villa, Di Wang, Francesca Porta, Dansheng Su, Laura Prati; *Journal of catalysis*; 2006
15. Synthesis characterisation and electrocatalytic activity of PtBi Nanoparticles prepared by the polyol process; Chandrani Roychowdhury, Futoshi Matsumoto, Paul F. Mutolo, Héctor D. Abruna, Francis J. DiSalvo; *Chemical Materials*; 2005
16. Propene Epoxidation with H<sub>2</sub>/H<sub>2</sub>O/O<sub>2</sub> mixtures over gold atoms supported on defective graphene: a theoretical study; Angeles Pulido, Mercedes Boronat, Avelino Corma; *Physical Chemistry C*; 2012
17. Influence of activated carbon surface chemistry on the activity of Au/C catalysts in glycerol oxidation; Elodie G. Rodrigues, Manuel F.R. Pereira, Xiaowei Chen, Juan J. Delgado, José J.M. Orfao; *Journal of Catalysis*; 2011
18. Gold on Carbon as a new catalyst for selective liquid phase oxidation of diols; Laura Prati, Michele Rossi, *Journal of catalysis*; 1998
19. The art of manufacturin gold catalysts; Laura Prati, Alberto Villa; *Catalysts Review*; 2012
20. Gold as a promoter for the activity of palladium in carbon-supported catalysts for the liquid phase oxidation of glyoxal to glyoxalic acid; Sophie Hermans and Michel Devillers; *Catalysts Letter*; 2005
21. Novel Process for 1,3-dihydroxyacetone production from glycerol, a technological feasibility study and process design; Zhi Zheng, Min Luo, Jianer Yu, Jianli Wang, Jianbing Ji; *Industrial and Engineering Chemistry Research*; 2012
22. Reduced transition metal colloids: a novel family of reusable catalysts?; Alain Roucoux, Jurgen Schulz, Henri Patin; *Chemical Review*; 2002
23. Small gold clusters formed in solution give reaction turnover numbers of 107 at room temperature; Judit oliver-meseguer, Jose R. Cabrero-Antonino, Irene Domínguez, Antonio Leyva-Pérez, Avelino Corma; *Science Mag*; 2012
24. Synthesis of gold nanoparticles modified with ionic liquid base on the imidazolium cation; Hideaki Itoh, Kensuke Naka, Yoshiki Chujo; *Journal of Americal Chemical Society*; 2004
25. Palladium-neocuproine catalyzed aerobic oxidation of alcohols in aqueos



- solvents; Isabel W.C.E. Arends, Gerd-jan Ten Brink, Roger A. Sheldon; *Journal of molecular catalysis*; 2006
26. CO oxidation on gold nanoparticles: theoretical studies; Ioannis N. Remediakis, Nuria Lopez, Jens K. Nørskov; *Applied Catalysis*; 2005
27. Gold on Carbon composite tubes and gold nanowires by impregnation templates with hydrogen tetrachloroaurate acetone solutions; Petra Goring, Eckhard Pippel, Herbert Hofmeister, Ralf B. Wehrspohn, Martin Steinhart, Ulrich Gosele; *Nano Letters*; 2004
28. High activity supported gold catalysts by incipient wetness impregnation; Michael Bowker, Abdullah Nuhu, Jorge Soares; *Catalysis Today*; 2007
29. Catalyst regeneration and activity enhancement of Au/TiO<sub>2</sub> by atmospheric pressure nonthermal plasma; H.H. Kim, S. Tsubota, M. Daté, A. Ogata, S. Futamura; *Applied Catalysis*; 2007
30. Preparation and characterization of a composite of gold nanoparticles and single-walled carbon nanotubes and its potential for heterogeneous catalysis; Anne E. Shanahan, James A. Sullivan, Mary McNamara, Hugh J. Byrne; *New Carbon Materials*, Science Direct, 2011
31. Prediction of oxygen solubility in pure water and brines up to high temperatures and pressures; Ming Geng, Zhenhao Duan; *Geochimica et Cosmochimica Acta*; 2010
32. Mechanism of Pd(OAc)<sub>2</sub>/DMSO – catalysed aerobic alcohol oxidation: mass transfer limitation effects and catalyst decomposition pathways; Bradley A. Steinhoff and Shannon S. Stahl; *Journal of American Chemical Society*; 2006
33. Metal complexes of organophosphate esters and open framework metal phosphates: synthesis, structure, transformations and applications; R. Murugavel, Amitava Choudhury, M.G. Walawalkar, R. Pothiraja, C.N.R. Rao; *Chemical Review*; 2008
34. The organometallic chemistry of the transition metals, fourth edition; Robert H. Crabtree, Yale University, Connecticut; 2005
35. Thermoanalytical, magnetic and structural study of Co(II) complexes with substituted salicylaldehydes and neocuproine; Maria Lalia Kantouri, Maria Gdaniec, Agnieszka Czapik, Konstantinos Chrissafis, Wiesława Ferenc, Jan Sarzynski, Christos D. Papadopoulos; 2011
36. Trinuclear Pd<sub>3</sub>O<sub>2</sub> intermediate in aerobic oxidation catalysis; Andrew J. Ingram, Diego Solis Ibarra, Richard N. Zare, Robert M. Waymouth; *Angewandte Communications*; 2014
37. Massive production of graphene oxide from expanded graphite; Ling Sun and Bunshi Fugetsu; Graduate School of Environmental Science, Hokkaido University, Japan; 2010
38. Interaction of acetonitrile with trifluoromethanesulfonic acid: unexpected formation of a wide variety of structures; George E. Salnikov, Alexander M. Genayev, Vladimir G. Vasiliev and Vyacheslav G. Shubin; *organic and Biomolecular Chemistry*; 2012

39. Supplementary material from [38]
40. HPLC methods for determination of Dihydroxyacetone and Glycerol in Fermentation Broth and Comparison with a Visible Spectrophotometric method to determine dihydroxyacetone; Jing Chen, Jianhua Chen and Changlin Zhou; *Journal of Chromatographic Science*; 2007
41. Preparation of metal nanoparticles in water-in-oil (w/o) microemulsion; I. Capek; *Advances in colloid and interface science*; 2004
42. H<sub>2</sub>SO<sub>4</sub>/HNO<sub>3</sub>/HCl – functionalisation and its effect on dispersion of carbon nanotubes in aqueous media; A.G. Osorio, I.C.L. Silveira, V.L. Bueno, C.P. Bergmann; *Applied Surface Science*; 2008
43. Chemoselective Pd-Catalyzed Oxidation of Polyols: synthetic scope and mechanistic studies; Kevin Chung, Steven M. Banik, Antonio G. De Crisci, David M. Pearson, Timothy R. Blake, Johan V. Olsson, Andrew J. Ingram, Richard N. Zare, Robert M. Waymouth; *Journal of the American Chemical Society*; 2013
44. Aerobic Alcohol oxidation with cationic Palladium complexes: insights into catalyst design and decomposition; Nicholas R. Conley, Liezel A. Labios, David M. Pearson, Charles C. I. McCrory, Robert M. Waymouth; *Organometallics*; 2007
45. Multiphase density functional theory parameterization of the Gupta potential for silver and gold; John T. Titantah, Mikko Karttunen; 2012
46. Study of 40-atom Pt-Au clusters using a combined empirical potential-density functional approach; Dung T. Tran, Roy L. Johnston; *Proceedings of the royal society*; 2014
47. Selective Oxidation of Glycerol to dihydroxyacetone over Pt-Bi/C catalyst: optimisation of catalyst and reaction conditions; Wenbin Hu, Daniel Knight, Brian Lowry, Arvind Varma; *Industrial Engineering Chemistry research*; 2010
48. Chemical-free growth of metal nanoparticles on graphene oxide sheets under visible light irradiation; Gun-hee Moon, Hyung-il Kim, Yongsoon Shin, Wonyong Choi; *The royal society of chemistry*; 2012
49. Improved synthesis of graphene oxide; Daniela C. Marcano, Dmitry V. Kosynkin, Jacob M. Berlin, Alexander Sinitskii, Zhengsong Sun, Alexander Slesarev, Lawrence B. Alemany, Wei Lu, James M. Tour; *American Chemical Society Nano*; 2010
50. Performance, structure and mechanism of Pd-Ag alloy catalyst for selective oxidation of glycerol to dihydroxyacetone; Shota Hirasawa, Hideo Watanabe, Tokushi Kizuka, Yoshinao Nakagawa, Keiichi Tomishige; *Journal of catalysis*; 2012
51. A novel glycerol valorization route: chemoselective dehydrogenation catalysed by iridium derivatives; Erica Farnetti, Jan Kaspar, Corrado Crotti; *Green Chemistry*; 2009
52. Preparation of the Graphite Oxide; William S. Hummers, Richard E. Offeman; March 1958

53. Selective oxidation of alcohols and aldehydes over supported metal nanoparticles; Sara E. Davis, Matthew S. Ide, Robert J. Davis; *Green Chemistry Review*; 2013
54. Corrigendum to “ Enhancement of the selectivity to di-hydroxyacetone in glycerol oxidation using gold nanoparticles supported on carbon nanotubes”, Elodie G.Rodrigues, Manuel F.R. Pereira, Juan J.Delgado, Xiaowei Chen, José J.M.Orfao; *Catalysis Communication*, 2013
55. Catalytic conversion in water. Part 23: steric effects and increased substrate scope in the Palladium-Neocuproine catalysed aerobic oxidation of alcohols in aqueous solvents; Gerd-Jan ten Brink, Isabel W.C.E. Arends, Marcel Hoogenraad, Goran Verspui, Roger A. Sheldon, *Advanced Synthesis of Catalysts*; 2003
56. Characterization of Peroxo and Hydroperoxo intermediates in the aerobic oxidation of N-Heterocyclic-Carbene-Coordinated Palladium(0); Michael M. Konnick, Llia A. Guzei, Shannon S. Stahl; *Journal of the American Chemical Society Communications*, 2004
57. *Chemical and Engineering Thermodynamics*, book, third edition; Stanley I. Sandler; 1997
58. The chemistry of graphene oxide; Daniel R. Dreyer, Sungjin Park, Christopher W. Bielawski, Rodney S. Ruoff; *Chemical Society Review*; 2009
59. Serinol: small molecule - big impact; Bjorn Andreeben and Alexander Steinbuchel; *Mini-Review AMB express* 2011
60. Oxidation of glycerol to biobased chemicals using supported mono- and bi-metallic noble metal catalysts; Ph.D. Thesis University of Groningen; 2013
61. C.H.C. Zhou, J.N. Beltramini, Y.X. Fan, G.Q.M. Lu, *Chem. Soc. Rev.* 37; 2008
62. P. McMorn, G.Roberts, G.J. Hutchings, *Catal.Letters* 63; 1999
63. Schultz M.J., Hamilton S.S., Jensen D.R., Sigman M.S.; *Chemical Communication* 2005
64. Nishimura T., Onoue T., Uemura S.; *Tetrahedron Letters*; 1998
65. Schultz M., Park C.C., Sigman M.S.; *Chem. Communications*, 2002
66. Brink G., Arends I., Sheldon R.A.; *Adv. Synthesis Catal.* 2002
67. Brink G., Arends I., Hoogenraad M., Verspui G., Sheldon R.A.; *Adv. Synthesis Catal.* 2003
68. Brink G., Arends I., Sheldon R.A.; *Science* 2000
69. Iwasawa T., Tokunaga M., Obora Y., Tsuji Y.J.; *American Chemical Society*; 2004
70. Komano T., Tokunaga M., Obora Y., Tsuji Y.J.; *Organometallics Letters*; 2005
71. Sigman M.S., Jensen D.R.; *Acc. Chem. Res.*; 2006
72. H.Kimura and K. Tsuto; *Applied Catalyst*; 1993
73. R.Garcia, m.Besson and P. Gallezot; *Applied Catalyst*; 1995
74. H.kimura and D.Keiichi (Kao Corporation); JP1992-224983, US5274187

(1993)

75. H.Kimura; Applied Catalyst, 1993
76. A. Brandner, K. Lehnert, A. Bienholz, M. Lucas and P. Claus; Top. Catal.; 2009
77. L.Xie and J.Hainan, Normal University (Natural Science); 2007
78. P. Claus, S. Demirel-Guelen, M. Lucas and K.Lehnert; Technische Universität Darmstadt; 2007
79. S. Demirel, K. Lehnert, M. Lucas and P. Claus: Applied Catalyst B; 2007
80. P.F.Fonseca Amaral, T.F.Ferreira, G.C.Fontes and M.A.Zarur Coelho; Food Bioprod. Process.; 2009
81. D.Liang, J.Gao, J.Wang, P.Chen, Z.Hou and X.Zheng; Catal. Communication; 2009
82. N.Dimistratos, A.Villa, C.L.Bianchi, L.Prati and M.Makkee; Applied Catal.; 2006
83. L.Prati and M.Rossi, J. Catal., 1998
84. S. Carretin, P. McMorn, P. Johnston, K.Griffin, C.Kiely and G.J.Hutchings; Physical Chem.; 2003
85. S. Carretin, P. McMorn, P. Johnston, K.Griffin, C.Kiely and G.J.Hutchings; Top. Catal. ; 2004
86. S. Carretin, P. McMorn, P. Johnston, K.Griffin, C.Kiely and G.J.Hutchings; Chem. Communication; 2002
87. F. Porta and L. prati; J. Catal; 2004
88. S. Demirel-Guelen, M.Lucas and P.Claus; Catal. Today; 2005
89. S. Demirel, P.Kern, M.Lucas, P.Claus; Catal. Today; 2007
90. J. Gao, D. Liang, P. Chen, Z. Hou and X. Zheng; Catal. Letters; 2009
91. A. Villa, C. Campione, L.Prati; Catal. Letters; 2007
92. L. Prati, P. Spontoni and A. Gaiassi; Top. Catal., 2009
93. A. Villa, M. Veith and L.Prati; Angew. Chem.; Int. Ed.; 2010
94. Mechanism of graphene oxide formation; Ayrat M. Dimiev and James M. Tour; ACSNano; 2014